

# BLOW-UP CRITERIA FOR THE 3D CUBIC NONLINEAR SCHRÖDINGER EQUATION

JUSTIN HOLMER, RODRIGO PLATTE, AND SVETLANA ROUDENKO

**ABSTRACT.** We consider solutions  $u$  to the 3d nonlinear Schrödinger equation  $i\partial_t u + \Delta u + |u|^2 u = 0$ . In particular, we are interested in finding criteria on the initial data  $u_0$  that predict the asymptotic behavior of  $u(t)$ , e.g., whether  $u(t)$  blows-up in finite time, exists globally in time but behaves like a linear solution for large times (scatters), or exists globally in time but does not scatter. This question has been resolved (at least for  $H^1$  data) in [18, 8, 9, 19] if  $M[u]E[u] \leq M[Q]E[Q]$ , where  $M[u]$  and  $E[u]$  denote the mass and energy of  $u$ , and  $Q$  denotes the ground state solution to  $-Q + \Delta Q + |Q|^2 Q = 0$ . Here we consider the complementary case  $M[u]E[u] > M[Q]E[Q]$ . In the first (analytical) part of the paper, we present a result due to Lushnikov [20], based on the virial identity and the uncertainty principle, giving a sufficient condition for blow-up. By replacing the uncertainty principle in his argument with an interpolation-type inequality, we obtain a new blow-up condition that in some cases improves upon Lushnikov's condition. Our approach also allows for an adaptation to radial infinite-variance initial data that has a conceptual interpretation: for real-valued initial data, if a certain fraction of the mass is contained within the ball of radius  $M[u]$ , then blow-up occurs. We also show analytically (if one takes the numerically computed value of  $\|Q\|_{\dot{H}^{1/2}}$ ) that there exist Gaussian initial data  $u_0$  with negative quadratic phase such that  $\|u_0\|_{\dot{H}^{1/2}} < \|Q\|_{\dot{H}^{1/2}}$  but the solution  $u(t)$  blows-up. In the second (numerical) part of the paper, we examine several different classes of initial data – Gaussian, super-Gaussian, off-centered Gaussian, and oscillatory Gaussian – and for each class give the theoretical predictions for scattering or blow-up provided by the above theorems as well as the results of numerical simulation. On the basis of the numerical simulations, we formulate several conjectures, among them that for *real* initial data, the quantity  $\|Q\|_{\dot{H}^{1/2}}$  provides the threshold for scattering.

## 1. INTRODUCTION

The nonlinear Schrödinger equation (NLS) or Gross-Pitaevskii equation is

$$(1.1) \quad i\partial_t u + \Delta u + |u|^2 u = 0,$$

with wave function  $u = u(x, t) \in \mathbb{C}$ . We consider  $x \in \mathbb{R}^n$  in dimensions  $n = 1, 2$ , or  $3$ . The initial-value problem is locally well-posed in  $H^1$  (see Cazenave [5] for exposition and references therein). In this now standard theory obtained from the Strichartz estimates, initial data  $u_0 \in H^1$  give rise to a unique solution  $u(t) \in C([0, T]; H^1)$  with the time interval  $[0, T]$  of existence specified in terms of  $\|u_0\|_{H^1}$ . In some situations,

an *a priori* bound on  $\|u(t)\|_{H^1}$  can be deduced from conservation laws which implies the solution  $u(t)$  exists globally in time. On the other hand, we say that a solution  $u(t)$  to NLS *blows-up in finite time*  $T^*$  provided

$$(1.2) \quad \lim_{t \nearrow T^*} \|\nabla u(t)\|_{L^2} = +\infty.$$

For  $n = 1$ , all  $H^1$  initial data yield global solutions, but large classes of initial data leading to solutions blowing-up in finite time are known for  $n = 2$  and  $n = 3$ . NLS arises as a model of several physical phenomena. We outline three important examples in a supplement to this introduction (§1.1 below), and emphasize that in each case the mathematical property of blow-up in finite time is realistic and relevant. It is therefore of interest to determine mathematical conditions on the initial data that guarantee the corresponding solution will blow-up in finite-time and conditions that guarantee it will exist globally in time. Moreover, if we know the solution is global, it is natural to ask whether we can predict the asymptotic ( $t \rightarrow +\infty$ ) behavior of the solution. If the solution asymptotically approaches a solution of the linear equation, we say it *scatters*. Nonlinear effects can persist indefinitely, however; for example, leading to formation of *solitons* or *long-range modulation of linear solutions*.

Partial answers to the above mathematical problem are known, and we will discuss separately the existing literature in the case of dimensions  $n = 1, 2$ , and  $3$ . Afterward, we will state our new findings in the  $n = 3$  case.

Before proceeding, we note that NLS satisfies conservation of mass  $M[u]$ , momentum  $P[u]$ , and energy  $E[u]$ , where

$$M[u] = \|u\|_{L^2}^2, \quad P[u] = \operatorname{Im} \int \bar{u} \nabla u,$$

$$E[u] = \frac{1}{2} \|\nabla u\|_{L^2}^2 - \frac{1}{4} \|u\|_{L^4}^4.$$

Also, NLS satisfies the scaling symmetry

$$(1.3) \quad u(x, t) \text{ solves NLS} \implies \lambda u(\lambda x, \lambda^2 t) \text{ solves NLS}.$$

Consequently, the critical (scale-invariant) Sobolev space  $H^s(\mathbb{R}^n)$  is  $s = \frac{n-2}{2}$ . The NLS equation also satisfies the Galilean invariance: For any  $v \in \mathbb{R}^n$ ,

$$u(x, t) \text{ solves NLS} \implies e^{ix \cdot v} e^{-it|v|^2} u(x - 2vt, t) \text{ solves NLS},$$

and thus, any solution can be transformed to one for which  $P[u] = 0$ . Let

$$V[u](t) = \|xu(t)\|_{L_x^2}^2$$

denote the variance. Assuming  $V[u](0) < \infty$ , then the virial identities (Vlasov-Petrishchev-Talanov [28], Zakharov [33], Glassey [13])

$$(1.4) \quad \partial_t V[u] = 4 \operatorname{Im} \int x \cdot \nabla u \bar{u} dx, \quad \partial_t^2 V[u] = 8nE[u] + (8 - 4n) \|\nabla u\|_{L_x^2}^2$$

hold. Let  $Q = Q(x)$  denote the real-valued, smooth, exponentially decaying ground state solution to

$$(1.5) \quad -Q + \Delta Q + Q^3 = 0.$$

Then  $u(x, t) = e^{it}Q(x)$  solves NLS, and is called the *ground state soliton*. The Pohozaev identities are

$$(1.6) \quad \|\nabla Q\|_{L^2}^2 = \frac{n}{4-n}\|Q\|_{L^2}^2, \quad \|Q\|_{L^4}^4 = \frac{4}{4-n}\|Q\|_{L^2}^2.$$

Weinstein [30] proved that the Gagliardo-Nirenberg inequality

$$(1.7) \quad \|\phi\|_{L^4}^4 \leq c_{\text{GN}} \|\phi\|_{L^2}^{4-n} \|\nabla \phi\|_{L^2}^n$$

is saturated by  $\phi = Q$ , i.e.,

$$c_{\text{GN}} = \frac{\|Q\|_{L^4}^4}{\|Q\|_{L^2}^{4-n} \|\nabla Q\|_{L^2}^n}$$

is the sharp constant.

*2d case.* Much of the mathematically rigorous literature has been devoted to the 2d case, of particular relevance to the optics model (item 1 in §1.1), and has the special mathematical property of being  $L^2$ -critical. The energy  $E[u]$  conservation combined with the Weinstein inequality (1.7) implies that if  $\|u_0\|_{L^2} < \|Q\|_{L^2}$ , an  $H^1$  solution is global. This result is in fact sharp, in the following sense. The  $L^2$  scale-invariance of the 2d equation allows for an additional symmetry, the pseudo-conformal transformation

$$(1.8) \quad u(x, t) \text{ solves 2d-NLS} \quad \implies \quad \tilde{u}(x, t) = \frac{1}{t} e^{\frac{i|x|^2}{4t}} \bar{u}\left(\frac{x}{t}, \frac{1}{t}\right) \text{ solves 2d-NLS.}$$

This gives rise to an explicit family of blow-up solutions

$$u_T(x, t) = \frac{1}{(T-t)} e^{i/(T-t)} e^{i|x|^2/(T-t)} Q\left(\frac{x}{T-t}\right)$$

obtained by the pseudoconformal transformation, time translation, and scaling. They blow-up at the origin at time  $T > 0$  (and  $T$  can be taken arbitrarily small), but  $\|u_T\|_{L^2} = \|Q\|_{L^2}$ . Note that they have initial data  $(u_T)_0(x) = e^{i|x|^2/T} Q(x/T)/T$ , indicating that the inclusion of a quadratic phase prefactor can create finite-time blow-up. Moreover, it was observed by Vlasov-Petrishchev-Talanov [28], Zakharov [33] and Glassey [13] that if the initial data has finite variance  $\|xu_0\|_{L^2} < \infty$  and  $E[u] < 0$  (which implies by (1.7) that  $\|u_0\|_{L^2} \geq \|Q\|_{L^2}$ ), then the solution  $u(t)$  blows-up in finite time. Blow-up solutions with  $E[u] > 0$  exist and global solutions with  $E[u] > 0$  exist. If  $E[u] > 0$ , then a sufficient condition for blow-up can be deduced

from the virial identity (see [28], [33])<sup>1</sup>:

$$(1.9) \quad V_t(0) < -\sqrt{16EV(0)}.$$

*1d case.* The 1d case is  $L^2$  subcritical; energy conservation and (1.7) prove that solutions never blow-up in finite time. One can still ask if there is a quantitative threshold for the formation of solitons. Such a threshold must be expressed in terms of a scale-invariant quantity, and the  $L^1$  norm is a natural candidate. We note that soliton solutions

$$u(x, t) = e^{it}Q(x), \quad Q(x) = \sqrt{2}\operatorname{sech} x$$

have  $\|u(t)\|_{L^1} = \|Q\|_{L^1} = \sqrt{2}\pi$  (as do rescalings and Galilean shifts of this solution). As the equation is completely integrable (see Zakharov-Shabat [32]), one has available the tools of inverse scattering theory (IST). IST has been applied by Klaus-Shaw [21] to show that if  $\|u_0\|_{L^1} < \frac{1}{2}\|Q\|_{L^1}$ , then no solitons form. See Holmer-Marzuola-Zworski [16], Apx. B for a calculation showing that this is sharp – for initial data  $u_0(x) = \alpha Q(x)$  with  $\alpha > \frac{1}{2}$ , a soliton emerges in the  $t \rightarrow +\infty$  asymptotic resolution. We remark that although no solitons appear if  $\|u_0\|_{L^1} < \frac{1}{2}\|Q\|_{L^1}$ , such solutions do not *scatter*, i.e., they do not approach a solution to the linear equation as  $t \rightarrow +\infty$  – see Barab [1]. In fact, there are long-range effects and one conjectures *modified scattering* – see Hayashi-Naumkin [15] for some results in this direction for small initial data.<sup>2</sup> The Hayashi-Naumkin paper, in fact, treats a more general equation and does not rely on IST; presumably IST could be applied to prove modified scattering for  $\|u_0\|_{L^1} < \frac{1}{2}\|Q\|_{L^1}$  for generic Schwartz  $u_0$ , although we are not aware of a reference.

*3d case.* We have previously studied the 3d case of NLS, which is  $L^2$  supercritical, in Holmer-Roudenko [17, 18, 19], Duyckaerts-Holmer-Roudenko [8], and Duyckaerts-Roudenko [9]. Scattering and blow-up criteria are most naturally expressed in terms of scale invariant quantities, and natural candidates are the  $L^3$  norm and the  $\dot{H}^{1/2}$  norm. We argue below that the  $L^3$  norm is completely inadequate, and while the  $\dot{H}^{1/2}$  norm is a more reasonable choice, it too appears deficient. In [18, 8], we work instead with two scale-invariant quantities:  $M[u]E[u]$  and

$$(1.10) \quad \eta(t) \stackrel{\text{def}}{=} \frac{\|u(t)\|_{L^2}\|\nabla u(t)\|_{L^2}}{\|Q\|_{L^2}\|\nabla Q\|_{L^2}}.$$

By the Weinstein inequality (1.7) and the Pohozaev identities (1.6) we have

$$(1.11) \quad 3\eta(t)^2 \geq \frac{M[u]E[u]}{M[Q]E[Q]} \geq 3\eta(t)^2 - 2\eta(t)^3.$$

<sup>1</sup>Blow-up solutions are also possible when  $E = 0$  provided  $V_t(0) < 0$ , for a general review refer to [26].

<sup>2</sup>[15] does not cover the full range  $\|u_0\|_{L^1} < \frac{1}{2}\|Q\|_{L^1}$ , and, in fact, the smallness condition is in terms of a stronger norm.

This results in two “forbidden regions” in the  $M[u]E[u]/M[Q]E[Q]$  versus  $\eta^2$  phase-plane – see the depiction in Figure 1.1. Note that since  $M[u]$  and  $E[u]$  are conserved, all time evolution in Figure 1.1 occurs along horizontal lines. In what follows for brevity and simplicity we assume  $P[u] = 0$  which can be obtained via Galilean transform. The most general case would follow as it is explained in Appendix B of [19].

**Theorem 1.1** (Duyckaerts-Holmer-Roudenko [8], Holmer-Roudenko [18, 19]). *Suppose that  $u_0 \in H^1$  and  $M[u]E[u] < M[Q]E[Q]$ .*

- (1) *If  $\eta(0) < 1$ , then  $u(t)$  is globally well-posed and, in fact, scatters in both time directions.*
- (2) *If  $\eta(0) > 1$  and either  $u_0$  has finite variance or  $u_0$  is radial, then  $u(t)$  blows-up in finite positive time and finite negative time.*
- (3) *If  $\eta(0) > 1$ , then either  $u(t)$  blows-up in finite forward time or there exists a sequence  $t_n \nearrow +\infty$  such that  $\|\nabla u(t_n)\|_{L^2} = \infty$ . A similar statement for negative time holds.*

It is a straightforward consequence of the linear decay estimate that scattering solutions satisfy

$$\lim_{t \nearrow +\infty} \|u(t)\|_{L^p} = 0, \quad 2 < p \leq 6.$$

It follows by using the  $p = 4$  case and the Pohozaev identities (1.6) that

$$\lim_{t \rightarrow +\infty} \eta(t)^2 = \frac{M[u]E[u]}{3M[Q]E[Q]}.$$

That is, in Figure 1.1, a scattering solution has  $\eta(t)^2$  asymptotically approaching boundary line ABC. On the other hand, since blow-up solutions satisfy (1.2), such solutions go off to right (along a horizontal line) in Figure 1.1. We note that Merle-Raphaël [24] strengthened (1.2): they proved that if  $u(t)$  blows-up in finite forward time  $T^* > 0$ , then

$$\lim_{t \nearrow T^*} \|u(t)\|_{L^3} = +\infty.$$

The blow up for finite variance as in Theorem 1.1, part (2), has previously been obtained by Kuznetsov et al. in [23].

The results of Duyckaerts-Roudenko [9] are contained in the next two theorems. First, they establish the existence of special solutions (besides  $e^{it}Q$ ) at the critical mass-energy threshold.

**Theorem 1.2** (Duyckaerts-Roudenko [9]). *There exist two radial solutions  $Q^+$  and  $Q^-$  of NLS with initial conditions  $Q_0^\pm$  such that  $Q_0^\pm \in \cap_{s>0} H^s(\mathbb{R}^3)$  and*

- (1)  *$M[Q^+] = M[Q^-] = M[Q]$ ,  $E[Q^+] = E[Q^-] = E[Q]$ ,  $[0, +\infty)$  is in the (time) domain of definition of  $Q^\pm$  and there exists  $e_0 > 0$  such that*

$$\forall t \geq 0, \quad \|Q^\pm(t) - e^{it}Q\|_{H^1} \leq Ce^{-e_0 t},$$

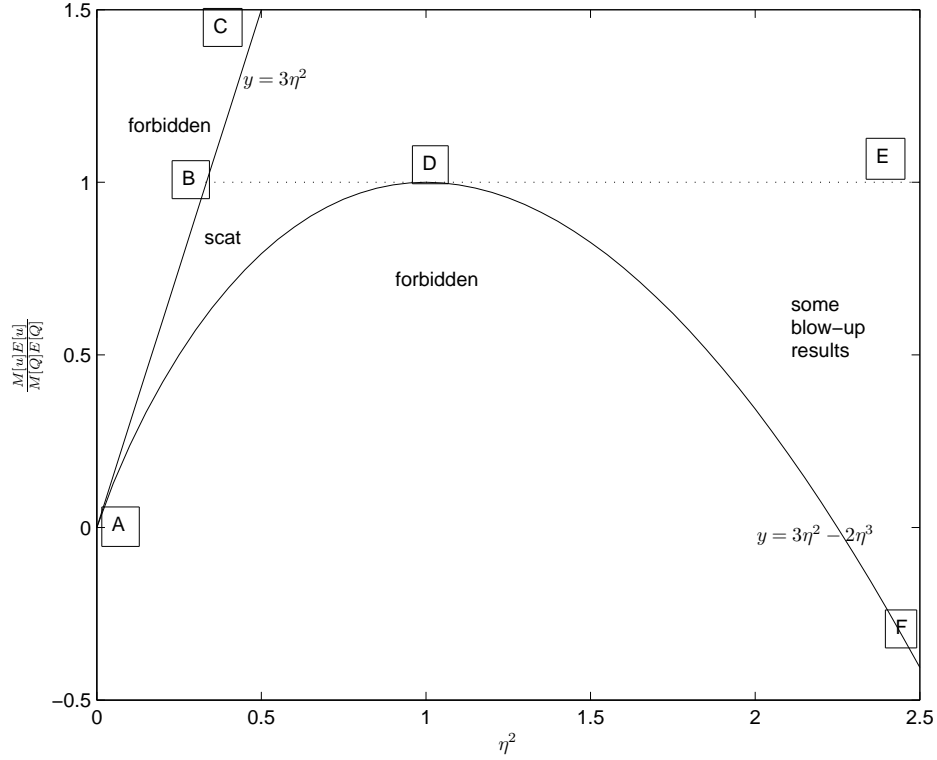


FIGURE 1.1. A plot of  $M[u]E[u]/M[Q]E[Q]$  versus  $\eta^2$ , where  $\eta$  is defined by (1.10). The area to the left of line ABC and inside region ADF are excluded by (1.11). The region inside ABD corresponds to case (1) of Theorem 1.1 (solutions scatter). The region EDF corresponds to case (2) of Theorem 1.1 (solutions blow-up in finite time). Behavior of solutions on the dotted line (mass-energy threshold line) is given by Theorem 1.3.

- (2)  $\|\nabla Q_0^-\|_2 < \|\nabla Q\|_2$ ,  $Q^-$  is globally defined and scatters for negative time,
- (3)  $\|\nabla Q_0^+\|_2 > \|\nabla Q\|_2$ , and the negative time of existence of  $Q^+$  is finite.

Next, they characterize all solutions at the critical mass-energy level as follows:

**Theorem 1.3** (Duyckaerts-Roudenko [9]). *Let  $u$  be a solution of NLS satisfying  $M[u]E[u] = M[Q]E[Q]$ .*

- (1) *If  $\eta(0) < 1$ , then either  $u$  scatters or  $u = Q^-$  up to the symmetries.*
- (2) *If  $\eta(0) = 1$ , then  $u = e^{it}Q$  up to the symmetries.*
- (3) *If  $\eta(0) > 1$ , and  $u_0$  is radial or of finite variance, then either the interval of existence of  $u$  is of finite length or  $u = Q^+$  up to the symmetries.*

A recent result of Beceanu [2] on (1.1) states that near the ground state soliton (and its Galilean, scaling and phase transformations) there exists a real analytic (center-stable) manifold in  $\dot{H}^{1/2}$  such that any initial data taken from it will produce a global in time solution decoupling into a moving soliton and a dispersive term scattering in  $\dot{H}^{1/2}$ .

In part I of this paper, we provide some alternate criteria for blow-up in the spirit of Lushnikov [20]. First, we state his result, adapted to our notation. Due to the complexity of the formulas, we will write  $M = M[u]$ ,  $E = E[u]$ , etc. For simplicity we restrict to the case  $E > 0$ , since  $E \leq 0$  is comparately well understood from Theorem 1.1.

**Theorem 1.4** (adapted from Lushnikov [20]). *Suppose that  $u_0 \in H^1$  and  $\|xu_0\|_{L^2} < \infty$ . The following is a sufficient condition for blow-up in finite time:*

$$(1.12) \quad \frac{V_t(0)}{M} < 2\sqrt{3} \, g\left(\frac{8EV(0)}{3M^2}\right),$$

where

$$(1.13) \quad g(\omega) = \begin{cases} \sqrt{\frac{2}{\omega^{1/2}} + \omega} - 3 & \text{if } 0 < \omega \leq 1 \\ -\sqrt{\frac{2}{\omega^{1/2}} + \omega} - 3 & \text{if } \omega \geq 1, \end{cases}$$

which is graphed in Figure 1.2.

For an explicit formulation of the condition (1.12) refer to §4.3, in particular, when initial datum is real-valued (1.12) becomes (4.4) and when it is complex-valued the condition rewrites as in (4.6)-(4.7).

Theorem 1.4 is based upon use of the uncertainty principle,

$$(1.14) \quad \|u\|_{L^2}^4 + \frac{4}{9} \left| \operatorname{Im} \int (x \cdot \nabla u) \bar{u} \, dx \right|^2 \leq \frac{4}{9} \|xu\|_{L^2}^2 \|\nabla u\|_{L^2}^2,$$

the virial identity, and a “mechanical analysis” of the resulting second-order ODE in  $V(t)$ . By replacing (1.14) with

$$(1.15) \quad \|u\|_{L^2} \leq \left( \frac{2^2 \cdot 7^5 \cdot \pi^2}{3^5 \cdot 5^2} \right)^{\frac{1}{14}} \|xu\|_{L^2}^{\frac{3}{7}} \|u\|_{L^4}^{\frac{4}{7}},$$

we can obtain a different condition which in some cases improves upon Theorem 1.4. The inequality (1.15) can be thought of as a variant of the Hölder interpolation inequality  $\|u\|_{L^2} \leq \|u\|_{L^{6/5}}^{3/7} \|u\|_{L^4}^{4/7}$ , since  $\|u\|_{L^{6/5}}$  and  $\|xu\|_{L^2}$  scale the same way. Both inequalities (1.14) and (1.15) are stated here with sharp constants and are proved in §2.

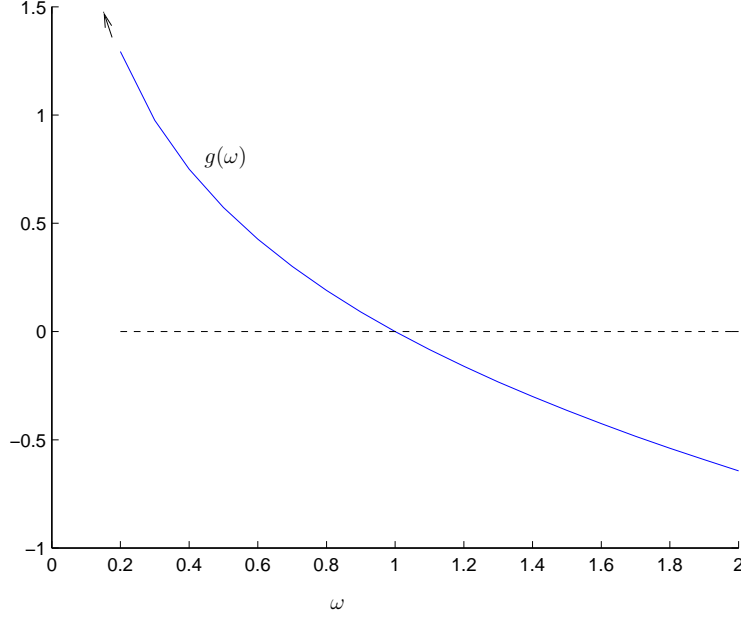


FIGURE 1.2. A plot of  $g(\omega)$  versus  $\omega$ , where  $g$  is defined in (1.13). This function appears in the blow-up conditions in Theorems 1.4 and 1.5.

**Theorem 1.5.** *Suppose that  $u_0 \in H^1$  and  $\|xu_0\|_{L^2} < \infty$ . The following is a sufficient condition for blow-up in finite time:*

$$(1.16) \quad \frac{V_t(0)}{M} < \frac{2\sqrt{2}(ME)^{\frac{1}{6}}}{C^{\frac{7}{3}}} g\left(\frac{4C^{\frac{14}{3}}E^{\frac{2}{3}}}{M^{\frac{7}{3}}}V(0)\right), \quad C = \left(\frac{2^2 \cdot 7^5 \cdot \pi^2}{3^5 \cdot 5^2}\right)^{\frac{1}{14}},$$

where  $g$  is defined in (1.13) and graphed in Figure 1.2.

For an explicit reformulation of (1.16) refer to §4.3, in particular, for the real-valued initial datum it becomes (4.5) and for the complex-valued datum it is equivalent to (4.12) - (4.13).

Note that (1.16) can be put into the form

$$\frac{V_t(0)}{M} < 2\sqrt{3} \tilde{g}\left(\frac{8EV(0)}{3M^2}\right), \quad \tilde{g}(\omega) = \mu g(\mu^{-2}\omega), \quad \mu = \frac{\sqrt{2}(ME)^{\frac{1}{6}}}{\sqrt{3}C^{\frac{7}{3}}},$$

which offers a comparison between Theorem 1.4 and 1.5. These conditions should be compared to the sufficient condition for  $E[u] > 0$  in the 2d case, namely (1.9).

The approach via the interpolation inequality (1.15) also allows us to prove a radial, infinite-variance version of Theorem 1.5 based upon a local virial identity, Strauss' radial Gagliardo-Nirenberg inequality [25], and a bootstrap argument. Select a smooth radial (nonstrictly) increasing function  $\psi(x)$  such that  $\psi(x) = |x|^2$  for



$0 \leq |x| \leq 1$  and  $\psi(x) = 2$  for  $|x| \geq 2$ . Define the *localized variance*

$$(1.17) \quad V_R \stackrel{\text{def}}{=} \int R^2 \psi(x/R) |u(x)|^2 dx.$$

Note that by the dominated convergence theorem, for any  $u_0 \in L^2$ , we have

$$\lim_{R \rightarrow +\infty} \frac{V_R(0)}{R^2 M} = 0.$$

Thus, there always exists  $R$  such that (1.18) below holds.

**Theorem 1.6.** *Suppose  $ME > 1$ . Fix  $\delta \ll 1$  (the smallness depends only on  $\psi(x)$  in (1.17)). Given  $u_0 \in H^1$  radial, take any  $R$  such that*

$$(1.18) \quad \frac{V_R(0)}{M} \leq \frac{1}{2} R^2, \quad R^2 \gtrsim \frac{M^2}{\delta}$$

*(the implicit constant in the second inequality again depends only on  $\psi(x)$  in (1.17)). Then the following is a sufficient condition for blow-up in finite time:*

$$(1.19) \quad \frac{(V_R)_t(0)}{M} < \frac{\sqrt{6}(8+\delta)^{\frac{1}{6}}(1-\delta)^{\frac{1}{3}}(ME)^{\frac{1}{6}}}{(C_\infty)^{\frac{7}{3}}} g \left( \frac{(8+\delta)^{\frac{2}{3}}(C_\infty)^{\frac{14}{3}}E^{\frac{2}{3}}}{(1-\delta)^{\frac{2}{3}}M^{\frac{7}{3}}} V_R(0) \right),$$

$$C_\infty = \left( \frac{2^{11}\pi^2}{3^2} \right)^{\frac{1}{14}},$$

where  $g$  is defined in (1.13) and graphed in Figure 1.2.

One way to generate examples of  $u_0$  satisfying the hypotheses of Theorem 1.6 but not Theorem 1.5 is to take any of the examples detailed below for which Theorem 1.5 applies, but tack on a slowly decaying tail of infinite variance but at very large radii. For example, redefine  $u_0$  at very large radii to be  $u_0(x) = |x|^{-2}$ . However, the main merit of Theorem 1.6 is the availability, in the case of real initial data, of a conceptual interpretation in terms of the way in which mass is initially distributed.

**Corollary 1.7.** *There is  $0 < \delta \ll 1$  such that the following holds. Suppose that  $ME > 1$ ,  $u_0 \in H^1$  is radial and real,*

$$(1.20) \quad \frac{1}{M} \int_{|x| \geq \delta^{1/2} M (ME)^{-1/3}} |u_0|^2 dx \leq \delta^2 (ME)^{-2/3}.$$

*Then blow-up occurs in finite time.*

Note that the quantity on the left-side of (1.20) is the fraction of initial mass occurring outside the ball of radius  $\delta M (ME)^{-1/3}$ . Thus, (1.20) states that most mass is *inside* the ball of radius  $\delta M (ME)^{-1/3}$ , and we intuitively expect an initially highly concentrated real solution to blow-up. By the scaling (1.3), it is natural that the radius scales linearly with  $M$ .

Theorems 1.4, 1.5, and 1.6, and Corollary 1.7 are proved in §3, and the reformulation of the conditions of Theorems 1.4 and 1.5 is in §4.3.

In the remainder of the paper, §5–9, we examine several specific *radial* initial data given as profiles with several parameters.<sup>3</sup> In each case, we report the predictions given by Theorems 1.1, 1.4, and 1.5, and also the results of numerical simulations. In general, Theorems 1.4, 1.5 may not give better results than Theorem 1.1 (we have one example where it does not, see Figure 5.3), however, we show that they give new information in many other cases, in particular, when initial data has a negative value of  $V_t(0)$ .

In §5, we consider initial data

$$u_0(x) = \lambda^{3/2} Q(\lambda r) e^{i\gamma r^2},$$

where  $Q$  is the ground state solution to (1.5). The case  $\gamma = 0$  is completely understood by Theorem 1.1. In fact,  $\lambda^{3/2} Q(\lambda r)$  corresponds to the parabolic-like boundary curve in Figure 1.1 which lies below the  $M[u]E[u] = M[Q]E[Q]$  line for all  $\lambda \neq 1$ , and we have blow-up for  $\lambda > 1$  and scattering for  $\lambda < 1$ . The case  $\gamma \neq 0$  is more interesting; in particular, for negative phase,  $\gamma < 0$ , Theorems 1.4 and 1.5 give new range on parameters  $(\lambda, \gamma)$  for which there will be a blow up, see Figure 5.2. Although for positive phase,  $\gamma > 0$ , there is no new information on blow up other than provided by Theorem 1.1, we show the numerical results for the blow up threshold in Figure 5.3, in particular, there is no blow up for  $\lambda < 1$  is expected.

In §6, we consider Gaussian initial data

$$u_0(x) = p e^{-\alpha r^2/2} e^{i\gamma r^2}.$$

By scaling, it suffices to consider  $\gamma = 0, \pm \frac{1}{2}$ . In the real case  $\gamma = 0$ , the behavior will be a function of  $p/\sqrt{\alpha}$ , and the results are depicted in Figure 6.1. The case  $\gamma = \frac{1}{2}$  appears in Figure 6.2, and the case  $\gamma = -\frac{1}{2}$  appears in Figure 6.3. For this initial data Theorem 1.4 gives the best range for blow up, although Theorem 1.5 gives an improvement over the Theorem 1.1.

In §7, we consider “super-Gaussian” initial data

$$u_0(x) = p e^{-\alpha r^4/2} e^{i\gamma r^2}.$$

By scaling, again it suffices to consider  $\gamma = 0, \pm \frac{1}{2}$ . In the real case  $\gamma = 0$ , the behavior will be a function of  $p/\alpha^{1/4}$ , and is depicted in Figure 7.1. The case  $\gamma = \frac{1}{2}$  is presented in Figure 7.3, and the case  $\gamma = -\frac{1}{2}$  is presented in Figure 7.2. For this initial data Theorem 1.5 gives the best theoretical range for blow up.

In §8, we consider “off-centered Gaussian” initial data

$$u_0(x) = p r^2 e^{-\alpha r^2} e^{i\gamma r^2}.$$

---

<sup>3</sup>Since we work exclusively with radial data, we write our functions as functions of  $r \in (0, +\infty)$ , but keep in mind that we are studying the 3d NLS equation.

By scaling, again it suffices to consider  $\gamma = 0, \pm \frac{1}{2}$ . In the real case  $\gamma = 0$ , the behavior will be a function of  $p/\alpha^{3/4}$ , and the results are presented in Figure 8.1. The case  $\gamma = +\frac{1}{2}$  is given in Figure 8.2 and the case  $\gamma = -\frac{1}{2}$  is given in Figure 8.3. For this initial data Theorem 1.5 gives as well the best theoretical range for blow up.

In §9, we consider “oscillatory Gaussian” initial data

$$u_0(x) = p \cos(\beta r) e^{-r^2} e^{i\gamma r^2}.$$

We restrict our attention to  $\gamma = 0, \pm \frac{1}{2}$ , presented in Figures 9.1, 9.2, and 9.3, respectively. For the oscillatory Gaussian the best theoretical range on blow up threshold is provided by a combination of Theorems 1.4, 1.5: for small oscillations,  $\beta \lesssim 1$ , Theorem 1.4 is stronger, and for fast oscillations,  $\beta \gtrsim 1$ , Theorem 1.5 provides a better range (for exact values see the above Figures).

The numerics described in §5–9 provide evidence to support the following conjectures.

**Conjecture 1.** For each  $\epsilon > 0$ , there exists radial Schwartz initial data  $u_0$  for which  $M[u]E[u] > M[Q]E[Q]$ ,  $\|u_0 - Q\|_{H^1} < \epsilon$ ,  $u(t)$  scatters as  $t \rightarrow -\infty$ , and  $u(t)$  blows-up in finite forward time.

That is, there exist initial data arbitrarily close to D in Figure 1.1 with the property that the backward time evolution results in scattering but the forward time evolution results in finite time blow-up. The numerical evidence of the existence of such solutions is a consequence of the study of initial data of the form  $\lambda^{3/2}Q(\lambda r)e^{i\gamma r^2}$  in §5. Take  $\lambda < 1$  but close to 1. Then we find that there exists a curve  $\gamma_0(\lambda)$  such that  $\lim_{\lambda \nearrow 1} \gamma_0(\lambda) = 0$  with the following property: If  $|\gamma| > \gamma_0(\lambda)$ , then  $M[u]E[u] > M[Q]E[Q]$ , and  $u_0$  evolves to a solution  $u(t)$  blowing up in finite positive time if  $\gamma < -\gamma_0(\lambda)$  but  $u_0$  evolves to a scattering solution in positive time if  $\gamma > \gamma_0(\lambda)$  (see Figures 5.2 and 5.3). By the time reversal property

$$u(t) \text{ solves NLS} \implies \bar{u}(-t) \text{ solves NLS}$$

we conclude that if  $\gamma < -\gamma_0(\lambda)$ ,  $u(t)$  scatters *backward* in time. We can take  $\lambda$  as close to 1 and  $\gamma$  as close to 0 as we please (while maintaining  $\gamma < -\gamma_0(\lambda)$ ), establishing the claimed conjecture (as a result of observed numerical behavior).

Before proceeding, let us remark on some consequences assuming this conjecture is valid. We see from Figure 1.1 that the smallest admissible value of  $\eta(0)^2$  that could lead to a finite-time blow-up solution is  $\frac{1}{3} +$  (Corner B).

**1st Corollary of Conjecture 1.** For each  $\epsilon > 0$ , there exist initial data  $u_0$  with  $M[u]E[u] > M[Q]E[Q]$  and  $\eta^2(0) < \frac{1}{3} + \epsilon$  for which the evolution  $u(t)$  blows-up in finite time. For each  $N \gg 1$ , there exists initial data  $u_0$  with  $M[u]E[u] > M[Q]E[Q]$  and  $\eta^2(0) \geq N$  leading to a scattering solution  $u(t)$ .

More loosely stated, there exist initial data as close to point B in Figure 1.1 leading to finite-time blow-up solutions, and there exist initial data as far to the right in

the direction of E in Figure 1.1 leading to scattering solutions. This establishes the irrelevance of the size of  $\eta(0)$  in predicting blow-up or scattering in the case  $M[u]E[u] > M[Q]E[Q]$ .

This follows from Conjecture 1 as follows. Taking  $u(t)$  to be a solution of the type described in Conjecture 1, note that  $\lim_{t \searrow -\infty} \eta^2(t) = \frac{1}{3}$ . Hence, for some large negative time  $-T$ , we have  $\frac{1}{3} < \eta^2(-T) < \frac{1}{3} + \epsilon$ . Resetting, by time translation, to make time  $-T$  into time 0 gives the first type of solution described here. On the other hand, if  $T^*$  denotes the blow-up time of  $u(t)$ , then  $\lim_{t \nearrow T^*} \eta^2(t) = +\infty$ . Therefore, there exists a time  $T' < T^*$  but close to  $T^*$  such that  $\eta^2(T') > N$ . Applying the time reversal symmetry and time translation gives the second type of solution described here.

**2nd Corollary of Conjecture 1.** For each  $\epsilon > 0$ , there exists initial data  $u_0$  with  $\|u_0\|_{L^3} < \epsilon$  for which  $u(t)$  blows-up in finite time. For each  $N \gg 1$ , there exists initial data  $u_0$  for which  $\|u_0\|_{L^3} \geq N$  and for which  $u(t)$  scatters.

Stated more loosely, the quantity  $\|u_0\|_{L^3}$  is irrelevant to predicting blow-up or scattering. Thus, the critical Lebesgue norm gives no prediction of dynamical behavior in the 3d case; note the contrast with the 1d case discussed above, where the critical Lebesgue norm  $L^1$  determines the threshold for soliton formation.

This follows from Conjecture 1 by the same type of reasoning used to justify the first corollary, since if  $u(t)$  scatters in negative time we have  $\lim_{t \searrow -\infty} \|u(t)\|_{L^3} = 0$  and if  $u(t)$  blows-up in finite forward time  $T^*$ , we have  $\lim_{t \nearrow T^*} \|u(t)\|_{L^3} = +\infty$ . This latter fact was proved by Merle-Raphaël [24].

What about the  $\dot{H}^{1/2}$  norm? The “small data scattering theory” (essentially a consequence of the Strichartz estimates – see [18] for exposition) states that there exists  $\delta > 0$  such that if  $\|u_0\|_{\dot{H}^{1/2}} < \delta$ , then  $u(t)$  scatters in both time directions. It is then natural to ask whether  $\delta$  in the above statement can be improved to  $\|Q\|_{\dot{H}^{1/2}}$ .

**Theorem 1.8.** *There exist radial initial data  $u_0$  for which  $\|u_0\|_{\dot{H}^{1/2}} < \|Q\|_{\dot{H}^{1/2}}$  and  $u(t)$  blows-up in finite forward time.*

This follows from Theorems 1.4 and 1.5 by considering certain Gaussian initial data with negative phase (see Figure 6.3). It needs to be remarked, however, that this theorem relies on one piece of numerical information – that value  $\|Q\|_{\dot{H}^{1/2}}^2 = 27.72665$ . It is an analytical result in the sense that one need not numerically solve the NLS equation.

This analytical result is further supported numerically for a variety of *nonreal* initial data with the inclusion of *negative* quadratic phase:  $u_0(x) = \phi(x)e^{i\gamma|x|^2}$  with  $\phi$  radial and real-valued and  $\gamma < 0$ . We note, however, that we did not observe any *real-valued* initial data  $u_0$  with  $\|u_0\|_{\dot{H}^{1/2}} < \|Q\|_{\dot{H}^{1/2}}$  evolving toward finite-time blow-up solutions. Hence, we pose the following conjecture:

**Conjecture 3.** If the initial data  $u_0$  is real-valued and  $\|u_0\|_{\dot{H}^{1/2}} < \|Q\|_{\dot{H}^{1/2}}$ , then  $u(t)$  scatters as  $t \rightarrow -\infty$  and  $t \rightarrow +\infty$ .

Assuming Conjecture 3 holds, we elaborate further in Conjecture 4 below. When working with a one-parameter family of profiles, the  $\dot{H}^{1/2}$  norm can apparently predict both scattering *and blow-up* if the profiles are monotonic; this is summarized in our next conjecture.

**Conjecture 4.** Consider a real-valued radial initial data profile  $\psi(r)$  that is strictly decreasing as  $r \rightarrow +\infty$ . Let  $\alpha_0 = \|Q\|_{\dot{H}^{1/2}}/\|\psi\|_{\dot{H}^{1/2}}$ . Then the solution with initial data  $u_0(x) = \alpha\psi(x)$  scatters if  $\alpha < \alpha_0$  and blows-up if  $\alpha > \alpha_0$ .

However, if the profile is not monotonic, then the  $\dot{H}^{1/2}$  norm appears to only give a sufficient condition for scattering. This is illustrated in the simulations for oscillatory Gaussian data – see Figure 9.1.

### 1.1. NLS as a model in physics.

1. *Laser propagation in a Kerr medium* [26, 10]. This model is inherently two dimensional (in  $xy$ ) and the time  $t$  in fact represents the  $z$ -direction, and is derived via the *paraxial approximation* for the Helmholtz equation. The nonlinearity arises from the dependence of the index of refraction on the amplitude of the propagating wave. Blow-up in finite time is observed in the laboratory as a sharp focusing of the propagating wave. Ultimately, the non-backscattering assumption, and hence the NLS model, breaks down.

2. *Langmuir turbulence in a weakly magnetized plasma* [33, 26]. A plasma is modeled as interpenetrating fluids of highly excited electrons and positive ions. The Langmuir waves propagate through the electron medium. The principle mathematical model is the Zakharov system [33], which is a nonlinearly coupled Schrödinger and wave system. The Schrödinger function is a slowly varying envelope for the electric potential and the wave function is the deviation of the ion density from its mean value. The NLS equation arises as the subsonic limit of the Zakharov system, which is obtained by sending the wave speed  $\rightarrow +\infty$ . Blow-up in finite time is the central phenomenon of study in [33], since it predicts the formation of a *cavern* of shrinking radius confining fast oscillating electrons whose collisions dissipate energy (at which point the model breaks down). The Zakharov model is inherently 3d, although certain experimental configurations can be modeled with the 1d or 2d equations.

3. *Bose-Einstein condensate (BEC)* [6]. BEC consists of ultracold (a few nK) dilute atomic gases where  $u$  gives the wave function (e.g. the number of atoms in a region  $E$  is  $\int_E |u|^2$ ) and the coefficient of the nonlinear term is related to the *scattering length* by  $g = 8\pi a$ . The scattering length depends upon the interatomic potential and can be either positive or negative. While the model is inherently 3d, the imposition of a strong confining potential in one or two directions can effectively reduce the model to

two or one dimensions, respectively. Experiments showing blow-up are reported for  $^{85}\text{Rb}$  condensates in [7] and for  $^7\text{Li}$  condensates in [14].

In each situation, blow-up is physically observed (although of course the model breaks down at some point prior to the blow-up time).

**1.2. Acknowledgements.** S.R. thanks Pavel Lushnikov for bringing to her attention his 1995 paper on the dynamic collapse criteria. J.H. and S.R. are grateful to Gadi Fibich for discussion and remarks on a preliminary version of this paper. S.R. is partially supported by NSF grant DMS-0808081. J.H. is partially supported by a Sloan fellowship and NSF grant DMS-0901582.

## 2. INEQUALITIES

In this section, we prove the two inequalities (1.14) and (1.15) needed for Theorems 1.4 and 1.5.

**2.1. Inequality (1.14).** Of course (1.14), the uncertainty principle, is standard, although we include a proof for completeness. By integration by parts,

$$\|u\|_{L^2}^2 = \frac{1}{3} \int (\nabla \cdot x) |u|^2 dx = -\frac{2}{3} \operatorname{Re} \int (x \cdot \nabla u) \bar{u} dx.$$

By Cauchy-Schwarz,

$$\frac{9}{4} \|u\|_{L^2}^4 + \left| \operatorname{Im} \int (x \cdot \nabla u) \bar{u} dx \right|^2 = \left| \int (x \cdot \nabla u) \bar{u} dx \right|^2 \leq \|xu\|_{L^2}^2 \|\nabla u\|_{L^2}^2.$$

This provides the sharp constant since the inequality is achieved by only the above application of Cauchy-Schwarz, which is saturated when  $xu = C\nabla u$ , i.e., when  $u$  is a Gaussian.

**2.2. Inequality (1.15).** In this section, we prove the following

**Proposition 2.1.** *The inequality*

$$(2.1) \quad \|u\|_{L^2} \leq C \|xu\|_{L^2}^{\frac{3}{7}} \|u\|_{L^4}^{\frac{4}{7}}$$

holds with sharp constant  $C = \left( \frac{2^{2.75} \cdot \pi^2}{3^{5.5^2}} \right)^{1/14} \approx 1.3983$ . Moreover, all functions for which equality is achieved are of the form  $\beta\phi(\alpha x)$ , where

$$\phi(x) = \begin{cases} (1 - |x|^2)^{1/2} & \text{if } 0 \leq |x| \leq 1 \\ 0 & \text{if } |x| > 1. \end{cases}$$

First we prove there exists *some* constant  $C$  for which (2.1) holds. Given  $u$  such that  $\|xu\|_{L^2} < \infty$  and  $\|u\|_{L^4} < \infty$ , define  $v$  by  $u(x) = \alpha v(\beta x)$  with  $\alpha$  and  $\beta$  chosen so that  $\|xv\|_{L^2} = 1$  and  $\|v\|_{L^4} = 1$ , i.e.,

$$\alpha = \|u\|_{L^4}^{\frac{10}{7}} \|xu\|_{L^2}^{-\frac{3}{7}}, \quad \beta = \|u\|_{L^4}^{\frac{4}{7}} \|xu\|_{L^2}^{-\frac{4}{7}}.$$

By Hölder,

$$\begin{aligned} \|v\|_{L^2}^2 &= \|v\|_{L^2(|x|\leq 1)}^2 + \|v\|_{L^2(|x|\geq 1)}^2 \\ &\leq \left(\frac{4}{3}\pi\right)^{1/2} \|v\|_{L^4(|x|\leq 1)}^2 + \|xv\|_{L^2(|x|\geq 1)}^2 \\ &\leq \left(\frac{4}{3}\pi\right)^{1/2} + 1, \end{aligned}$$

which completes the proof of (2.1) with nonsharp constant  $C = ((\frac{4}{3}\pi)^{1/2} + 1)^{1/2} \approx 1.7455$ .

*Remark 2.2.* We can optimize the above splitting argument by splitting at radius  $r = (\frac{4}{3\pi})^{1/7}$ , which gives the constant  $C \approx 1.7265$ . However, this is still off from the sharp constant  $C \approx 1.3983$  stated in Prop. 2.1. The reason is that the estimates applied after the splitting lead to an optimizing function which is the characteristic function of the ball of radius  $r$ . However, such a function fails to have both  $\|u\|_{L^4} = 1$  and  $\|xu\|_{L^2} = 1$ .

We now proceed to identify the sharp constant  $C$  in (2.1) and the family of optimizing functions. Consider the Lagrangian

$$L(\phi) = \frac{\|x\phi\|_{L^2}^{\frac{3}{2}} \|\phi\|_{L^4}^{\frac{4}{7}}}{\|\phi\|_{L^2}},$$

defined on  $X \stackrel{\text{def}}{=} L^4 \cap L^2(\langle x \rangle^2 dx)$ ,  $x \in \mathbb{R}^3$ .

**Lemma 2.3.**

- (1) *Any minimizer  $\phi$  (without loss of generality taken real-valued and nonnegative) of  $L$  in  $X$  is radial and (nonstrictly) decreasing.*
- (2) *There exists a minimizer  $\phi$  of  $L$  in  $X$ .*

*Remark 2.4.* Lemma 2.3 does not say that a minimizer  $\phi$  needs to be continuous, *strictly* decreasing, or compactly supported. We only discover this to be the case in the next step of the proof.

*Proof.* We first argue that any  $\phi \in X$  can be replaced by a radial, monotonically (perhaps not strictly) decreasing function  $\tilde{\phi}$  such that

$$(2.2) \quad \|\tilde{\phi}\|_{L^2} = \|\phi\|_{L^2}, \quad \|\tilde{\phi}\|_{L^4} = \|\phi\|_{L^4},$$

$$(2.3) \quad \|x\tilde{\phi}\|_{L^2} \leq \|x\phi\|_{L^2}.$$

Moreover, we have equality in (2.3) if and only if  $\tilde{\phi} = \phi$ , which occurs if and only if  $\phi$  itself is radial, nonnegative, and (nonstrictly) decreasing. Given  $\phi$ , let

$$E_{\phi,\lambda} = \{x \mid |\phi(x)| > \lambda\}, \quad \mu_{\phi}(\lambda) = |E_{\phi,\lambda}|.$$

Recall that (by Fubini's theorem)

$$(2.4) \quad \|\phi\|_{L^p}^p = \int_{\lambda=0}^{+\infty} p\lambda^{p-1}\mu_\phi(\lambda) d\lambda.$$

Note that  $\mu_\phi : [0, +\infty) \rightarrow [0, +\infty)$  is a nonstrictly decreasing right-continuous function. Thus,

$$\lim_{\sigma \searrow \lambda} \mu_\phi(\lambda) = \mu_\phi(\lambda) \leq \lim_{\sigma \nearrow \lambda} \mu_\phi(\sigma)$$

with equality if and only if  $\lambda$  is a point of continuity. Since  $\mu_\phi$  is *nonstrictly* decreasing, there may be intervals on which  $\mu_\phi$  is constant that we need to exclude in order to achieve invertibility. Let  $F_\phi$  be the set of all  $r$  such that  $\mu_\phi^{-1}(\{\frac{4}{3}\pi r^3\})$  has positive measure (is a nontrivial interval). Note that  $F_\phi$  is an at most countable set (because  $\mu_\phi$  is nonstrictly decreasing). For all  $r \notin F$ , define the radial function  $\tilde{\phi}$  on  $\mathbb{R}^3$  by

$$\tilde{\phi}(r) = \lambda \quad \text{iff} \quad \mu_\phi(\lambda) \leq \frac{4}{3}\pi r^3 \leq \lim_{\sigma \nearrow \lambda} \mu_\phi(\sigma).$$

Note that  $\mu_\phi = \mu_{\tilde{\phi}}$ , i.e.,  $\phi$  and  $\tilde{\phi}$  are equidistributed. By (2.4), we have (2.2). Let

$$h_\phi(\lambda) \stackrel{\text{def}}{=} \int_{E_{\phi,\lambda}} |x|^2 dx.$$

By Fubini,

$$\|x\phi\|_{L^2}^2 = 2 \int_{\lambda=0}^{+\infty} \lambda h_\phi(\lambda) d\lambda,$$

and similarly for  $\tilde{\phi}$ . For each  $\lambda$ , we have  $h_{\tilde{\phi}}(\lambda) \leq h_\phi(\lambda)$ , since  $|E_{\tilde{\phi},\lambda}| = |E_{\phi,\lambda}|$  but  $E_{\tilde{\phi},\lambda}$  is uniformly positioned around the origin (it is a ball centered at 0). Consequently, (2.3) holds.

We note that the above argument establishes (1) in the theorem statement. To prove (2), we need to construct a minimizer by a limiting argument. Let

$$m \stackrel{\text{def}}{=} \inf_{\phi \in X} L(\phi).$$

Let  $\phi_n$  be a minimizing sequence. By approximation and the above argument, we can assume that each  $\phi_n$  is continuous, compactly supported, radial, nonnegative, and nonstrictly decreasing. By scaling ( $\phi_n(x) \mapsto \alpha \phi_n(\beta x)$ ) we can also assume that  $\|\phi_n\|_{L^2} = 1$  and  $\|\phi_n\|_{L^4} = 1$ . We have  $\|x\phi_n\|_{L^2} \leq \|x\phi_1\|_{L^2} \stackrel{\text{def}}{=} A$ . Since for each  $n$ , the function  $\phi_n(r)$  is decreasing in  $r$ , we have

$$A^2 \geq \|x\phi_n\|_{L^2(|x| \leq r)}^2 = \int_{\rho=0}^r 4\pi \rho^4 |\phi_n(\rho)|^2 d\rho \geq |\phi_n(r)|^2 \frac{4\pi r^5}{5},$$

i.e.,  $|\phi_n(r)| \lesssim r^{-5/2}$ . Similarly, working with the fact that  $\|\phi_n\|_{L^4} = 1$ , we have that for all  $n$ ,  $|\phi_n(r)| \lesssim r^{-3/4}$ . Combining these two pointwise bounds, we have

$$(2.5) \quad |\phi_n(r)| \lesssim r^{-3/4}(1+r)^{-7/4},$$



with implicit constant uniform in  $n$ . Thus, for each  $r > 0$ , the sequence of nonnegative numbers  $\{\phi_n(r)\}_{n=1}^{+\infty}$  is bounded and hence has a convergent subsequence. By a diagonal argument, we can pass to a subsequence of  $\phi_n$  (still labeled  $\phi_n$ ) such that for each  $r \in \mathbb{Q}$ , we have that  $\lim_{n \rightarrow +\infty} \phi_n(r)$  exists. Denote by  $\phi(r)$  the limiting function (for now only defined on  $\mathbb{Q}$ ).

We claim that  $\phi_n$  converges pointwise a.e.<sup>4</sup> Pass to a subsequence (still labeled  $\phi_n$ ) such that for each  $r \in 2^{-n}\mathbb{N}$ ,  $\frac{1}{n} < r < n$ , we have  $|\phi_n(r) - \phi(r)| \leq 2^{-2n}$ . Let

$$\phi_n^-(r) \stackrel{\text{def}}{=} \phi((j+1)2^{-n}) - 2^{-2n} \text{ for } j2^{-n} < r < (j+1)2^{-n},$$

$$\phi_n^+(r) \stackrel{\text{def}}{=} \phi(j2^{-n}) + 2^{-2n} \text{ for } j2^{-n} < r < (j+1)2^{-n}.$$

Then for each  $n$ ,

$$\phi_n^-(r) \leq \phi_n(r) \leq \phi_n^+(r)$$

and  $\phi_n^-$  is a pointwise nonstrictly increasing sequence of functions, while  $\phi_n^+$  is pointwise nonstrictly decreasing sequence of functions. Since  $\phi$  is a decreasing function,

$$\sum_{j=2^{n-\log n}}^{n2^n} (\phi(j2^{-n}) - \phi((j+1)2^{-n})) = \phi(1/n) - \phi(n) \lesssim n^{3/4}$$

by (2.5). Thus, there can exist at most  $n^{3/4}2^{n/2}$  indices  $j$  for which the jump  $\phi(j2^{-n}) - \phi((j+1)2^{-n}) \geq 2^{-n/2}$ . Thus, the measure of the set  $H_n$  on which  $\phi_n^+(r) - \phi_n^-(r) > 2^{-n/2}$  satisfies  $|H_n| \leq n^{3/4}2^{n/2}2^{-n} \leq n^{3/4}2^{-n/2}$ . This establishes that for a.e.  $r$ ,  $\phi(r) \stackrel{\text{def}}{=} \lim_{n \rightarrow +\infty} \phi_n(r)$  exists and moreover for a.e.  $r$ ,

$$\lim_{n \rightarrow +\infty} \phi_n^-(r) = \phi(r) = \lim_{n \rightarrow +\infty} \phi_n^+(r).$$

We know that  $\|x\phi_n^-(x)\|_{L^2(\frac{1}{n} \leq r \leq n)} \leq \|x\phi_n\|_{L^2}$ . By monotone convergence, we conclude that

$$\|x\phi(x)\|_{L^2} = \lim_{n \rightarrow +\infty} \|x\phi_n^-(x)\|_{L^2(\frac{1}{n} \leq r \leq n)} \leq \lim_{n \rightarrow +\infty} \|x\phi_n\|_{L^2} = m^{7/3}.$$

Similarly, we have that

$$\|\phi\|_{L^4} \leq 1.$$

By (2.5) and dominated convergence, we conclude that

$$\|\phi\|_{L^2} = \lim_{n \rightarrow +\infty} \|\phi_n\|_{L^2} = 1.$$

Hence,  $L(\phi) \leq m$  (and thus,  $L(\phi) = m$ ), i.e.,  $\phi \in X$  is a minimizer.  $\square$

<sup>4</sup>Note that  $\phi_n$  is a sequence of functions each of which is decreasing, but it is not the case that for each  $r$ , the sequence of numbers  $\phi_n(r)$  is decreasing. Thus, proving that  $\phi_n(r)$  converges for a.e.  $r > 0$  is a little more subtle.

**Lemma 2.5.** *If  $\phi \in X$ ,  $\phi$  is radial, nonnegative, (nonstrictly) decreasing, and solves  $L'(\phi) = 0$ , then there exist  $\alpha > 0$ ,  $\beta > 0$ ,  $0 < \gamma \leq 1$  such that  $\phi(x) = \beta\phi_\gamma(\alpha x)$ , where*

$$(2.6) \quad \phi_\gamma(x) = \begin{cases} (1 - |x|^2)^{1/2} & \text{for } |x| \leq \gamma \\ 0 & \text{for } |x| > \gamma. \end{cases}$$

*Proof.* Writing

$$\log L(\phi) = \frac{3}{14} \log \|x\phi\|_{L^2}^2 + \frac{1}{7} \log \|\phi\|_{L^4}^4 - \frac{1}{2} \|\phi\|_{L^2}^2,$$

it follows that for each  $\psi$ ,

$$0 = L'(\phi)(\psi) = L(\phi) \int \left( \frac{3|x|^2\phi}{7\|x\phi\|_{L^2}^2} + \frac{4}{7} \frac{\phi^3}{\|\phi\|_{L^4}^4} - \frac{\phi}{\|\phi\|_{L^2}^2} \right) \psi \, dx.$$

From this, we see that it must have the form

$$(2.7) \quad \phi(x) = \beta(1 - \alpha^2|x|^2)^{1/2}.$$

on the set where  $\phi(x) \neq 0$ . Since  $\phi(x)$  is decreasing, we see that (2.7) holds on  $0 \leq |x| \leq \gamma/\alpha$  for some  $0 < \gamma \leq 1$ , and  $\phi(x) = 0$  for  $|x| > \gamma/\alpha$ .  $\square$

Let  $\phi \in X$  be a minimizer for  $L(\phi)$  as in Lemma 2.3. We know that  $\phi$  must solve the Euler-Lagrange equation  $L'(\phi) = 0$ , and hence, Lemma 2.5 is applicable, which establishes that  $\phi(x) = \beta\phi_\gamma(\alpha x)$  for some  $\gamma$ ,  $0 < \gamma \leq 1$ , where  $\phi_\gamma$  is given by (2.6). We now plug  $\phi(x) = \beta\phi_\gamma(\alpha x)$  into  $L(\phi)$  to determine  $\gamma$ . However, since  $L(\phi)$  is invariant under the rescaling  $\phi(x) \mapsto \beta\phi(\alpha x)$ , it suffices to take  $\alpha = 1$ ,  $\beta = 1$  in this computation. We compute

$$\begin{aligned} \|\phi\|_{L^4}^4 &= 4\pi \left( \frac{1}{3} - \frac{2\gamma^2}{5} + \frac{\gamma^4}{7} \right), \quad \|x\phi\|_{L^2}^2 = 4\pi \left( \frac{1}{5} - \frac{\gamma^2}{7} \right), \\ \|\phi\|_{L^2}^2 &= 4\pi \left( \frac{1}{3} - \frac{\gamma^2}{5} \right), \end{aligned}$$

and we thus obtain

$$L(\phi)^{14} = \frac{\left( \frac{1}{3} - \frac{2\gamma^2}{5} + \frac{\gamma^4}{7} \right)^2 \left( \frac{1}{5} - \frac{\gamma^2}{7} \right)^3}{(4\pi)^2 \left( \frac{1}{3} - \frac{\gamma^2}{5} \right)^7}.$$

A tedious computation shows that  $\gamma = 1$  produces the minimum value, which is

$$L(\phi)^{14} = \frac{3^5 \cdot 5^2}{2^2 \cdot 7^5 \cdot \pi^2}.$$

This completes the proof of Prop. 2.1.

### 3. NEW BLOW-UP CRITERIA

In this section, we prove Theorem 1.4, 1.5, and 1.6.

**3.1. The blow up criteria of Lushnikov.** Here, we prove Theorem 1.4. It is an adaptation and further investigation of the dynamic criterion for collapse proposed by P. Lushnikov in [20].

We write  $M = M[u]$ ,  $E = E[u]$ , etc., for simplicity. By the virial identity (1.4) in the case  $n = 3$ ,

$$(3.1) \quad V_{tt}(t) = 24E - 4\|\nabla u(t)\|_2^2,$$

and the bound (1.14), we obtain

$$(3.2) \quad V_{tt}(t) \leq 24E - 9 \frac{M^2}{V(t)} - \frac{1}{4} \frac{|V_t(t)|^2}{V(t)}.$$

Now, rewritting the equation (3.2) to remove the last term with  $V_t^2$  by making a substitution  $V = B^{4/5}$ , we get

$$(3.3) \quad B_{tt} \leq 30EB^{1/5} - \frac{45}{4} \frac{M^2}{B^{3/5}}.$$

This differential inequality is an equality with some unknown non-negative quantity:

$$(3.4) \quad B_{tt} \leq 30EB^{1/5} - \frac{45}{4} \frac{M^2}{B^{3/5}} - g^2(t).$$

The equation (3.4) is the key in further analysis and in [20] is called the *dynamic criterion for collapse*. To analyze this equation, Lushnikov proposes to use a mechanical analogy of a particle moving in a field with a potential barrier. Let  $B = B(t)$  be the position of a particle (with mass 1) in motion under 2 forces:

$$B_{tt} = F_1 + F_2,$$

where

$$(3.5) \quad F_1 = -\frac{\partial U}{\partial B} \quad \text{with the potential} \quad U = -25EB^{6/5} + \frac{225}{8}M^2B^{2/5},$$

and

$$F_2 = -g^2(t), \quad \text{some unknown force which pulls the particle towards zero.}$$

If this particle reaches the origin in a finite period of time,

$$B(t^*) = 0 \quad \text{for some} \quad 0 < t^* < \infty,$$

then collapse necessarily occurs at some time  $t \leq t^*$ .

Several observations are due:

- If the particle reaches the origin without the force  $-g^2(t)$  (i.e., if  $B(t_1) = 0$  some  $0 < t_1 < \infty$ ), then it also reaches the origin in the situation when this force is applied ( $B(t_2) = 0$  for some  $0 < t_2 \leq t_1$ ).
- If  $E < 0$ , then  $B$  always reaches the origin and collapse always happens. Thus, the more interesting case to consider is  $E > 0$ .

- The potential  $U$  in (3.5) as a function of  $B$  is a convex function (at least for positive  $B$ ) with the maximum attained at

$$B_{max} = \left( \frac{3}{8} \frac{M^2}{E} \right)^{5/4} \quad \text{and} \quad U_{max} = U(B_{max}) = \frac{75\sqrt{3}}{8\sqrt{2}} \frac{M^3}{E^{1/2}}.$$

Define the “energy” of the particle  $B$ :

$$(3.6) \quad \mathcal{E}(t) = \frac{B_t(t)^2}{2} + U(B(t)),$$

which is time dependent due to the term  $g(t)^2$  in (3.4). However, recall that for our purposes it is sufficient for  $B$  to reach the origin if  $B$  satisfies only  $B_{tt} = F_1$  (see the first observation above), for which the energy  $\mathcal{E}(t)$  is conserved.

The analysis is facilitated if we introduce the rescaled variables  $\tilde{B}(s)$  and  $\tilde{\mathcal{E}}(s)$ , where

$$B(t) = B_{max} \tilde{B} \left( \frac{16Et}{\sqrt{3}M} \right), \quad \mathcal{E}(t) = U_{max} \tilde{\mathcal{E}} \left( \frac{16Et}{\sqrt{3}M} \right), \quad s = \frac{16E}{\sqrt{3}M} t.$$

We obtain

$$\tilde{B}_{ss} \leq \frac{15}{16} \left( \tilde{B}^{1/5} - \frac{1}{\tilde{B}^{3/5}} \right).$$

If we set

$$\tilde{U}(\tilde{B}) \stackrel{\text{def}}{=} -\frac{1}{2}\tilde{B}^{6/5} + \frac{3}{2}\tilde{B}^{2/5},$$

then (3.6) converts to

$$\tilde{\mathcal{E}}(s) = \frac{8}{25}\tilde{B}_s(s)^2 + \tilde{U}(\tilde{B}(s)).$$

The potential  $\tilde{U}(\tilde{B})$  is depicted in Figure 3.1. From this energy diagram, we can identify two sufficient conditions under which  $\tilde{B}(s)$  necessarily reaches 0 in finite time:

- (1)  $\tilde{\mathcal{E}}(0) < 1$  and  $\tilde{B}(0) < 1$ . In this case, the value of  $\tilde{B}_s(0)$  does not matter.
- (2)  $\tilde{\mathcal{E}}(0) \geq 1$  and  $\tilde{B}_s(0) < 0$ . In this case, the value of  $\tilde{B}(0)$  does not matter.

Now define  $\tilde{V} = \tilde{B}^{4/5}$ . Then

$$\tilde{\mathcal{E}} = \frac{1}{2}\tilde{V}^{1/2}(\tilde{V}_s^2 - \tilde{V} + 3).$$

Introduce the function

$$(3.7) \quad f(\tilde{V}) = \sqrt{\frac{2}{\tilde{V}^{1/2}} + \tilde{V} - 3}.$$

We obtain

$$\begin{aligned} \tilde{\mathcal{E}} < 1 &\Leftrightarrow |\tilde{V}_s| < f(\tilde{V}) \\ \tilde{\mathcal{E}} \geq 1 &\Leftrightarrow |\tilde{V}_s| \geq f(\tilde{V}) \end{aligned}$$

Thus, we see that sufficient condition (1) for blow-up above equates to

$$\tilde{V}(0) < 1 \quad \text{and} \quad -f(\tilde{V}(0)) < \tilde{V}_s(0) < f(\tilde{V}(0))$$

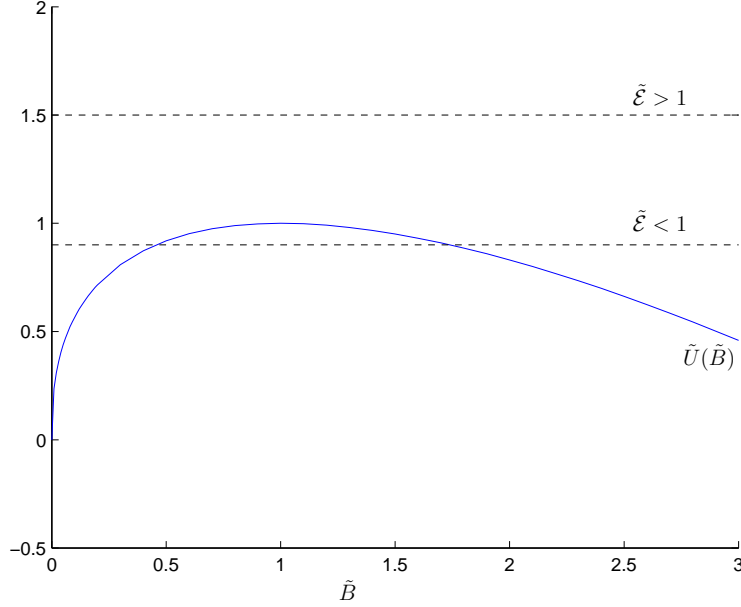


FIGURE 3.1. A depiction of the rescaled potential  $\tilde{U}$  as a function of position  $\tilde{B}$ . In the case  $\tilde{\mathcal{E}} < 1$ , a particle starting at  $\tilde{B}(0) < 1$  is trapped in that region and moves to the origin in finite time. In the case  $\tilde{\mathcal{E}} > 1$ , a particle with initial velocity  $\tilde{B}_s(0) < 1$  has sufficient energy to reach the origin in finite time, regardless of its initial position  $\tilde{B}(0)$ .

and condition (2) equates to

$$\tilde{V}_s(0) \geq -f(\tilde{V}(0)).$$

This is graphed in Figure 3.2.

The two separate conditions can be merged into one: the solution blows-up in finite time if

$$\tilde{V}_s(0) < \begin{cases} +f(\tilde{V}(0)) & \text{if } \tilde{V}(0) \leq 1 \\ -f(\tilde{V}(0)) & \text{if } \tilde{V}(0) \geq 1 \end{cases}$$

Tracing back through the rescalings, we see that the relationship with  $V(t)$  and  $\tilde{V}(s)$  is

$$V(t) = B_{\max}^{4/5} \tilde{V}\left(\frac{16Et}{\sqrt{3}M}\right),$$

which completes the proof of Theorem 1.4.

**3.2. An adaptation.** In this subsection, we prove Theorem 1.5. The analysis here is similar to that used above in the proof of Theorem 1.4, except that we use (1.15) in place of (1.14).

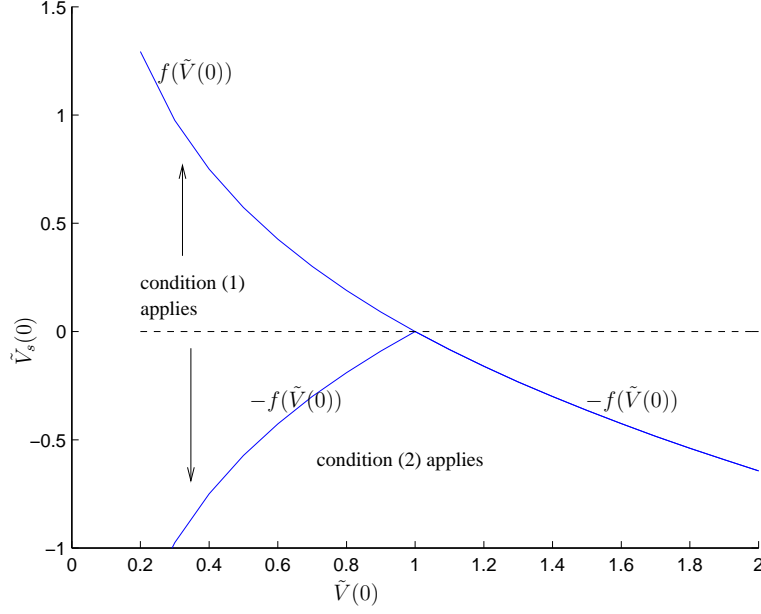


FIGURE 3.2. The two sufficient conditions (1) and (2) described in the text §3.1 for blow-up in finite time convert to the conditions on  $\tilde{V}_s(0)$  in terms of  $V(0)$  depicted in this figure.

By energy conservation, we can rewrite the virial identity as

$$(3.8) \quad \begin{aligned} V_{tt} &= 24E - 4\|\nabla u\|_{L^2}^2 \\ &= 16E - 2\|u\|_{L^4}^4. \end{aligned}$$

By (1.15),

$$(3.9) \quad V_{tt} \leq 16E - \frac{2M^{\frac{7}{2}}}{C^7 V^{\frac{3}{2}}}.$$

Let

$$U(V) = -16EV - \frac{4M^{\frac{7}{2}}}{C^7 V^{\frac{1}{2}}}.$$

Then, as in the previous subsection, we can interpret  $V(t)$  as giving the position of a particle subject to a conservative force  $-\partial_V U(V)$  plus another unknown nonconservative force pulling  $V(t)$  toward 0. The corresponding mechanical energy is

$$(3.10) \quad \mathcal{E}(t) = \frac{1}{2}V_t^2 + U(V).$$

Restricting to the case  $E > 0$ , we compute that  $U(V)$  achieves its maximum  $U_{max}$  at  $V_{max}$ , with

$$V_{max} = \frac{M^{\frac{7}{3}}}{4C^{\frac{14}{3}}E^{\frac{2}{3}}}, \quad U_{max} = \frac{-12M^{\frac{7}{3}}E^{\frac{1}{3}}}{C^{\frac{14}{3}}}.$$

To facilitate the rest of the analysis, we introduce a rescaling. Define  $\tilde{V}(s)$  and  $\tilde{\mathcal{E}}(s)$  by the relations

$$V(t) = V_{max} \tilde{V}(\alpha t), \quad \mathcal{E}(t) = |U_{max}| \tilde{\mathcal{E}}(\alpha t), \quad \alpha = \frac{8\sqrt{3}C^{\frac{7}{3}}E^{\frac{5}{6}}}{M^{\frac{7}{6}}}, \quad s = \alpha t.$$

Then

$$\tilde{V}_{ss}(s) \leq \frac{1}{3} \left(1 - \tilde{V}^{-3/2}(s)\right)$$

and (3.10) equates to

$$\tilde{\mathcal{E}} = \frac{1}{2} \tilde{V}_s^2 - \frac{1}{3} \tilde{V} - \frac{2}{3} \tilde{V}^{-\frac{1}{2}}.$$

From this, we identify two sufficient conditions for blow-up in finite time.

$$(1) \quad \tilde{\mathcal{E}}(0) < -1 \text{ and } \tilde{V}(0) < 1.$$

$$(2) \quad \tilde{\mathcal{E}}(0) \geq -1 \text{ and } \tilde{V}_s(0) < 0.$$

Let  $f(\tilde{V})$  be defined by (3.7). Then

$$\tilde{\mathcal{E}} < -1 \quad \Leftrightarrow \quad |\tilde{V}_s| < \sqrt{\frac{2}{3}} f(\tilde{V}),$$

$$\tilde{\mathcal{E}} \geq -1 \quad \Leftrightarrow \quad |\tilde{V}_s| \geq \sqrt{\frac{2}{3}} f(\tilde{V}).$$

Thus, condition (1) above holds if and only if

$$\tilde{V}(0) < 1 \quad \text{and} \quad -\sqrt{\frac{2}{3}} f(\tilde{V}(0)) < \tilde{V}_s(0) < \sqrt{\frac{2}{3}} f(\tilde{V}(0))$$

and condition (2) holds if and only if

$$\tilde{V}_s(0) \leq -\sqrt{\frac{2}{3}} f(\tilde{V}(0)).$$

Clearly, we can merge the two conditions into one: we have blow-up in finite time provided

$$\tilde{V}_s(0) < \sqrt{\frac{2}{3}} \begin{cases} f(\tilde{V}(0)) & \text{if } \tilde{V}(0) \leq 1, \\ -f(\tilde{V}(0)) & \text{if } \tilde{V}(0) \geq 1. \end{cases}$$

Substituting back  $V(t)$ , we obtain with  $\omega = 4C^{14/3}E^{2/3}M^{-7/3}V(0)$

$$\frac{V_t(0)}{M} \frac{C^{7/3}}{2\sqrt{3}(ME)^{1/6}} < \sqrt{\frac{2}{3}} \begin{cases} f(\omega) & \text{if } \omega \leq 1 \\ -f(\omega) & \text{if } \omega \geq 1, \end{cases}$$

which gives (1.16) and finishes the proof of Theorem 1.5.

**3.3. Infinite variance radial case.** Let  $\psi(x)$  be a smooth, radial, (nonstrictly) increasing function such that

$$\psi(x) = \begin{cases} |x|^2 & \text{if } |x| \leq 1 \\ 2 & \text{if } |x| \geq 2 \end{cases}$$

Let  $V_R$  denote the *localized variance*, defined in (1.17). Note that  $V_R/M \leq 2R^2$ . We need to replace inequality (1.15) with a localized version.

**Lemma 3.1.** *Suppose that  $V_R/M \leq \frac{1}{2}R^2$ . Then*

$$\|u\|_{L^2} \leq \left( \frac{2^{\frac{11}{2}} \pi}{3} \right)^{\frac{1}{7}} \|u\|_{L_x^4}^{\frac{4}{7}} V_R^{\frac{3}{14}}.$$

*Proof.* Let  $r^2 = 2V_R/M$  so that, by assumption, we have  $r^2 \leq R^2$ . Then

$$\begin{aligned} M &= \|u\|_{L^2}^2 = \|u\|_{L^2(|x| \leq r)}^2 + \|u\|_{L^2(|x| \geq r)}^2 \\ &\leq \left( \frac{4}{3} \pi r^3 \right)^{1/2} \|u\|_{L^4(|x| \leq r)}^2 + \frac{1}{r^2} V_R \\ &\leq \left( \frac{4}{3} \pi r^3 \right)^{1/2} \|u\|_{L^4(|x| \leq r)}^2 + \frac{M}{2}, \end{aligned}$$

where we note that the inequality  $\|u\|_{L^2(|x| \geq r)}^2 \leq \frac{1}{r^2} V_R$  requires  $r^2 \leq R^2$ . The result follows.  $\square$

We have not made any effort to identify the sharp constant here.

Now we turn to the proof of Theorem 1.6. By direct calculation, we have the local virial identity:

$$V_R''(t) = 4 \int \partial_j \partial_k \psi \left( \frac{x}{R} \right) \partial_j u \partial_k \bar{u} - \int \Delta \psi \left( \frac{x}{R} \right) |u|^4 - \frac{1}{R^2} \int \Delta^2 \psi \left( \frac{x}{R} \right) |u|^2.$$

Note that

$$V_R''(t) = 16E - 2\|u(t)\|_{L_x^4}^4 + A_R(u(t)),$$

where

$$A_R(u(t)) \lesssim \frac{1}{R^2} \|u\|_{L^2(|x| \geq R)}^2 + \|u\|_{L^4(|x| \geq R)}^4.$$

Recall that we are assuming  $ME > 1$ . Then, if we take

$$(3.11) \quad R^2 \gtrsim \delta^{-1} M^2,$$

we have

$$\frac{1}{R^2} \|u\|_{L^2(|x| \geq R)}^2 \leq \frac{\delta}{M} \leq \delta E.$$



Also, by the radial Gagliardo-Nirenberg inequality,

$$\begin{aligned}
\|u\|_{L^4(|x|\geq R)}^4 &\leq \frac{1}{2\pi R^2} \|u\|_{L_x^2}^3 \|\nabla u\|_{L_x^2} \\
&\leq \frac{\delta}{2\pi} \frac{\|\nabla u\|_{L^2}^2}{\|u\|_{L^2}} \\
&\leq \frac{\delta}{2\pi} \|\nabla u\|_{L^2} E^{1/2}, \quad \text{since } ME > 1 \\
&\leq \frac{1}{4} \delta E + \frac{1}{4} \delta \|\nabla u\|_{L^2}^2 \\
&\leq \delta E + \delta \|u\|_{L^4}^4.
\end{aligned}$$

Hence,

$$V_R''(t) \leq (16 + 2\delta)E - (2 - \delta)\|u\|_{L^4}^4.$$

Now we follow the analysis in §3.2 but we must ensure that for all  $t$ ,

$$(3.12) \quad \frac{V_R(t)}{M} \leq \frac{1}{2}R^2.$$

In fact, (3.12) will act as a bootstrap assumption that will be reinforced by the mechanical analysis. Suppose that (3.12) holds, and thus, Lemma 3.1 is applicable. Then

$$V_R'' \leq (16 + 2\delta)E - (2 - \delta)M^{7/2}(C_\infty)^{-7}V_R^{-3/2}, \quad \text{where } C_\infty = \left(\frac{2^{11/2}\pi}{3}\right)^{1/7}.$$

Let

$$U(V_R) = -(16 + 2\delta)EV_R - 2(2 - \delta)(C_\infty)^{-7}M^{7/2}V_R^{-1/2},$$

and define the mechanical energy as

$$\mathcal{E} = \frac{1}{2}(V_R')^2 + U(V_R).$$

The maximum of  $U(V_R)$  occurs at  $V_{max}$  and is equal to  $U_{max}$ , where

$$V_{max} = \frac{(1 - \delta)^{\frac{2}{3}}M^{\frac{7}{3}}}{(8 + \delta)^{\frac{2}{3}}(C_\infty)^{\frac{14}{3}}E^{\frac{2}{3}}}, \quad U_{max} = -\frac{6(8 + \delta)^{\frac{1}{3}}(1 - \delta)^{\frac{2}{3}}M^{\frac{7}{3}}E^{\frac{1}{3}}}{(C_\infty)^{\frac{14}{3}}}.$$

We introduce a rescaling: Define  $\tilde{V}(s)$  and  $\tilde{\mathcal{E}}(s)$  by the relations

$$V(t) = V_{max}\tilde{V}(\alpha t), \quad \mathcal{E}(t) = |U_{max}|\tilde{\mathcal{E}}(\alpha t), \quad \alpha = \frac{6^{\frac{1}{2}}(8 + \delta)^{\frac{5}{6}}(C_\infty)^{\frac{7}{3}}E^{\frac{5}{6}}}{(1 - \delta)^{\frac{1}{3}}M^{\frac{7}{6}}}.$$

Then

$$\tilde{\mathcal{E}} = \frac{1}{2}\tilde{V}_s^2 + \tilde{U}(\tilde{V}), \quad \tilde{U}(\tilde{V}) \stackrel{\text{def}}{=} -\frac{1}{3}\tilde{V} - \frac{2}{3}\tilde{V}^{-\frac{1}{2}}.$$

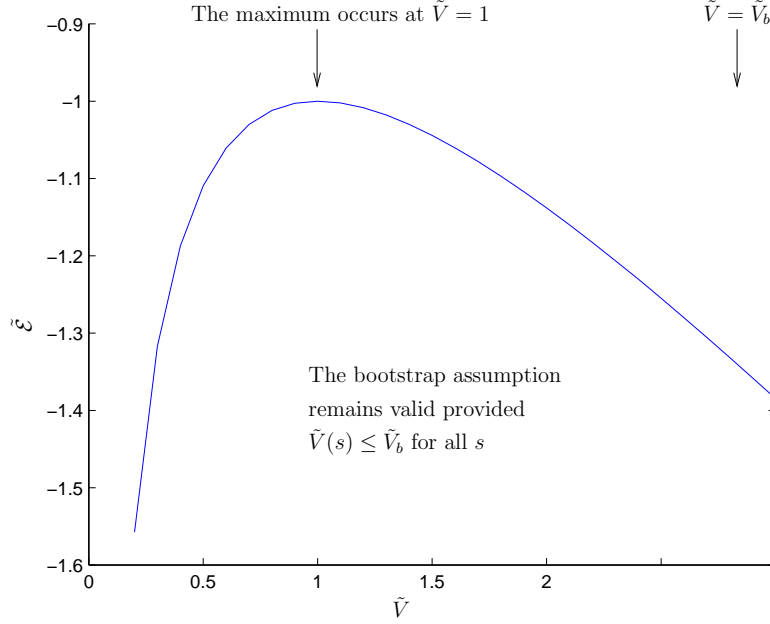


FIGURE 3.3. A depiction of  $\tilde{U}(\tilde{V})$ , with  $\tilde{V}_b$  indicated. Note that  $\tilde{V}(0) \ll \tilde{V}_b$  and always  $\tilde{V}_b \gg 1$ .

The maximum of  $\tilde{U}(\tilde{V})$  now occurs at  $\tilde{V} = 1$ . The bootstrap assumption (3.12) equates to

$$(3.13) \quad \tilde{V}_R(s) \leq \frac{R^2(8+\delta)^{\frac{2}{3}}(C_\infty)^{\frac{14}{3}}E^{\frac{2}{3}}}{2(1-\delta)^{\frac{2}{3}}M^{\frac{4}{3}}} =: \tilde{V}_b,$$

where we have defined the right-hand side as  $\tilde{V}_b$ , the “bootstrap threshold”. But by (3.11) and the assumption  $ME > 1$ , we have

$$\tilde{V}_b \geq \frac{(8+\delta)^{\frac{2}{3}}}{(1-\delta)^{\frac{2}{3}}\delta}.$$

We thus have  $\tilde{V}_b \gg 1$ , provided  $\delta$  is taken sufficiently small.<sup>5</sup>

The (rescaled) potential  $\tilde{U}(\tilde{V})$ , and  $\tilde{V}_b$  are depicted in Figure 3.3. From this, we identify two sufficient conditions for blow-up in finite time, noting that in each case, if (3.13) holds initially, then it will hold for all times:

- (1)  $\tilde{\mathcal{E}}(0) < -1$  and  $\tilde{V}(0) < 1$ .
- (2)  $\tilde{\mathcal{E}}(0) \geq -1$  and  $\tilde{V}_s(0) < 0$ .

<sup>5</sup>The smallness on  $\delta$  here does not depend on  $M$ ,  $E$ , etc. It depends only on  $\psi(x)$ , the weight appearing in the local virial identity.

The remainder of the analysis is the same as in the previous section, and thus, Theorem 1.6 is established.

Finally, we present the proof of Corollary 1.7.

*Proof of Cor. 1.7 assuming Theorem 1.6.* Take  $R = \mu M \delta^{-1/2}$ , where  $\mu$  is the constant in the second equation in (1.18). Since  $u_0$  is real, (1.19) converts to the statement

$$(3.14) \quad (ME)^{\frac{2}{3}} \frac{V_R(0)}{M^3} = \frac{E^{\frac{2}{3}} V_R(0)}{M^{\frac{7}{3}}} \ll 1$$

(see the graph of  $g$  in Fig. 1.2.) Decompose

$$\begin{aligned} \frac{V_R(0)}{MR^2} &= \frac{1}{M} \int_{|x| \leq \delta^{1/2} M (ME)^{-1/3}} \psi(x/R) |u_0|^2 dx \\ &\quad + \frac{1}{M} \int_{|x| \geq \delta^{1/2} M (ME)^{-1/3}} \psi(x/R) |u_0|^2 dx \\ &= \text{I} + \text{II}. \end{aligned}$$

For I, note that, when  $|x| \leq \delta^{1/2} M (ME)^{-1/3} \leq R$ ,

$$\psi(x/R) = |x|^2/R^2 = |x|^2 \delta / \mu^2 M^2 \leq \delta^2 (ME)^{-2/3} \mu^{-2},$$

and thus,  $|\text{I}| \leq \delta^2 (ME)^{-2/3} \mu^{-2}$ . For II, just use  $|\psi(x/R)| \lesssim 1$  and the assumption (1.20) to obtain  $|\text{II}| \leq \delta^2 (ME)^{-2/3}$ . Hence,

$$\frac{V_R(0)}{MR^2} \leq \delta^2 (ME)^{-2/3}.$$

Thus, the first condition in (1.18) is satisfied, and moreover,

$$\frac{V_R(0)}{M^3} = \frac{V_R(0) \mu^2}{MR^2 \delta} \leq \mu^2 \delta (ME)^{-2/3}.$$

Therefore, (3.14) holds provided  $\delta$  is sufficiently small.  $\square$

#### 4. PRELIMINARIES FOR THE PROFILE ANALYSES

In the sections that follow (§5–9), we consider several different initial data families. Here we record some facts needed.

**4.1.  $\dot{H}^{1/2}$  norm.** For radially symmetric data  $u_0$ , the Fourier transform can be expressed as

$$\begin{aligned} \hat{u}_0(R) &= 2 R^{-1} \int_0^\infty u_0(r) \sin(2\pi Rr) r dr \\ (4.1) \quad &= 2\pi R^{-1/2} \int_0^\infty u_0(r) J_{1/2}(2\pi Rr) r^{3/2} dr, \end{aligned}$$

where  $J_{1/2}$  is the Bessel function of index  $\frac{1}{2}$  given by

$$J_{1/2}(2\pi Rr) = \frac{\sin(2\pi Rr)}{\pi\sqrt{Rr}}.$$

We can then obtain

$$(4.2) \quad \|u_0\|_{\dot{H}^{1/2}(\mathbb{R}^3)}^2 = 8\pi^2 \int_0^\infty R^3 |\hat{u}_0(R)|^2 dR.$$

**4.2. Properties of  $Q$ .** Recall that the Pohozaev identities (1.6) hold, which in the case  $n = 3$  take the form

$$(4.3) \quad \|\nabla Q\|_{L^2}^2 = 3\|Q\|_{L^2}^2 \quad \text{and} \quad \|Q\|_{L^4}^4 = 4\|Q\|_{L^2}^2.$$

It then follows that  $E[Q] = \frac{1}{2}M[Q]$  or  $\frac{1}{6}\|\nabla Q\|_{L^2}^2$ .

We computed numerically:

$$\begin{aligned} \|Q\|_{L^2(\mathbb{R}^3)}^2 &= 4\pi \int_0^\infty Q^2(r) r^2 dr \approx 18.94, \\ \|yQ\|_{L^2(\mathbb{R}^3)}^2 &= 4\pi \int_0^\infty Q^2(r) r^4 dr \approx 20.32, \\ \|Q\|_{\dot{H}^{1/2}(\mathbb{R}^3)}^2 &= 8\pi^2 \int_0^\infty |\hat{Q}(R)|^2 R^3 dR \approx 27.72665. \end{aligned}$$

**4.3. Reformulation of blow up conditions.** For real valued initial data, Theorem 1.4 condition (1.12) can be simplified to

$$(4.4) \quad V(0) < \frac{3}{8} \frac{M^2}{E}.$$

Similarly, the condition (1.16) from Theorem 1.5 can be simplified to

$$(4.5) \quad V(0) < c \frac{M^{7/3}}{E^{2/3}} \quad \text{with} \quad c = \frac{1}{4C^{14/3}} \quad \text{and} \quad C \quad \text{from (1.16)}.$$

Observe that the second condition (4.4) is an improvement over (4.5) for real valued initial data when

$$M[u]E[u] > \frac{7^5\pi^2}{450} M[Q]E[Q] \approx 2.06 M[Q]E[Q].$$

Thus, when discussing the real valued initial data, we will refer to (4.4) and (4.5) instead of Theorems 1.4 and 1.5, correspondingly; the blow up conditions look simple in this case.

For complex valued initial data, Theorem 1.4 condition (1.12) has to be considered separately for positive and negative values of  $V_t(0)$ . Define (a scale invariant quantity)

$$\omega = \frac{8}{3} \frac{E V(0)}{M^2},$$

then for positive valued  $V_t(0)$  blow up happens

- in the intersection of the regions:

$$(4.6) \quad 0 < \omega \leq 1 \quad \text{and} \quad \frac{V_t(0)}{M} < 2\sqrt{3} \left( \frac{3^{1/2}M}{2^{1/2}E^{1/2}V(0)^{1/2}} + \frac{8EV(0)}{3M^2} - 3 \right)^{1/2},$$

and for the negative valued  $V_t(0)$  blow up happens

- in all of the region  $0 < \omega \leq 1$
- and in the intersection of the regions:

$$(4.7) \quad \omega \geq 1 \quad \text{and} \quad \frac{|V_t(0)|}{M} > 2\sqrt{3} \left( \frac{3^{1/2}M}{2^{1/2}E^{1/2}V(0)^{1/2}} + \frac{8EV(0)}{3M^2} - 3 \right)^{1/2}.$$

In this paper we consider the complex valued initial data with the quadratic phase

$$(4.8) \quad u_0(r) = f(r) e^{i\gamma r^2},$$

with  $f(r)$  - real valued radial function and  $\gamma \in \mathbb{R}$ . For such initial condition we have

$$V(0) = 4\pi F, \quad V_t(0) = 32\pi\gamma F \quad \text{with} \quad F = \int_0^\infty r^4 |f(r)|^2 dr.$$

Also

$$E = \left( 2\pi \int_0^\infty r^2 |\nabla f|^2 dr - \pi \int_0^\infty r^4 |f|^2 dr \right) + 8\pi\gamma^2 F = E^0 + E^\gamma.$$

Since

$$(4.9) \quad V_t(0)^2 - 32V(0)E^\gamma = 0,$$

the second condition in (4.6) is simplified further to

$$(4.10) \quad \sqrt{\frac{3}{2}} \frac{M}{[EV(0)]^{1/2}} + \frac{8}{3} \frac{E^0 V(0)}{M^2} - 3 > 0,$$

and analogously, the second condition in (4.7) will be as above inequality with the reversed sign (we write it out for future reference)

$$(4.11) \quad \sqrt{\frac{3}{2}} \frac{M}{[EV(0)]^{1/2}} + \frac{8}{3} \frac{E^0 V(0)}{M^2} - 3 < 0.$$

Similarly, Theorem 1.5 condition (1.16) has to be studied separately for positive and negative values of  $V_t(0)$ . Denoting (also a scale invariant quantity)

$$\kappa = 4C^{14/3} \frac{E^{2/3}V(0)}{M^{7/3}},$$

we obtain that for the positive valued  $V_t(0)$  blow up happens

- in the intersection of the regions:

$$(4.12) \quad 0 < \kappa \leq 1 \quad \text{and} \quad \frac{V_t(0)}{M} < \frac{2\sqrt{2}}{C^{7/3}} \left( \frac{M^{3/2}}{C^{7/3}V(0)^{1/2}} + \frac{4C^{14/3}EV(0)}{M^2} - 3(ME)^{1/3} \right)^{1/2},$$

and for the negative valued  $V_t(0)$  blow up happens

- in all of the region  $0 < \kappa \leq 1$
- and in the intersection of the regions:

$$(4.13) \quad \kappa \geq 1 \quad \text{and} \quad \frac{|V_t(0)|}{M} > \frac{2\sqrt{2}}{C^{7/3}} \left( \frac{M^{3/2}}{C^{7/3}V(0)^{1/2}} + \frac{4C^{14/3}EV(0)}{M^2} - 3(ME)^{1/3} \right)^{1/2}.$$

For the initial data with the quadratic phase as in (4.8), the second condition in (4.12) reduces to

$$(4.14) \quad \frac{M^{3/2}}{C^7V(0)^{1/2}} + 4 \frac{E^0V(0)}{M^2} - 3 \left( \frac{ME}{C^{14}} \right)^{1/3} > 0,$$

due to (4.9). The second inequality in (4.13) reduces to the same inequality as above except with the reversed sign (again, we write it out for the convenience of future reference):

$$(4.15) \quad \frac{M^{3/2}}{C^7V(0)^{1/2}} + 4 \frac{E^0V(0)}{M^2} - 3 \left( \frac{ME}{C^{14}} \right)^{1/3} < 0.$$

In computations below we study the conditions (4.6)-(4.7), (4.10)-(4.11) and (4.12)-(4.15) instead of (1.12) and (1.16), respectively. In graphical presentation we refer to the set of conditions (4.6)-(4.7), (4.10)-(4.11) as “*Condition from Thm. 1.4*” and (4.12) - (4.15) as “*Condition from Thm. 1.5*”.

## 5. $Q$ PROFILE

In this section we study initial data of the form

$$(5.1) \quad u_0(r) = \lambda^{3/2} Q(\lambda r) e^{i\gamma r^2},$$

where  $Q$  is the ground state defined by (1.5). Note that  $u_0$  has been scaled so that  $M[u] = M[Q]$  for all  $\lambda > 0$ .

We compute

$$\frac{E[u]}{E[Q]} = 3\lambda^2 - 2\lambda^3 + \frac{3\tilde{\gamma}^2}{\lambda^2}, \quad \frac{\|\nabla u_0\|_{L^2}^2}{\|\nabla Q\|_{L^2}^2} = \lambda^2 + \frac{\tilde{\gamma}^2}{\lambda^2},$$

where, by a Pohozaev identity (4.3),

$$(5.2) \quad \tilde{\gamma}^2 = 4\gamma^2 \frac{\|yQ\|_{L^2(\mathbb{R}^3)}^2}{\|\nabla Q\|_{L^2(\mathbb{R}^3)}^2} = \frac{4}{3}\gamma^2 \frac{\|yQ\|_{L^2(\mathbb{R}^3)}^2}{\|Q\|_{L^2(\mathbb{R}^3)}^2}.$$

The blow up when energy is negative occurs when

$$(5.3) \quad \tilde{\gamma}^2 < \frac{2}{3}\lambda^5 - \lambda^4.$$

For positive energy blow-up is analytically proven in the case  $\frac{E[u]}{E[Q]} \leq 1$  and  $\frac{\|\nabla u_0\|_{L^2}^2}{\|\nabla Q\|_{L^2}^2} > 1$  by Theorem 1.1. These conditions equate to

$$\lambda^2(1 - \lambda^2) < \tilde{\gamma}^2 < \frac{1}{3}\lambda^2(1 - 3\lambda^2 + 2\lambda^3) = \frac{1}{3}(1 - \lambda)^2(1 + 2\lambda),$$

which is not possible for any  $0 < \lambda < 1$ . On the other hand, scattering is proved in the case  $\frac{E[u]}{E[Q]} < 1$  and  $\frac{\|\nabla u_0\|_{L^2}^2}{\|\nabla Q\|_{L^2}^2} < 1$ , which just reduces to the condition  $0 < \lambda < 1$  and

$$\tilde{\gamma}^2 < \frac{1}{3}\lambda^2(1 - 3\lambda^2 + 2\lambda^3).$$

This is depicted in Figure 5.1.

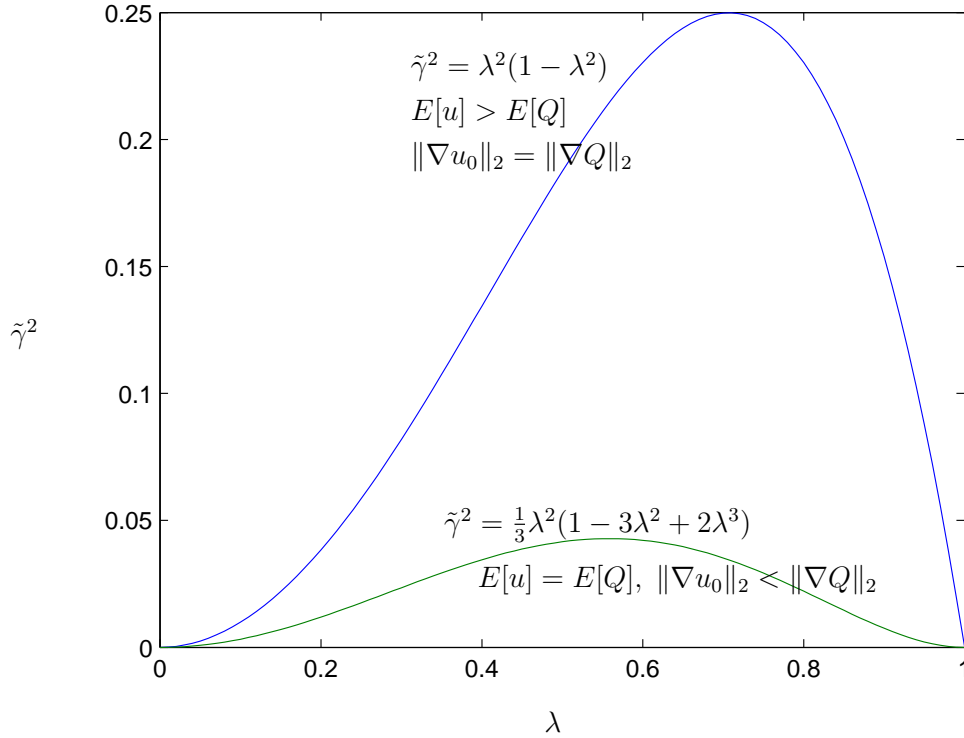


FIGURE 5.1. The curves for the mass-gradient and mass-energy thresholds for the  $Q$  profile in (5.1).

We now investigate the conditions for blow up from Theorems 1.4 and 1.5. Note that

$$V(0) = \frac{1}{\lambda^2} \|yQ\|_2^2 \quad \text{and} \quad V_t(0) = \gamma \frac{8}{\lambda^2} \|yQ\|_2^2.$$

Hence, depending on the sign of  $\gamma$ , Theorems 1.4, 1.5 provide different ranges of values  $(\lambda, \gamma)$  for which blow up occurs. We start with  $\gamma < 0$ . In what follows we use  $\tilde{\gamma}$  instead of  $\gamma$ , recall their simple relation (5.2).

• Theorem 1.4: we investigate the region given by  $0 < \omega \leq 1$ , see notation in (4.6), and then its complement with an additional restriction (4.11). The condition  $\omega \leq 1$  is

$$(5.4) \quad \tilde{\gamma}^2 \leq \frac{2}{3}\lambda^5 + \left( \frac{1}{4} \frac{\|Q\|_2^2}{\|yQ\|_2^2} - 1 \right) \lambda^4,$$

note that the right side is nonnegative when  $\lambda \geq \frac{3}{2}(1 - \frac{\|Q\|_2^2}{4\|yQ\|_2^2}) \approx 1.15$ . The condition (4.11) is

$$(5.5) \quad \tilde{\gamma}^2 > \frac{2}{3}\lambda^5 - \left( \frac{\|Q\|_2^2}{\|yQ\|_2^2} \frac{1}{\left(4(\frac{2}{3}\lambda - 1) \frac{\|yQ\|_2^2}{\|Q\|_2^2} + 3\right)^2} - 1 \right) \lambda^4,$$

provided  $\lambda \geq \frac{3}{2} \left( 1 - \frac{3}{4} \frac{\|Q\|_2^2}{\|yQ\|_2^2} \right) \approx .45$ .

Thus, for  $\gamma < 0$ , or negative  $V_t(0)$ , union of (5.4) and (5.5) will give a region where solution will blow up in finite time. It turns out that the first condition (5.4) is a part of the region covered by (5.5), and the last one is depicted in Figure 5.2 under the name “*Blow up by Thm. 1.4*”.

For  $\gamma > 0$ , the blow up region by Theorem 1.4 is an intersection of (5.4) and the inequality (5.5) with the reversed sign, which is depicted in Figure 5.3 under the name “*Blow up by Thm. 1.4*”. It turns out that this region has previously been covered by our Theorem 1.1.

Summarizing, Theorem 1.4 provides a nontrivial blow up condition for the pair  $(\lambda, \tilde{\gamma}^2)$  only if  $0.45 \leq \lambda \leq 1.15$  and  $\gamma < 0$  (see Figure 5.2).

• Theorem 1.5: similarly to the above, we start with  $\gamma < 0$  and investigate the region given by  $0 < \kappa \leq 1$ , see notation in (4.12), and then its complement with an additional restriction (4.15). The condition  $\kappa \leq 1$  is

$$(5.6) \quad \tilde{\gamma}^2 < \left( \frac{5 \cdot 3^{3/2}}{8\pi \cdot 7^{5/2}} \frac{\|Q\|_2^5}{\|yQ\|_2^3} + \frac{2}{3} \right) \lambda^5 - \lambda^4,$$

with the right side being nonnegative when  $\lambda \geq \left( \frac{5 \cdot 3^{3/2}}{8\pi \cdot 7^{5/2}} \frac{\|Q\|_2^5}{\|yQ\|_2^3} + \frac{2}{3} \right)^{-1} \approx 1.25$ . The condition (4.15) is

$$(5.7) \quad \tilde{\gamma}^2 > \frac{2}{3}\lambda^5 - \lambda^4 + \frac{2}{3} \frac{C^{14}}{\|Q\|_2^4} \lambda^2 \left( \left( \frac{1}{C^7} \frac{\|Q\|_2^3}{\|yQ\|_2} - 4 \frac{\|yQ\|_2^2}{\|Q\|_2^2} \right) \lambda + 2 \frac{\|yQ\|_2^2}{\|Q\|_2^2} \right)^3,$$



where  $C$  is from (1.16), and is valid for any  $\lambda > 0$ . Again, it turns out that the first condition (5.6) is a part of the region covered by (5.7), and the last one is depicted in Figure 5.2 under the name “*Blow up by Thm. 1.5*”.

For  $\gamma > 0$ , the blow up region by Theorem 1.5 is an intersection of (5.6) and the inequality (5.7) but with the reversed sign, which is depicted in Figure 5.3 under the name “*Blow up by Thm. 1.5*”. This region has also been previously covered by our Theorem 1.1.

In summary, Theorem 1.5 provides a nontrivial blow up condition for the pair  $(\lambda, \tilde{\gamma}^2)$  for any  $0 \leq \lambda \leq 1.25$  and  $\gamma < 0$  (see Figure 5.2). In comparison with Theorem 1.4, it provides a wider range for  $0 < \lambda < 0.762$ .

Note that Theorems 1.4 and 1.5 provide new information on the blow up behavior for the  $Q$  profile of the form (5.1) with negative phase. In particular, Theorem 1.4 gives a nontrivial range of  $\gamma$  when  $0.45 < \lambda < 1.15$ . Further extension is given by Theorem 1.5 for any  $\lambda < 0.762$ , see Figure 5.2. Both Theorems provide a blow up range “under” the mass-gradient condition, thus, showing that the last condition is irrelevant for determining long time behavior in the region when  $M[u]E[u] < M[Q]E[Q]$ .

Lastly, we compute  $\|u_0\|_{\dot{H}^{1/2}}$  norm using (4.2) numerically and then compare all conditions about the global behavior for this initial data together with numerical data in Figures 5.2 and 5.3 with negative and positive signs in the initial phase, correspondingly. For the positive phase Theorems 1.4 and 1.5 do not provide any new information, however, we have numerical range on blow up threshold and include the plot for illustration and completeness.

**Example 5.1.** Consider  $u_0 = Q(r) e^{i\gamma r^2}$  (i.e., take  $\lambda = 1$  in (5.1)). Note that

$$M[u_0]E[u_0] = \left(1 + 4\gamma^2 \frac{\|yQ\|_2^2}{\|Q\|_2^2}\right) M[Q]E[Q] > M[Q]E[Q],$$

and thus, Theorems 1.1 and 1.3 can not be applied. However, the solution with such initial condition will blow up in finite time if

$$\gamma < - \left( \frac{3}{4} \frac{\|Q\|_2^4}{\|yQ\|_2^4 \left(3 - \frac{4}{3} \frac{\|Q\|_2^2}{\|yQ\|_2^2}\right)^2} - \frac{\|Q\|_2^2}{4\|yQ\|_2^2} \right)^{1/2} \approx -0.177,$$

by Theorem 1.4, or when

$$\gamma < - \left( \frac{\|Q\|_2^4}{54C^7\|yQ\|_2^2} \left( \frac{\|Q\|_2}{\|yQ\|_2} + \frac{2C^7\|yQ\|_2^2}{\|Q\|_2^4} \right)^3 - \frac{\|Q\|_2^2}{4\|yQ\|_2^2} \right)^{1/2} \approx -0.279,$$

by Theorem 1.5. In this example, Theorem 1.4 is more powerful than Theorem 1.5, however, this is not always the case, as can be seen from Figure 5.2 (for example, for  $\lambda < .762$  Theorem 1.5 gives a larger range for blow up).

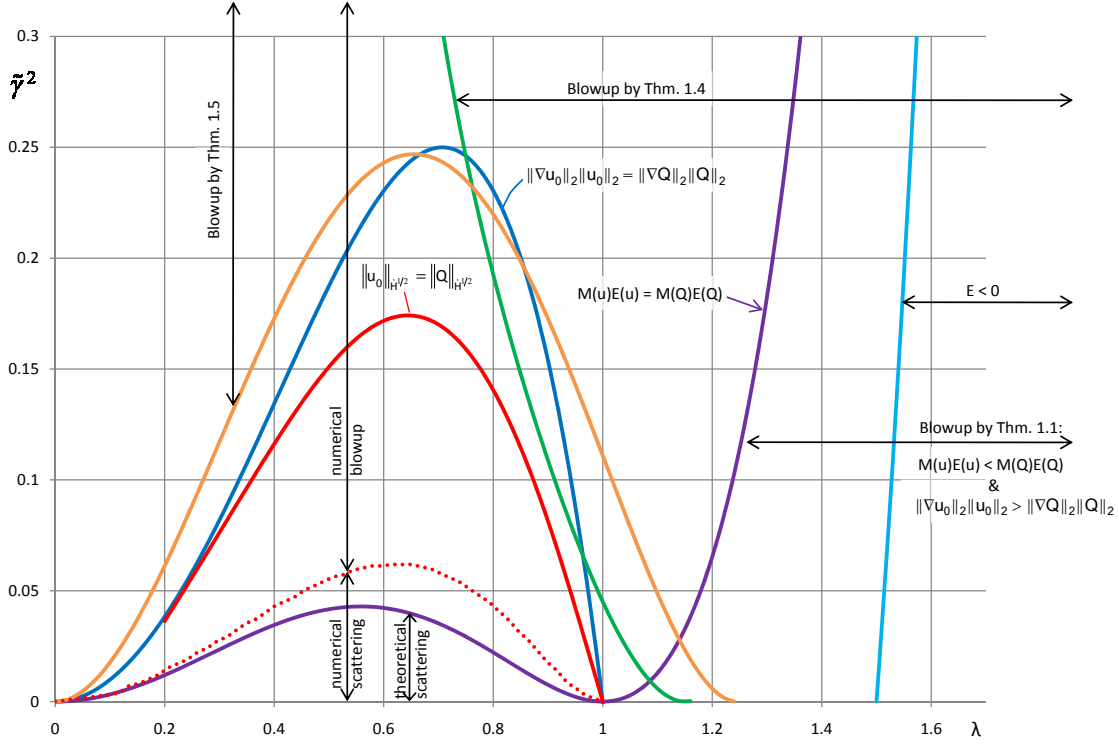


FIGURE 5.2. Global behavior of the solutions to the  $Q$  profile initial data with the negative quadratic phase:  $u_0(r) = \lambda^{3/2}Q(\lambda r)e^{-i|\gamma|r^2}$ . Here,  $\tilde{\gamma}$  is the renormalized  $\gamma$ , see (5.2), namely,  $\tilde{\gamma}^2 \approx 1.43\gamma^2$ . The region of “theoretical scattering” is provided by Thm. 1.1, see also Figure 5.1. “Blowup by Thm. 1.4” is given by (5.5) and “Blowup by Thm. 1.5” is given by (5.7). The intersection of these two conditions occurs at  $\lambda \approx 0.762$ .

### 5.1. Conclusions.

- (1) The condition “ $\|u_0\|_{\dot{H}^{1/2}} < \|Q\|_{\dot{H}^{1/2}}$  implies scattering” is not valid; the numerical blow-up curve is *below* the  $\|u_0\|_{\dot{H}^{1/2}}^2 = \|Q\|_{\dot{H}^{1/2}}^2$  curve in Figure 5.2. This supports Conjecture 2.
- (2) The condition “ $\|u_0\|_{L^2}\|\nabla u_0\|_{L^2} < \|Q\|_{L^2}\|\nabla Q\|_{L^2}$  implies scattering” is not valid (unless  $M[u]E[u] < M[Q]E[Q]$  as in Theorem 1.1); not only the numerical blow-up curve is *below* the  $\|u_0\|_{L^2}\|\nabla u_0\|_{L^2} = \|Q\|_{L^2}\|\nabla Q\|_{L^2}$  curve in Figure 5.2, but also both Theorems 1.4 and 1.5 provide range of  $(\lambda, \gamma)$  for which blow up from the initial data 5.1 occurs and this range is *below* the  $\|u_0\|_{L^2}\|\nabla u_0\|_{L^2} = \|Q\|_{L^2}\|\nabla Q\|_{L^2}$  curve in Figure 5.2.
- (3) Previously, no theoretical blow-up result for the profile (5.1) with  $0 < \lambda \leq 1$  could be obtained from Theorem 1.1. The new blow-up criteria in Theorems

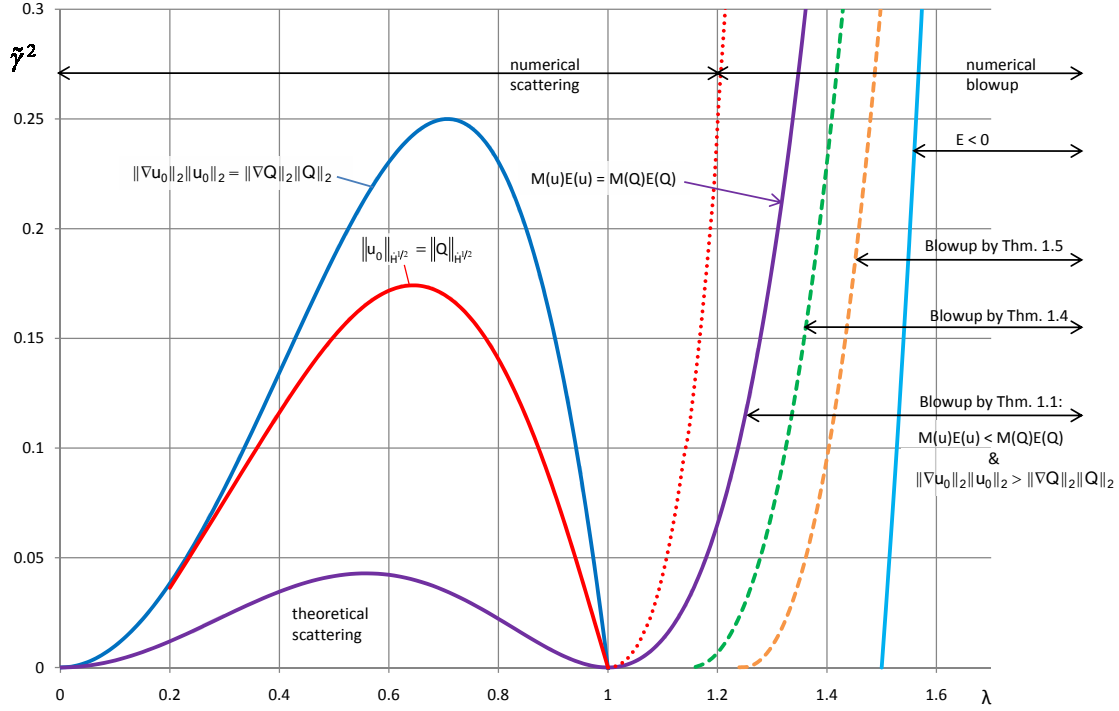


FIGURE 5.3. Global behavior of the solutions to the  $Q$  profile initial data with the positive quadratic phase:  $u_0(r) = \lambda^{3/2}Q(\lambda r)e^{+i|\gamma|r^2}$ . As before,  $\tilde{\gamma}$  is the renormalized  $\gamma$ , see (5.2), namely,  $\tilde{\gamma}^2 \approx 1.43\gamma^2$ . The region of “theoretical scattering” is the same as in Fig. 5.2 and is provided by Thm. 1.1. “Blowup by Thm. 1.4” is given by the complement of (5.5) intersected with (5.4) and “Blowup by Thm. 1.5” is given by the complement of (5.7) intersected with (5.6).

1.4 and 1.5 give a nonempty set of  $(\lambda, \gamma)$  with  $\gamma < 0$  for which blow up occurs, see conditions (5.4)-(5.5) and (5.6)-(5.7) as well as the illustration in Figure 5.2.

## 6. GAUSSIAN PROFILE

In this section, we study initial data  $u_0$  of the form

$$(6.1) \quad u_0(x) = p e^{-\alpha r^2/2} e^{i\gamma r^2}, \quad r = |x|, \quad x \in \mathbb{R}^3.$$

By scaling, it suffices to consider the cases  $\gamma = 0$  (real data) and  $\gamma = \pm \frac{1}{2}$ . The main parameters are

$$\begin{aligned} M[u] &= \frac{\pi^{3/2} p^2}{\alpha^{3/2}}, & \|\nabla u_0\|_{L^2}^2 &= \frac{3\pi^{3/2} p^2}{2\alpha^{1/2}} \left(1 + 4\frac{\gamma^2}{\alpha^2}\right), \\ E[u] &= \frac{\pi^{3/2} p^2}{4\alpha^{1/2}} \left(3 \left(1 + 4\frac{\gamma^2}{\alpha^2}\right) - \frac{p^2}{2\sqrt{2}\alpha}\right), \\ V(0) &= \frac{3\pi^{3/2} p^2}{2\alpha^{5/2}}, & V_t(0) &= \frac{12\gamma\pi^{3/2} p^2}{\alpha^{5/2}}, \\ \|u_0\|_{\dot{H}^{1/2}}^2 &= \frac{2\pi p^2}{\alpha} \left(1 + 4\frac{\gamma^2}{\alpha^2}\right)^{1/2}. \end{aligned}$$

To compute the last expression  $\|u_0\|_{\dot{H}^{1/2}}$ , consider the Fourier transform of  $u_0^\gamma$  (here,  $R^2 = |\xi|^2$ ,  $\xi \in \mathbb{R}^3$ )

$$\hat{u}_0(R) = p \left( \frac{2\pi}{\alpha - 2i\gamma} \right)^{3/2} e^{-\frac{2\pi^2 \alpha}{\alpha^2 + 4\gamma^2} R^2} e^{-i\frac{4\pi^2 \gamma}{\alpha^2 + 4\gamma^2} R^2},$$

where we used  $\int_{-\infty}^{\infty} e^{i(az^2 + 2bz)} dz = \sqrt{\frac{\pi i}{a}} e^{-ib^2/a}$ ,  $a, b \in \mathbb{C}$ . By (4.2) we have

$$(6.2) \quad \|u_0\|_{\dot{H}^{1/2}(\mathbb{R}^3)}^2 = \frac{64\pi^5 p^2}{(\alpha^2 + 4\gamma^2)^{3/2}} \int_0^\infty e^{-\frac{4\pi^2 \alpha}{\alpha^2 + 4\gamma^2} R^2} R^3 dR = \frac{2\pi p^2}{\alpha^2} (\alpha^2 + 4\gamma^2)^{1/2}.$$

**6.1. Real Gaussian.** Take  $\gamma = 0$  in (6.1). Then by scaling, the behavior of solutions is a function of  $p/\sqrt{\alpha}$ . We have

- $E[u] > 0$  if

$$(6.3) \quad p < \left(6\sqrt{2}\right)^{1/2} \sqrt{\alpha} \approx 2.91 \sqrt{\alpha};$$

- the condition on the mass and gradient  $\|u_0\|_{L^2}^2 \|\nabla u_0\|_{L^2}^2 < \|Q\|_{L^2}^2 \|\nabla Q\|_{L^2}^2$  implies

$$(6.4) \quad p < 2^{1/4} \pi^{-3/4} \|Q\|_{L^2} \sqrt{\alpha} \approx 2.19 \sqrt{\alpha};$$

- the mass-energy condition  $M[u]E[u] < M[Q]E[Q]$  is

$$\frac{\pi^3 p^4}{4\alpha^2} \left(3 - \frac{p^2}{2\sqrt{2}\alpha}\right) < \frac{1}{2} \|Q\|_{L^2}^4,$$

which gives

$$(6.5) \quad p < 1.92\sqrt{\alpha} \quad \text{and} \quad p > 2.69\sqrt{\alpha}.$$

- the invariant norm condition  $\|u_0\|_{\dot{H}^{1/2}}^2 < \|Q\|_{\dot{H}^{1/2}}^2$  is

$$(6.6) \quad p < (2\pi)^{-1/2} \|Q\|_{\dot{H}^{1/2}} \sqrt{\alpha} \approx 2.10\sqrt{\alpha}.$$

- (Theorem 1.4) the condition (4.4) is

$$(6.7) \quad p > \left(4\sqrt{2}\right)^{1/2} \sqrt{\alpha} \approx 2.38\sqrt{\alpha},$$

- (Theorem 1.5) the condition (4.5) is

$$(6.8) \quad p > \left(\frac{3 \cdot 2^{3/2} \cdot 7^{5/2}}{30\pi^{1/2} + 7^{5/2}}\right)^{1/2} \sqrt{\alpha} \approx 2.45\sqrt{\alpha},$$

- Numerical simulations: the results for the real Gaussian initial data (6.1) are in Table 6.1. For  $p \geq p_b$  the blow up was observed, for  $p \leq p_s$  the solution dispersed over time. For example, for  $\alpha = 1$  the threshold is between 2.07 and 2.08. This is consistent with the previously reported threshold by Vlasov et al. in [29] ( $p = 2.0764$ ). From this table it also follows that  $p_s/\sqrt{\alpha} \in (2.07, 2.075)$  and  $p_b/\sqrt{\alpha} \in (2.077, 2.08)$ .

$\alpha$	0.5	1.0	2.0	4.0	6.0	8.0	10.0
$p_s$	1.46	2.07	2.93	4.15	5.08	5.87	6.56
$p_b$	1.47	2.08	2.94	4.16	5.09	5.88	6.57

TABLE 6.1. Thresholds for blow up/scattering from numerical simulations for the Gaussian initial data: for  $p \leq p_s$  scattering was observed and for  $p \geq p_b$  blow up in finite time was observed. For comparison the values of  $p$  from (6.6) are also listed.

In Kuznetsov et. al. [23] it is reported that for the Gaussian initial data (6.1) with  $\gamma = 0$ , the numerical condition for collapse is when two conditions hold:

$$(6.9) \quad \frac{\|\nabla u_0\|_2^2 \|u_0\|_2^2}{\|\nabla Q\|_2^2 \|Q\|_2^2} > 0.80255 \quad \text{or} \quad p > \frac{(2 \cdot 0.80255)^{1/4}}{\pi^{3/4}} \|Q\|_{L^2} \sqrt{\alpha} \approx 2.0759 \sqrt{\alpha},$$

and

$$(6.10) \quad \frac{E[u_0]M[u_0]}{E[Q]M[Q]} > 1.1855 \quad \text{or} \quad 2.0764\sqrt{\alpha} < p < 2.6105\sqrt{\alpha}.$$

Thus, the numerical threshold  $p/\sqrt{\alpha} \approx 2.0764$  is reported in [23]. Our data is consistent with this report, see also Figure 6.1.

To compare the conditions (6.4) - (6.8) with the numerics, we graph them in Figure 6.1. For clarity of presentation, and also for comparison with the  $\gamma \neq 0$  case considered next, we plot  $\frac{p}{\sqrt{\alpha}}$  on the vertical axis vs  $\alpha$  on the horizontal.

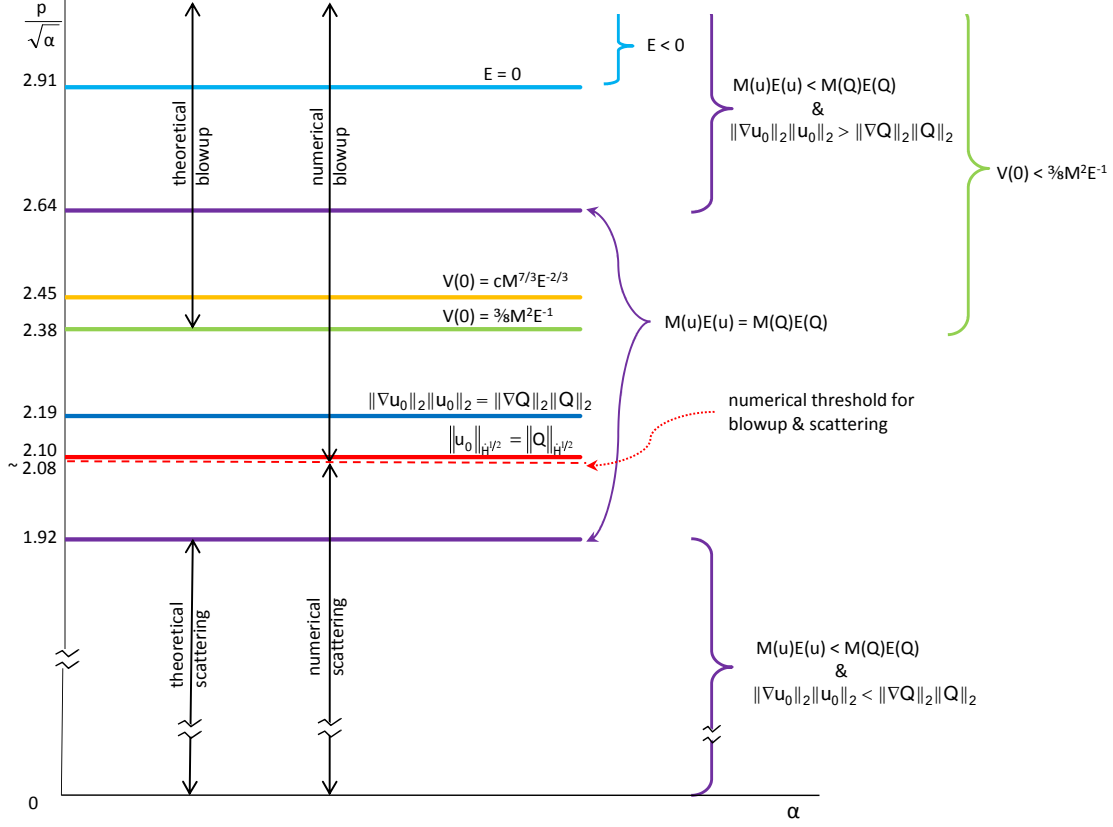


FIGURE 6.1. Global behavior of the solutions with the (real) Gaussian initial data  $u_0(r) = p e^{\alpha r^2/2}$ . The line denoted by  $V(0) = 3/8M^2E^{-1}$  is the threshold for blow up from Theorem 1.4, see (6.7); similarly, the line denoted by  $V(0) = cM^{7/3}E^{-2/3}$  is the threshold for blow up from Theorem 1.5, see (6.8). The line “theoretical scattering” is given by Thm. 1.1, see (6.5). The numerical threshold (dashed line) comes from Table 6.1 normalized by  $\sqrt{\alpha}$ . For all other values refer to text in §6.1.

**6.2. Gaussian with a quadratic phase.** Now we consider (6.1) with  $\gamma \neq 0$ . (By scaling it suffices to consider  $\gamma = \pm \frac{1}{2}$ .) We compute

- $E[u] > 0$  if

$$(6.11) \quad p < \left(6\sqrt{2}\right)^{1/2} \sqrt{\alpha} \left(1 + 4\frac{\gamma^2}{\alpha^2}\right)^{1/2} \approx 2.91 \sqrt{\alpha} \left(1 + 4\frac{\gamma^2}{\alpha^2}\right)^{1/2};$$

- the condition on the mass and gradient  $\|u_0\|_{L^2}^2 \|\nabla u_0\|_{L^2}^2 < \|Q\|_{L^2}^2 \|\nabla Q\|_{L^2}^2$  is

$$(6.12) \quad p < \frac{2^{1/4} \|Q\|_{L^2}}{\pi^{3/4}} \frac{\sqrt{\alpha}}{(1 + 4\frac{\gamma^2}{\alpha^2})^{1/4}} \approx 2.19 \sqrt{\alpha} \left(1 + 4\frac{\gamma^2}{\alpha^2}\right)^{-1/4};$$

- the mass-energy condition  $M[u]E[u] < M[Q]E[Q]$  is

$$(6.13) \quad \frac{\pi^3 p^4}{4\alpha^2} \left(3 \left(1 + 4\frac{\gamma^2}{\alpha^2}\right) - \frac{p^2}{2\sqrt{2}\alpha}\right) < \frac{1}{2} \|Q\|_{L^2}^4.$$

The left hand side is a cubic polynomial in  $y^2 = p^2/\alpha$  and can be solved explicitly to obtain  $\frac{p}{\alpha^{1/2}}$  as a function of  $\alpha$ , though with a very complicated expression. We list a few values for  $\gamma = \pm \frac{1}{2}$  in Table 6.2. The inequality in (6.13) holds for  $p < p_1$

$\alpha$	0.25	0.5	1	2	4	6	8	10
$p_1$	0.41	0.79	1.45	2.42	3.70	4.62	5.38	6.04
$p_2$	6.01	4.60	4.09	4.46	5.65	6.75	7.71	8.58

TABLE 6.2. The positive real roots of the equation in (6.13).

and  $p > p_2$ .

- the invariant norm condition  $\|u_0\|_{\dot{H}^{1/2}}^2 < \|Q\|_{\dot{H}^{1/2}}^2$  is

$$(6.14) \quad p < \alpha \left( \frac{27.72665}{2\pi(\alpha^2 + 4\gamma^2)^{1/2}} \right)^{1/2} \approx 2.10 \sqrt{\alpha} \left(1 + 4\frac{\gamma^2}{\alpha^2}\right)^{-1/4};$$

- (Theorem 1.4) the condition  $\omega \leq 1$  from (4.6) amounts to

$$(6.15) \quad p \geq \left(4\sqrt{2}\right)^{1/2} \sqrt{\alpha} \left(1 + 6\frac{\gamma^2}{\alpha^2}\right)^{1/2} \approx 2.38 \sqrt{\alpha} \left(1 + 6\frac{\gamma^2}{\alpha^2}\right)^{1/2},$$

similarly,  $\omega \geq 1$  from (4.7) will be the above with the reversed sign. The condition (4.10) for positive  $\gamma$  with  $y = p/\sqrt{\alpha}$  is

$$(6.16) \quad y^6 - 6\sqrt{2} \left(1 + 4\frac{\gamma^2}{\alpha^2}\right) y^4 + 64\sqrt{2} > 0$$

and with the reversed inequality sign for negative  $\gamma$ . The last inequality is cubic in  $y^2$  producing two positive roots, which are listed in Table 6.3 for  $\gamma = \pm \frac{1}{2}$ .

$\alpha$	0.25	0.5	1	2	4	6	8	10
$p_b$	0.45	0.86	1.58	2.68	4.22	5.37	6.33	7.16
$p_t$	6.01	4.60	4.08	4.39	5.42	6.35	7.17	7.91

TABLE 6.3. The positive real roots,  $p_t$  and  $p_b$ , of the function in (6.15) for the condition (4.10) (Theorem 1.4).

- (Theorem 1.5) the condition  $\kappa \leq 1$  from (4.12) amounts to

$$(6.17) \quad p \geq \left( \frac{3 \cdot 2^{3/2} \cdot 7^{5/2}}{30\pi^{1/2} + 7^{5/2}} \right)^{1/2} \sqrt{\alpha} \left( 1 + 4 \frac{\gamma^2}{\alpha^2} \right)^{1/2} \approx 2.45 \sqrt{\alpha} \left( 1 + 4 \frac{\gamma^2}{\alpha^2} \right)^{1/2},$$

similarly,  $\kappa \geq 1$  from (4.13) is the above inequality with the reversed sign. The condition (4.14) with  $y = p/\sqrt{\alpha}$  for positive  $\gamma$  is

$$(6.18) \quad \left( \frac{15\sqrt{2\pi}}{7^{5/2}} - \frac{1}{2^{3/2}} \right) y^2 + 3 - \left( \frac{3^5 \cdot 5^2 \pi}{2 \cdot 7^5} \right)^{1/3} \left( 3 \left( 1 + 4 \frac{\gamma^2}{\alpha^2} \right) y^4 - \frac{y^6}{2^{3/2}} \right)^{1/3} > 0,$$

and with the reversed sign for negative  $\gamma$ . The positive real zeros of the function in (6.18) for  $\gamma = \pm \frac{1}{2}$  are listed in Table 6.4.

$\alpha$	0.25	0.5	1	2	4	6	8	10
$p_b$	0.48	0.93	1.68	2.81	4.39	5.57	6.55	7.41
$p_t$	6.01	4.61	4.10	4.46	5.54	6.51	7.36	8.13

TABLE 6.4. The positive real roots,  $p_t$  and  $p_b$ , of the function in (6.18) for the condition (4.14) (Theorem 1.5).

- Numerical simulations: we fix the quadratic phase  $\gamma = \pm 0.5$  and vary the parameter  $\alpha$  in our numerical simulations in order to obtain the blow up threshold, see data in Table 6.2. Note that we obtain different thresholds depending on the sign of  $\gamma$ .

To compare conditions (6.11) - (6.18) with the numerics, we graph the dependence of  $p$  on  $\alpha$  in Figures 6.2 and 6.3 separately for positive and negative values of the phase  $\gamma = \pm \frac{1}{2}$ . We plot  $\frac{p}{\sqrt{\alpha}}$  on the vertical axis to observe the asymptotics as  $\alpha \rightarrow \infty$ , and thus, approaches the case of the real Gaussian initial data.

**6.3. Conclusions.** The above computations show

- (1) Consistency with Conjecture 3: if  $u_0$  is *real*, then  $\|u_0\|_{\dot{H}^{1/2}} < \|Q\|_{\dot{H}^{1/2}}$  implies  $u(t)$  scatters (numerical data).
- (2) Consistency with Conjecture 4 (since  $u_0$  is based upon a radial profile that is *monotonically decreasing*): if  $\|u_0\|_{\dot{H}^{1/2}} > \|Q\|_{\dot{H}^{1/2}}$ , then  $u(t)$  blows-up in finite time (numerical data) .



$\alpha$	0.5	1.0	2.0	4.0	6.0	8.0	10.0
$p_s^+$	2.8	3.00	3.56	4.58	5.43	6.17	6.83
$p_b^+$	2.8	3.01	3.57	4.59	5.44	6.18	6.835
$p_s^-$	0.79	1.44	2.42	3.76	4.76	5.59	6.313
$p_b^-$	0.80	1.45	2.43	3.77	4.77	5.60	6.315

TABLE 6.5. Thresholds from numerical simulations for the Gaussian initial data with phase  $\gamma = \pm 5$ : for  $p \geq p_b^\pm$  blow up in finite time was observed and for  $p \leq p_s^\pm$  scattering was observed; + superscript indicates the threshold for the positive phase  $\gamma = .5$  and – superscript indicates the negative phase  $\gamma = -.5$ .

- (3) Theoretical proof of the Conjecture 2, i.e., “ $\|u_0\|_{\dot{H}^{1/2}} < \|Q\|_{\dot{H}^{1/2}}$  implies scattering” is false for an arbitrary radial data. We show that it is possible to produce a radial Gaussian initial data with negative phase (e.g., for  $0 < \lambda < 3.3$  by Theorem 1.4) such that  $\|u_0\|_{\dot{H}^{1/2}} < \|Q\|_{\dot{H}^{1/2}}$  and the solution  $u(t)$  blows up in finite time.
- (4) The condition “ $\|u_0\|_{L^2}\|\nabla u_0\|_{L^2} < \|Q\|_{L^2}\|\nabla Q\|_{L^2}$  implies scattering” is not valid (unless  $M[u]E[u] < M[Q]E[Q]$  as in Theorem 1.1).
- (5) In all three cases (real data, data with positive phase and with negative phase) Theorems 1.4 and 1.5 provide new range on blow up than was previously known from our Theorem 1.1.
- (6) For the Gaussian initial data with negative phase and small values of  $\alpha$  ( $0 < \alpha \lesssim 2$ , see Figure 6.3) the numerical threshold for scattering and blow up coincides with the scattering threshold provided by Theorem 1.1. As  $\alpha \rightarrow \infty$  the numerical threshold (for both positive and negative phases) approaches the values  $\|u_0\|_{\dot{H}^{1/2}} = \|Q\|_{\dot{H}^{1/2}}$ .

## 7. SUPER-GAUSSIAN PROFILE

Now we modify the initial Gaussian data to the “super Gaussian” profile:

$$(7.1) \quad u_0(r) = p e^{-\alpha r^4/2} e^{i\gamma r^2}, \quad r = |x|, \quad x \in \mathbb{R}^3.$$

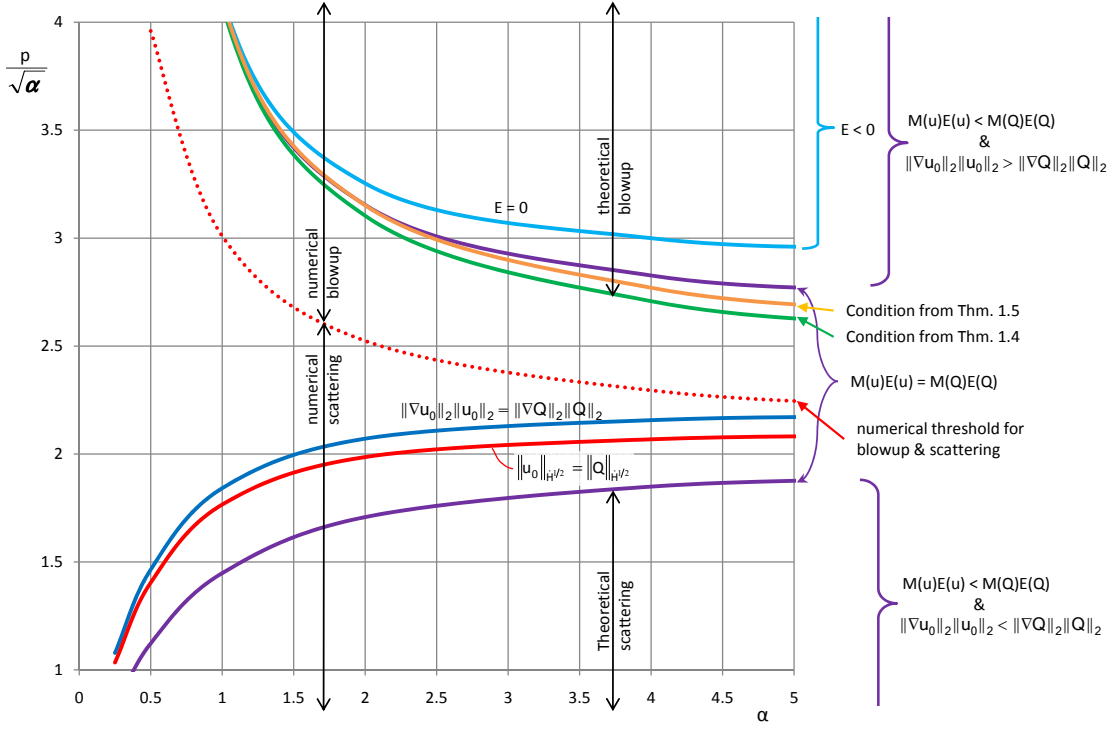


FIGURE 6.2. Global behavior of the solutions to the Gaussian initial data with the positive quadratic phase  $u_0(r) = p e^{-\alpha r^2/2} e^{+i\frac{1}{2}r^2}$ . The curve denoted by “Condition from Thm. 1.4” comes from the largest positive root of the equation in (6.15), namely, values  $p_t/\sqrt{\alpha}$  in Table 6.3. Similarly, the curve denoted by “Condition from Thm. 1.5” comes from the largest positive root of the equation in (6.18), namely, values  $p_t/\sqrt{\alpha}$  in Table 6.4. The curve “theoretical scattering” is provided by Thm. 1.1, see (6.13) and values  $p_1$  in Table 6.2. The numerical threshold (dotted curve) comes from values  $p_s^+$ ,  $p_b^+$  in Table 6.2 normalized by  $\sqrt{\alpha}$ .

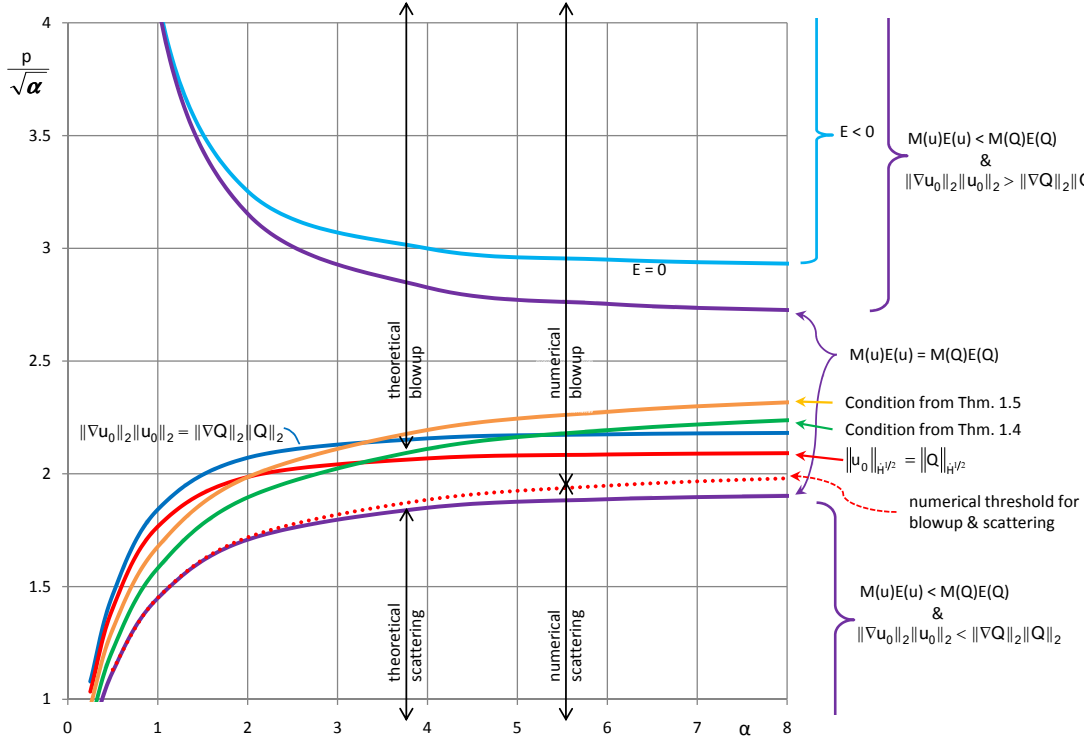


FIGURE 6.3. Global behavior of the solutions to the Gaussian initial data with the negative quadratic phase  $u_0(r) = p e^{-\alpha r^2/2} e^{-i\frac{1}{2}r^2}$ . The curve denoted by “Condition from Thm. 1.4” comes from the smallest positive root of the equation in (6.15), namely, values  $p_b/\sqrt{\alpha}$  in Table 6.3. Similarly, the curve denoted by “Condition from Thm. 1.5” comes from the smallest positive root of the equation in (6.18), namely, values  $p_b/\sqrt{\alpha}$  in Table 6.4. The curve “theoretical scattering” is the same as in Fig. 6.2 and is provided by Thm. 1.1, see (6.13) and values  $p_1$  in Table 6.2. The numerical threshold (dotted curve) comes from values  $p_s^-, p_b^-$  in Table 6.2 normalized by  $\sqrt{\alpha}$ . This plot illustrates that both Theorems 1.4 and 1.5 provide ranges of the Gaussian initial data  $u_0$  such that  $\|u_0\|_{\dot{H}^{1/2}} < \|Q\|_{\dot{H}^{1/2}}$  and  $u(t)$  blows up in finite time.

For this initial data we calculate

$$\begin{aligned} M[u] &= \frac{\pi p^2}{\alpha^{3/4}} \Gamma\left(\frac{3}{4}\right), \quad \|\nabla u_0\|_{L^2}^2 = \frac{\pi^2 p^2}{2\sqrt{2} \alpha^{1/4} \Gamma(\frac{3}{4})} \left(5 + 4\frac{\gamma^2}{\alpha}\right), \\ E[u] &= \frac{\pi p^2}{4\sqrt{2} \alpha^{1/4} \Gamma(\frac{3}{4})} \left( \pi \left(5 + 4\frac{\gamma^2}{\alpha}\right) - \frac{[\Gamma(\frac{3}{4})]^2}{2^{1/4}} \frac{p^2}{\sqrt{\alpha}} \right), \\ V(0) &= \frac{\pi^2 p^2}{2\sqrt{2} \alpha^{5/4} \Gamma(\frac{3}{4})}, \quad V_t(0) = \frac{2\sqrt{2} \pi^2 p^2 \gamma}{\alpha^{5/4} \Gamma(\frac{3}{4})}. \end{aligned}$$

Here,  $\Gamma(s+1) = \int_0^\infty e^{-t} t^s dt$ .

**7.1. Real super Gaussian.** When  $\gamma = 0$ , we have

- $E[u] > 0$  if

$$(7.2) \quad p < \frac{2^{1/8} \sqrt{5\pi}}{\Gamma(\frac{3}{4})} \alpha^{1/4} \approx 3.53 \alpha^{1/4};$$

- the condition on the mass and gradient  $\|u_0\|_{L^2}^2 \|\nabla u_0\|_{L^2}^2 < \|Q\|_{L^2}^2 \|\nabla Q\|_{L^2}^2$  implies

$$(7.3) \quad p < \frac{2^{3/8} 3^{1/4}}{5^{1/4} \pi^{3/4}} \|Q\|_{L^2} \alpha^{1/4} \approx 2.10 \alpha^{1/4};$$

- the mass-energy condition  $M[u]E[u] < M[Q]E[Q]$  is

$$\frac{\pi^2 p^4}{4\sqrt{2}\alpha} \left( 5\pi - \frac{[\Gamma(\frac{3}{4})]^2}{2^{1/4}} \frac{p^2}{\sqrt{\alpha}} \right) < \frac{1}{2} \|Q\|_{L^2}^4,$$

and thus, we obtain

$$(7.4) \quad p < 1.71 \alpha^{1/4} \quad \text{and} \quad p > 3.44 \alpha^{1/4}.$$

- (Theorem 1.4) the condition (4.4) is

$$(7.5) \quad p > \frac{2^{1/8} \pi^{1/2}}{\Gamma(\frac{3}{4})} \left( 5 - \frac{6}{\pi^2} \left[ \Gamma\left(\frac{3}{4}\right) \right]^4 \right)^{1/2} \alpha^{1/4} \approx 3.00 \alpha^{1/4}.$$

- (Theorem 1.5) the condition (4.5) is

$$(7.6) \quad p > \frac{2^{1/8} \cdot 5^{1/2} \cdot \pi^{3/4} C^{7/2}}{\Gamma(\frac{3}{4}) (C^7 \pi^{1/2} + 4[\Gamma(\frac{3}{4})]^4)^{1/2}} \alpha^{1/4} \approx 2.89 \alpha^{1/4}.$$

- the invariant norm condition  $\|u_0\|_{\dot{H}^{1/2}}^2 < \|Q\|_{\dot{H}^{1/2}}^2$  is given in Table 7.1. Here, we first compute the Fourier transform of  $u_0$  using (4.1) and then  $\dot{H}^{1/2}$  norm by (4.2) which is listed in the second row of the Table 7.1 for various  $\alpha$ . The third row indicates the values of  $p$ , denoted by  $p_{1/2}$ , for the threshold in the invariant norm condition. We observe that  $p_{1/2}/\sqrt[4]{\alpha} \approx 2.02$ .

- Numerical simulations: the results with the super Gaussian initial data (7.1) are in Table 7.1. For  $p \geq p_b$  the blow up was observed, for  $p \leq p_s$  the solution dispersed over time. We observe that  $p_s/\sqrt[4]{\alpha} \approx 2.01$  and  $p_b\sqrt[4]{\alpha} \approx 2.02$ . For convenience Table 7.1 contains the  $\dot{H}^{1/2}$  norm calculations.

$\alpha$	.25	.5	1	2	4	6	8	10
$\frac{1}{p^2} \ u_0\ _{\dot{H}^{1/2}}$	13.54	9.58	6.77	4.79	3.39	2.76	2.39	2.14
$p_{1/2}$	1.43	1.70	2.02	2.41	2.86	3.17	3.41	3.60
$p_s$	1.42	1.69	2.01	2.39	2.85	3.15	3.39	3.58
$p_b$	1.43	1.70	2.02	2.40	2.86	3.16	3.40	3.59

TABLE 7.1. The  $\dot{H}^{1/2}$  norm of the super Gaussian initial data depending on  $\alpha$  and values of  $p$  for the  $\dot{H}^{1/2}$  condition as well as the numerical results for blow up threshold and global existence -  $p \geq p_b$  and  $p \leq p_s$ , correspondingly.

To compare the conditions (7.2) - (7.6) with numerical data, we graph the dependence of  $p$  on  $\alpha$  in Figure 7.1. For clarity of presentation we plot  $\frac{p}{\sqrt[4]{\alpha}}$  on the vertical axis.

**7.2. Super Gaussian with a quadratic phase.** When  $\gamma \neq 0$ , we have

- $E[u] > 0$  if

$$(7.7) \quad p < \frac{2^{1/8} \pi^{1/2}}{\Gamma(\frac{3}{4})} \left(5 + 4 \frac{\gamma^2}{\alpha}\right)^{1/2} \alpha^{1/4} \approx 1.58 \alpha^{1/4} \left(5 + 4 \frac{\gamma^2}{\alpha}\right)^{1/2};$$

- the condition on the mass and gradient  $\|u_0\|_{L^2}^2 \|\nabla u_0\|_{L^2}^2 < \|Q\|_{L^2}^2 \|\nabla Q\|_{L^2}^2$  implies

$$(7.8) \quad p < \frac{2^{3/8} 3^{1/2}}{\pi^{3/4} (5 + 4 \frac{\gamma^2}{\alpha})^{1/4}} \|Q\|_{L^2} \alpha^{1/4} \approx 3.15 \alpha^{1/4} \left(5 + 4 \frac{\gamma^2}{\alpha}\right)^{-1/4};$$

- the mass-energy threshold  $M[u]E[u] = M[Q]E[Q]$  is

$$(7.9) \quad \frac{\pi^2 p^4}{4\sqrt{2}\alpha} \left( \pi \left(5 + 4 \frac{\gamma^2}{\alpha}\right) - \frac{[\Gamma(\frac{3}{4})]^2}{2^{1/4}} \frac{p^2}{\sqrt{\alpha}} \right) = \frac{1}{2} \|Q\|_{L^2}^4,$$

the real positive zeros of the above expression when  $\gamma = \pm \frac{1}{2}$  are in Table 7.2.

- for the invariant norm condition  $\|u_0\|_{\dot{H}^{1/2}}^2 < \|Q\|_{\dot{H}^{1/2}}^2$ , we compute the Fourier Transform of  $u_0(r) = p e^{-\alpha r^4/2} e^{i\gamma r^2}$  again by (4.1) and then  $\dot{H}^{1/2}$  norm by (4.2). The values of  $p$  when the condition  $\|u_0\|_{\dot{H}^{1/2}} = \|Q\|_{\dot{H}^{1/2}}$  are in Table 7.3 as well.

$\alpha$	.25	.5	1	2	4	6	8	10
$p_1$	1.00	1.28	1.60	1.96	2.37	2.64	2.85	3.02
$p_2$	3.34	3.48	3.81	4.32	5.01	5.49	5.88	6.20

TABLE 7.2. The positive real roots of the equation in (7.9).

$\alpha$	.25	.5	1	2	4	6	8	10
$\frac{1}{p^2} \ u_0\ _{\dot{H}^{1/2}}$	17.53	11.03	7.29	4.97	3.45	2.80	2.42	2.16
$p_{1/2}$	1.26	1.59	1.95	2.36	2.83	3.15	3.39	3.59

TABLE 7.3. The  $\dot{H}^{1/2}$  norm of the super Gaussian initial data with the phase  $\gamma = \pm \frac{1}{2}$  depending on  $\alpha$  is listed in the second row and values of  $p$  for this condition are in the last.

- (Theorem 1.4) the condition  $\omega \leq 1$  from (4.6) is  
(7.10)

$$p > \frac{2^{1/8} \pi^{1/2}}{\Gamma(\frac{3}{4})} \left( \left( 5 + 4 \frac{\gamma^2}{\alpha} \right) - \frac{6}{\pi^2} \left[ \Gamma\left(\frac{3}{4}\right) \right]^4 \right)^{1/2} \alpha^{1/4} \approx 1.58 \left( 3.63 + 4 \frac{\gamma^2}{\alpha} \right)^{1/2} \alpha^{1/4},$$

and the condition (4.10) (with  $y = p/\alpha^{1/4}$ ) is

$$(7.11) \quad \frac{5\pi^2}{6[\Gamma(\frac{3}{4})]^4} - 3 - \frac{\pi}{2^{5/4} 3 [\Gamma(\frac{3}{4})]^2} y^2 + \frac{2^{3/2} 3^{1/2} [\Gamma(\frac{3}{4})]^2}{\pi \left( 5 + \frac{4\gamma^2}{\alpha} - \frac{[\Gamma(\frac{3}{4})]^2}{2^{1/4} \pi} y^2 \right)^{1/2}} > 0,$$

the positive real zeros of the left hand side with  $\gamma = \pm \frac{1}{2}$  are in Table 7.4.

$\alpha$	.25	.5	1	2	4	6	8	10
$p_b$	1.62	2.04	2.56	3.18	3.90	4.38	4.75	5.05
$p_t$	3.32	3.43	3.71	4.13	4.69	5.10	5.42	5.68

TABLE 7.4. The positive real roots,  $p_t$  and  $p_b$ , of the function in (7.11) for the condition (4.10) (Theorem 1.4).

- (Theorem 1.5) the condition (4.12) is

$$(7.12) \quad p > \frac{2^{1/8} \pi^{3/4} C^{7/2}}{\Gamma(\frac{3}{4}) (C^7 \pi^{1/2} + 4 [\Gamma(\frac{3}{4})]^4)^{1/2}} \left( 1 + 4 \frac{\gamma^2}{\alpha} \right)^{1/2} \alpha^{1/4} \\ \approx 1.29 \left( 1 + 4 \frac{\gamma^2}{\alpha} \right)^{1/2} \alpha^{1/4},$$

and the condition (4.14) with  $y = p/\alpha^{1/4}$  is

$$(7.13) \quad \left( \frac{2^{7/4}[\Gamma(\frac{3}{4})]^2}{C^7\pi^{1/2}} - \frac{1}{2^{5/4}[\Gamma(\frac{3}{4})]^2} \right) y^2 + \frac{5\pi}{2[\Gamma(\frac{3}{4})]^4} - \frac{3 \cdot 2^{1/6}}{C^{14/3}} \left( \left( 5 + 4\frac{\gamma^2}{\alpha} \right) y^4 - \frac{[\Gamma(\frac{3}{4})]^2}{2^{1/4}\pi} y^6 \right)^{1/3} > 0,$$

the positive real zeros of the left hand side with  $\gamma = \pm \frac{1}{2}$  are in Table 7.5.

$\alpha$	.25	.5	1	2	4	6	8	10
$p_b$	1.41	1.84	2.36	2.50	3.68	4.15	4.51	4.80
$p_t$	3.30	3.41	3.66	4.05	4.59	4.97	5.27	5.53

TABLE 7.5. The positive real roots,  $p_t$  and  $p_b$ , of the function in (7.13) for the condition (4.14) (Theorem 1.5).

- Numerical simulations: the results for the super Gaussian with the quadratic phase  $\gamma = \pm \frac{1}{2}$  are given in Table 7.6. The rows denoted by  $p_b^+$ ,  $p_s^+$ ,  $p_b^-$  and  $p_s^-$  are thresholds for blow up and global existence/scattering for the positive phase  $\gamma = +\frac{1}{2}$  and negative phase  $\gamma = -\frac{1}{2}$ , correspondingly.

To compare the conditions (7.7) - (7.13) with the numerics, we graph the dependence of  $p$  on  $\alpha$  in Figures 7.3 and 7.2 separately for positive and negative values of the phase  $\gamma = \pm \frac{1}{2}$ . We plot  $\frac{p}{\sqrt[4]{\alpha}}$  on the vertical axis to observe the asymptotics as  $\alpha \rightarrow \infty$ .

$\alpha$	.25	.5	1	2	4	6	8	10
$p_s^+$	2.18	2.27	2.47	2.76	3.14	3.41	3.63	3.81
$p_b^+$	2.19	2.28	2.48	2.77	3.15	3.42	3.64	3.82
$p_s^-$	1.02	1.33	1.69	2.12	2.60	2.92	3.17	3.38
$p_b^-$	1.03	1.34	1.70	2.11	2.61	2.93	3.18	3.39

TABLE 7.6. Numerical results for blow up threshold ( $p \geq p_b^\pm$ ) and global existence ( $p \leq p_s^\pm$ ). The sign in the superscript indicates the positive or negative sign of  $\gamma$ , correspondingly.

*Remark 7.1.* Numerical simulations showed that, for example, when  $\alpha = 2$  for  $2.3995 \leq p \leq 6$  the blow up occurs over the origin. When  $p \geq 10$  the blow up happens on a *contracting sphere*. This phenomena we originally discussed in our heuristic analysis in [17], it was also numerically obtained in [11].

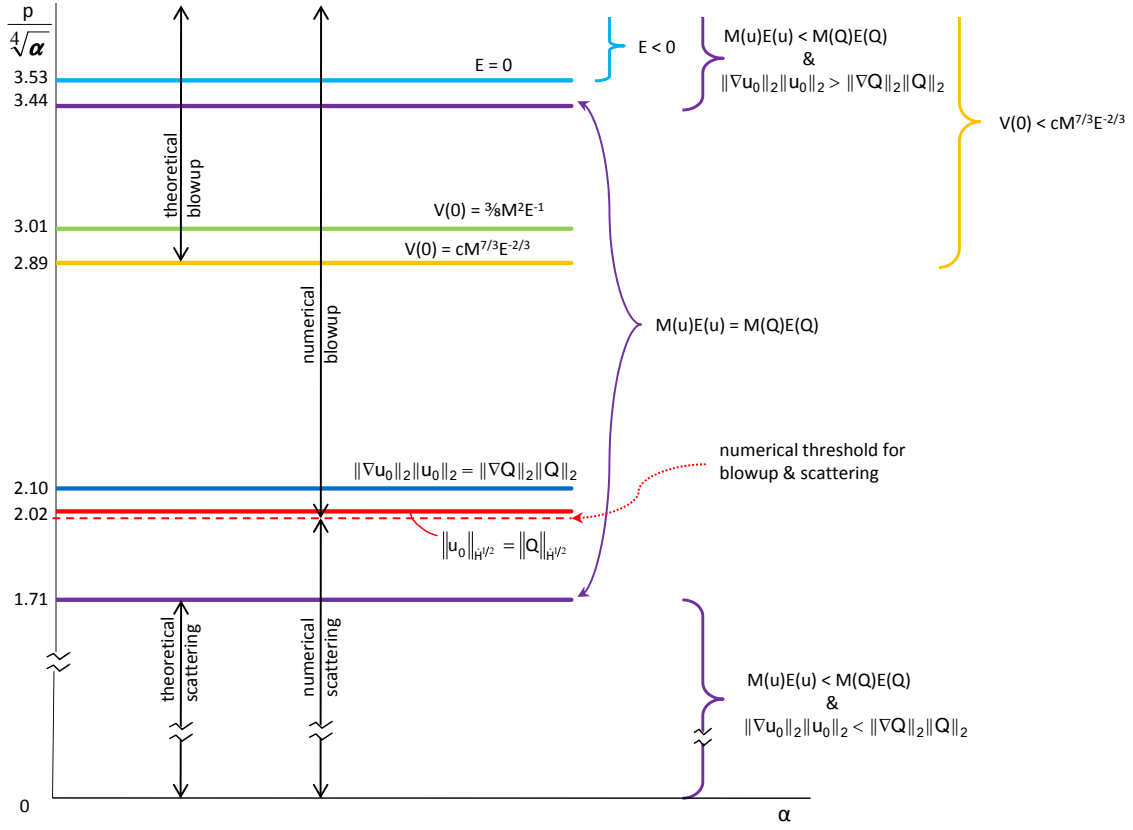


FIGURE 7.1. Global behavior of the solutions with the super Gaussian initial data  $u_0(r) = p e^{-\alpha r^4/2}$ . The line denoted by  $V(0) = 3/8 M^2 E^{-1}$  is the threshold for blow up from Theorem 1.4, see (7.5); similarly, the line denoted by  $V(0) = c M^{7/3} E^{-2/3}$  is the threshold for blow up from Theorem 1.5, see (7.6). The line “theoretical scattering” is given by Thm. 1.1, see (7.4). The numerical threshold (dashed line) comes from Table 7.1 normalized by  $\sqrt[4]{\alpha}$ . For all other values refer to text.



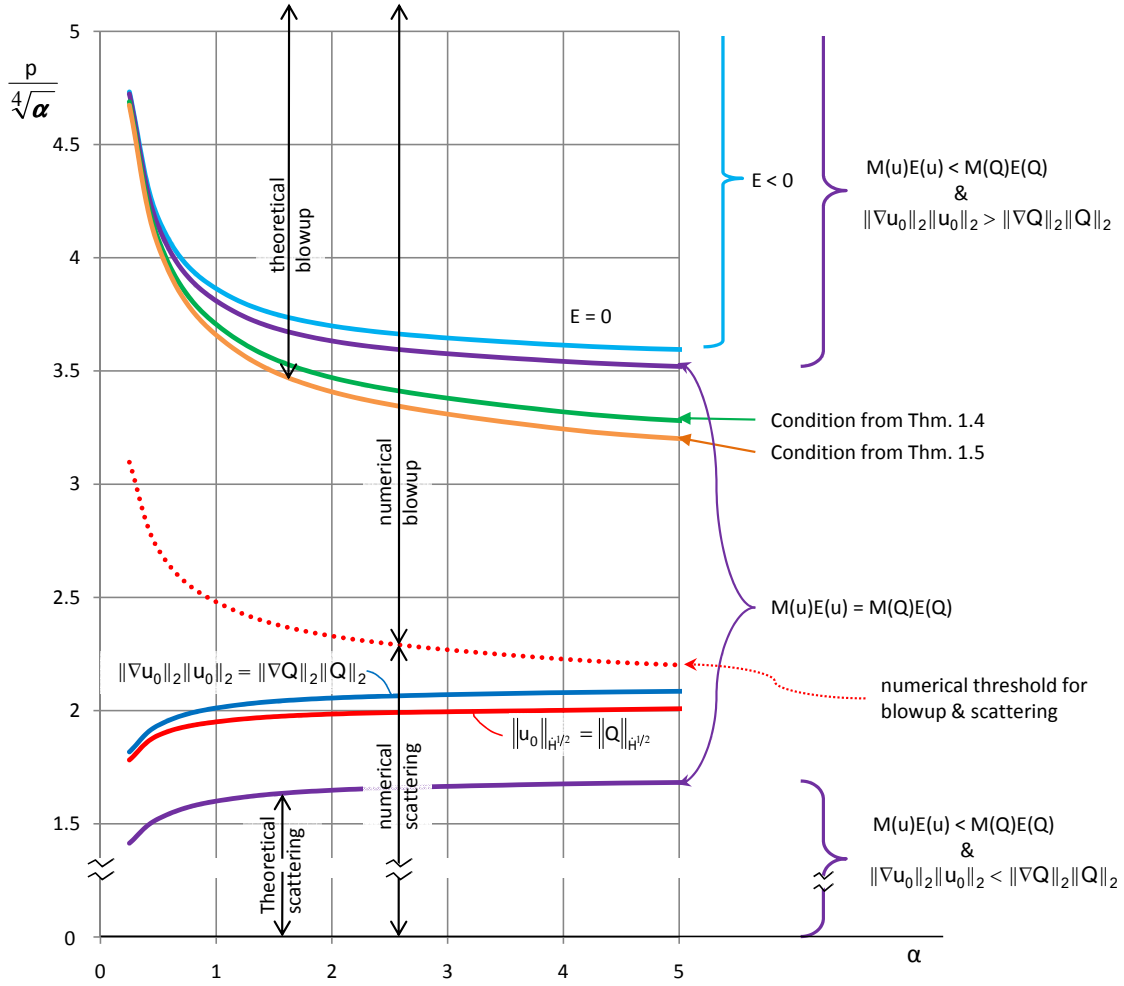


FIGURE 7.2. Global behavior of solutions to (1.1) with the super Gaussian initial data with the positive quadratic phase  $u_0(r) = p e^{-\alpha r^4/2} e^{+i\frac{1}{2}r^2}$ . The curve denoted by “Condition from Thm. 1.4” comes from the largest positive root of the equation in (7.11), namely, values  $p_t/\sqrt[4]{\alpha}$  in Table 7.4. Similarly, the curve denoted by “Condition from Thm. 1.5” comes from the largest positive root of the equation in (7.13), namely, values  $p_t/\sqrt[4]{\alpha}$  in Table 7.5. The dotted line “numerical threshold” is plotted from the values  $p_s^+/\sqrt[4]{\alpha}$  and  $p_b^+/\sqrt[4]{\alpha}$  (indistinguishable) from Table 7.6. The curve “theoretical scattering” is provided by Thm. 1.1, see (7.9) and values  $p_1$  in Table 7.2.

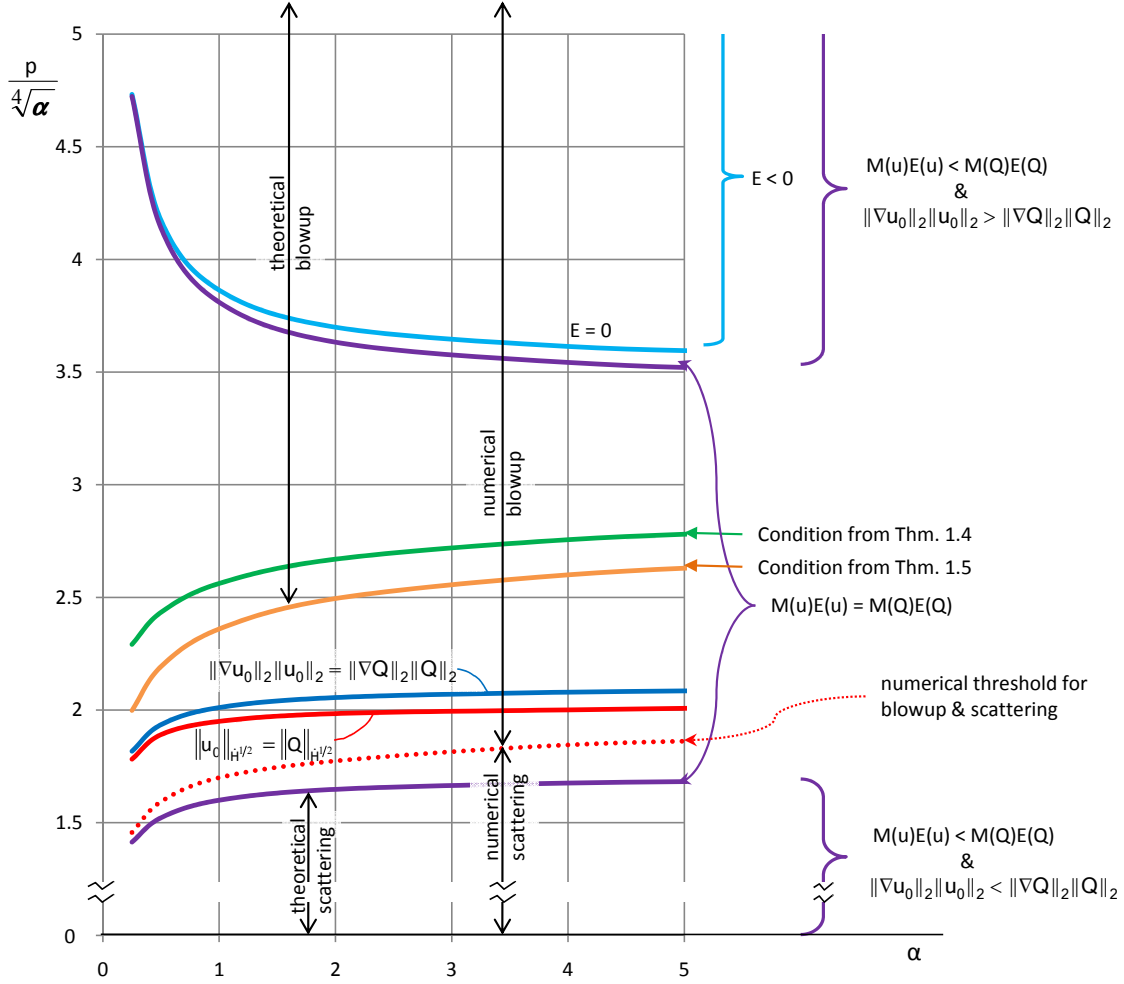


FIGURE 7.3. Global behavior of solutions to (1.1) with the super Gaussian initial data with the negative quadratic phase  $u_0(r) = p e^{-\alpha r^4/2} e^{-i\frac{1}{2}r^2}$ . The curve denoted by “Condition from Thm. 1.4” comes from the smallest positive root of the equation in (7.11), namely, values  $p_b/\sqrt[4]{\alpha}$  in Table 7.4. Similarly, the curve denoted by “Condition from Thm. 1.5” comes from the smallest positive root of the equation in (7.13), namely, values  $p_b/\sqrt[4]{\alpha}$  in Table 7.5. The dotted line “numerical threshold” is plotted from the values  $p_s^-/\sqrt[4]{\alpha}$  and  $p_b^-/\sqrt[4]{\alpha}$  (indistinguishable) from Table 7.6. The curve “theoretical scattering” is the same as in Fig. 7.3 and is provided by Thm. 1.1, see (7.9) and values  $p_1$  in Table 7.2.

**7.3. Conclusions.** The above computations show

- (1) Consistency with Conjecture 3: if  $u_0$  is *real*, then  $\|u_0\|_{\dot{H}^{1/2}} < \|Q\|_{\dot{H}^{1/2}}$  implies  $u(t)$  scatters.
- (2) Consistency with Conjecture 4 (since  $u_0$  is based upon a radial profile that is *monotonically decreasing*): if  $\|u_0\|_{\dot{H}^{1/2}} > \|Q\|_{\dot{H}^{1/2}}$ , then  $u(t)$  blows-up in finite time.
- (3) The condition “ $\|u_0\|_{L^2}\|\nabla u_0\|_{L^2} < \|Q\|_{L^2}\|\nabla Q\|_{L^2}$  *implies scattering*” is not valid (unless  $M[u]E[u] < M[Q]E[Q]$  as in Theorem 1.1).
- (4) In all three cases (real data, data with positive phase and with negative phase) Theorems 1.4 and 1.5 provide new range on blow up than was previously known from our Theorem 1.1. Furthermore, Theorem 1.5 provides the best results.

## 8. OFF-CENTERED GAUSSIAN PROFILE

Next we consider the off-centered Gaussian profile:

$$(8.1) \quad u_0(x) = p r^2 e^{-\alpha r^2} e^{i\gamma r^2}, \quad r = |x|, x \in \mathbb{R}^3.$$

For this initial data we calculate

$$\begin{aligned} M[u] &= \frac{15\pi^{3/2}p^2}{32\sqrt{2}\alpha^{7/2}}, \quad \|\nabla u_0\|_{L^2}^2 = \frac{3\pi^{3/2}p^2}{32\sqrt{2}\alpha^{5/2}} \left(11 + 35\frac{\gamma^2}{\alpha^2}\right), \\ E[u] &= \frac{3\pi^{3/2}p^2}{64\sqrt{2}\alpha^{5/2}} \left(11 + 35\frac{\gamma^2}{\alpha^2} - \frac{315p^2}{2^{10}\sqrt{2}\alpha^3}\right), \\ V(0) &= \frac{105\pi^{3/2}p^2}{128\sqrt{2}\alpha^{9/2}}, \quad V_t(0) = \frac{105\gamma\pi^{3/2}p^2}{16\sqrt{2}\alpha^{9/2}} \\ \|u_0\|_{\dot{H}^{1/2}}^2 &= 32\pi^2 \int_0^\infty R \left| \int_0^\infty r^3 \sin(2\pi Rr) e^{-\alpha r^2} e^{i\gamma r^2} dr \right|^2 dR = \frac{3\pi p^2}{4\alpha^3} \frac{(1 + 2\frac{\gamma^2}{\alpha^2})}{(1 + \frac{\gamma^2}{\alpha^2})^{1/2}}. \end{aligned}$$

**8.1. Real off-centered Gaussian.** When  $\gamma = 0$ , we have

- $E[u] > 0$  if

$$(8.2) \quad p < \frac{32}{3} \left( \frac{11\sqrt{2}}{35} \right)^{1/2} \alpha^{3/2} \approx 7.11 \alpha^{3/2};$$

- the condition on the mass and gradient  $\|u_0\|_{L^2}^2 \|\nabla u_0\|_{L^2}^2 < \|Q\|_{L^2}^2 \|\nabla Q\|_{L^2}^2$  implies

$$(8.3) \quad p < \left( \frac{2^{11}}{165\pi^3} \right)^{1/4} \|Q\|_2 \alpha^{3/2} \approx 3.46 \alpha^{3/2};$$

- the mass-energy condition  $M[u]E[u] < M[Q]E[Q]$  is

$$\frac{45\pi^3 p^4}{2^{12}\alpha^6} \left( 11 - \frac{315p^2}{2^{10}\sqrt{2}\alpha^3} \right) < \frac{1}{2} \|Q\|_{L^2}^4,$$

and thus, we obtain

$$(8.4) \quad p < 2.73 \alpha^{3/2} \quad \text{and} \quad p > 7.04 \alpha^{3/2}.$$

- the invariant norm condition  $\|u_0\|_{\dot{H}^{1/2}}^2 < \|Q\|_{\dot{H}^{1/2}}^2$  is

$$(8.5) \quad p < \frac{2}{(3\pi)^{1/2}} \|Q\|_{\dot{H}^{1/2}} \alpha^{3/2} \approx 3.43 \alpha^{3/2}.$$

- (Theorems 1.4) the condition (4.4) is

$$(8.6) \quad p > \frac{32}{21} \left( \frac{62\sqrt{2}}{5} \right)^{1/2} \alpha^{3/2} \approx 6.38 \alpha^{3/2}$$

- (Theorems 1.5) the condition (4.5) is

$$(8.7) \quad p > \frac{2^5 \cdot 2^{1/4} \cdot 7^2 \cdot 11^{1/2}}{3 \cdot 5^{1/2} (7^5 + 2^5 \cdot 3^{3/2} \cdot 5^2 \pi^{1/2})^{1/2}} \alpha^{3/2} \approx 5.93 \alpha^{3/2},$$

- Numerical simulations: the results for the off-centered Gaussian initial data (8.1) are in Table 8.1. For  $p \geq p_b$  the blow up was observed, for  $p \leq p_s$  the solution dispersed over time. We obtain that  $p_s/\alpha^{3/2} \approx 3.57$  and  $p_b/\alpha^{3/2} \approx 3.58$ .

$\alpha$	.25	.5	1	1.5	2	3	4	5
$p_s$	0.44	1.26	3.57	6.57	10.11	18.5	28.4	40.0
$p_b$	0.45	1.27	3.58	6.58	10.12	18.6	28.5	40.1

TABLE 8.1. The numerical results for blowing up ( $p \geq p_b$ ) and global existence ( $p \leq p_s$ ) for the off-centered Gaussian initial data depending on the parameter  $\alpha$ .

To compare all the above conditions (8.2) - (8.7) with the numerics, we graph the dependence of  $p$  on  $\alpha$  in Figure 6.1. For clarity of presentation we plot  $\frac{p}{\alpha^{3/2}}$  on the vertical axis.

**8.2. Off-centered Gaussian with quadratic phase.** When  $\gamma \neq 0$ , we have

- $E[u] > 0$  if

$$(8.8) \quad p < \frac{32}{3} \left( \frac{\sqrt{2}}{35} \right)^{1/2} \left( 11 + 35 \frac{\gamma^2}{\alpha^2} \right)^{1/2} \alpha^{3/2} \approx 2.14 \left( 11 + 35 \frac{\gamma^2}{\alpha^2} \right)^{1/2} \alpha^{3/2};$$

- the condition on the mass and gradient  $\|u_0\|_{L^2}^2 \|\nabla u_0\|_{L^2}^2 < \|Q\|_{L^2}^2 \|\nabla Q\|_{L^2}^2$  implies

$$(8.9) \quad p < \left( \frac{2^{11}}{15\pi^3} \right)^{1/4} \|Q\|_2 \left( 11 + 35 \frac{\gamma^2}{\alpha^2} \right)^{-1/4} \alpha^{3/2} \approx 6.29 \left( 11 + 35 \frac{\gamma^2}{\alpha^2} \right)^{-1/4} \alpha^{3/2};$$

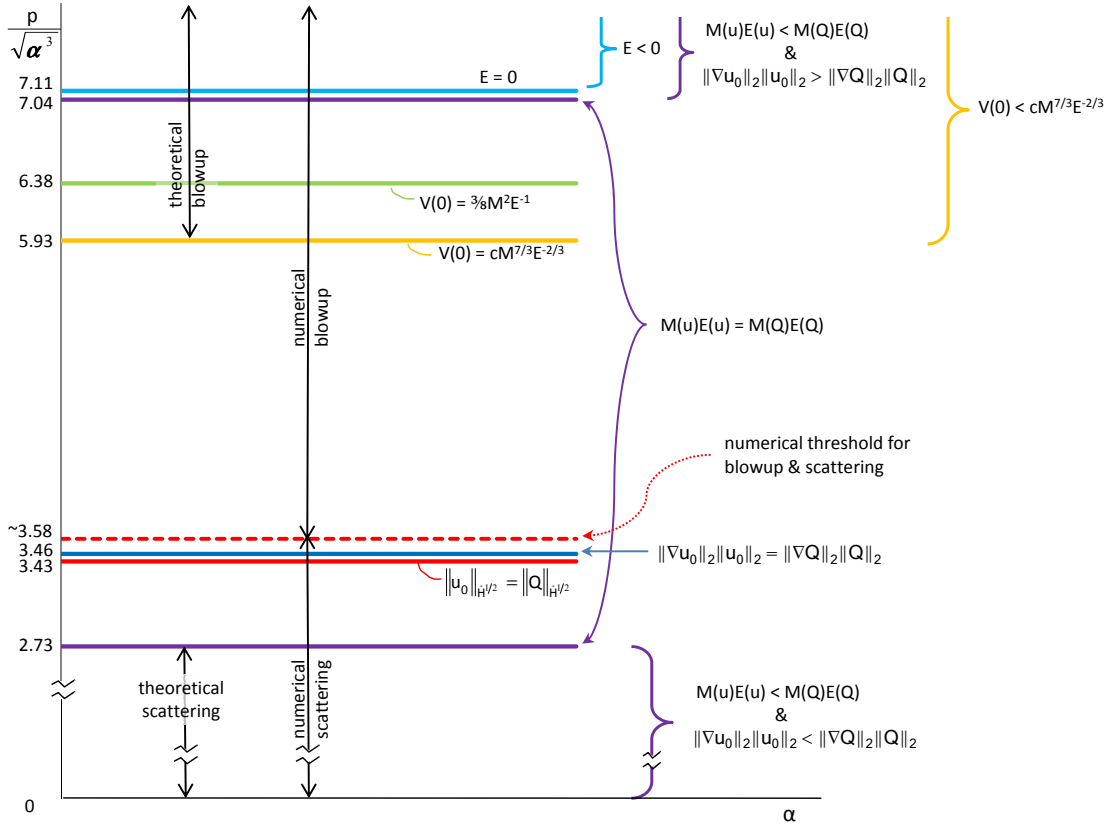


FIGURE 8.1. Global behavior of the solutions to (1.1) with the real off-centered Gaussian initial data (8.1). The line denoted by  $V(0) = \frac{3}{8}M^2E^{-1}$  is the threshold for blow up from Theorem 1.4, see (8.6); similarly, the line denoted by  $V(0) = cM^{7/3}E^{-2/3}$  is the threshold for blow up from Theorem 1.5, see (8.7). The line “theoretical scattering” is given by Thm. 1.1, see (8.4). Observe that the numerical threshold (dashed line, values are given in Table 8.1) is away from the line  $\|u_0\|_{\dot{H}^{1/2}} = \|Q\|_{\dot{H}^{1/2}}$ , see (8.5), which is different compared to real Gaussian and real super Gaussian initial data, see Fig. 6.1 and 7.1.

- the mass-energy condition  $M[u]E[u] < M[Q]E[Q]$  is

$$(8.10) \quad \frac{45\pi^3 p^4}{2^{12}\alpha^6} \left( 11 + 35\frac{\gamma^2}{\alpha^2} - \frac{315p^2}{2^{10}\sqrt{2}\alpha^3} \right) - \frac{1}{2} \|Q\|_2^4 < 0,$$

the real positive zeros of the left hand side when  $\gamma = \pm\frac{1}{2}$  given in Table 8.2.

$\alpha$	.25	.5	1	1.5	2	3	4	5
$p_1$	0.17	0.65	2.3	4.58	7.31	13.84	21.54	30.27
$p_2$	3.29	5.14	9.51	15.14	21.9	38.26	57.8	80.05

TABLE 8.2. Real positive zeros of the function in (8.10) when  $\gamma = \pm\frac{1}{2}$ .

- the invariant norm condition  $\|u_0\|_{\dot{H}^{1/2}}^2 < \|Q\|_{\dot{H}^{1/2}}^2$  is

$$(8.11) \quad p < \frac{2}{(3\pi)^{1/2}} \|Q\|_{\dot{H}^{1/2}} \frac{(1 + \frac{\gamma^2}{\alpha^2})^{1/4}}{(1 + 2\frac{\gamma^2}{\alpha^2})^{1/2}} \alpha^{3/2} \approx 3.43 \frac{(1 + \frac{\gamma^2}{\alpha^2})^{1/4}}{(1 + 2\frac{\gamma^2}{\alpha^2})^{1/2}} \alpha^{3/2}.$$

- (Theorems 1.4) the condition (4.4) is

$$(8.12) \quad p > \frac{32 \cdot 2^{1/4}}{3} \left( \frac{62}{5 \cdot 7^2} + \frac{\gamma^2}{\alpha^2} \right)^{1/2} \alpha^{3/2} \approx 12.68 \left( 0.253 + \frac{\gamma^2}{\alpha^2} \right) \alpha^{3/2}$$

and the condition (4.10) with  $y = p/\alpha^{3/2}$  is

$$(8.13) \quad \frac{2^6 \sqrt{105}}{7 \sqrt{2^{11}(11 + \frac{35\gamma^2}{\alpha^2}) - 315\sqrt{2}y^2}} - \frac{3 \cdot 7^2}{2^{11}} y^2 + \frac{32}{15\sqrt{2}} > 0,$$

the positive real roots of which when  $\gamma = \pm\frac{1}{2}$  are in Table 8.3.

$\alpha$	.25	.5	1	1.5	2	3	4	5
$p_b$	0.60	1.79	5.37	10.25	16.18	30.63	47.97	67.80
$p_t$	3.29	5.14	9.49	14.99	21.50	37.00	55.27	75.91

TABLE 8.3. The positive real roots of the function in (8.13) when  $\gamma = \pm\frac{1}{2}$  for the off-centered Gaussian initial data.

- (Theorems 1.5) the condition (4.5) is

$$(8.14) \quad p > \frac{2^5 \cdot 2^{1/4} \cdot 7^2}{3 \cdot 5^{1/2}(7^5 + 2^5 \cdot 3^{3/2} \cdot 5^2 \pi^{1/2})^{1/2}} \left( 11 + 35\frac{\gamma^2}{\alpha^2} \right)^{1/2} \alpha^{3/2} \\ \approx 1.79 \left( 11 + 35\frac{\gamma^2}{\alpha^2} \right)^{1/2} \alpha^{3/2}$$

and the condition (4.14) with  $y = p/\alpha^{3/2}$  is

$$(8.15) \quad \left( \frac{(2^6 \cdot 3^{3/2} \cdot 5^2 \pi^{1/2} - 7^5)}{2^{5/2} \cdot 105} y^2 + \frac{2^8 \cdot 7^3 \cdot 11}{3^3 \cdot 5^2} \right)^3 - 84\pi \left( 2^{11} (11 + 35 \frac{\gamma^2}{\alpha^2}) - 315\sqrt{2} y^2 \right) y^4 > 0,$$

the positive real zeros of which with  $\gamma = \pm \frac{1}{2}$  is in Table 8.4.

$\alpha$	.25	.5	1	1.5	2	3	4	5
$p_b$	0.30	1.16	4.15	8.46	13.79	26.94	42.92	61.04
$p_t$	3.29	5.14	9.45	14.80	21.05	35.75	52.97	72.38

TABLE 8.4. The positive real roots of the function in (8.15) when  $\gamma = \pm \frac{1}{2}$  for the off-centered Gaussian initial data.

- Numerical simulations: the results for the off-centered Gaussian initial data with nonzero phase (8.1) are in Table 8.5. For  $p \geq p_b$  the blow up was observed, for  $p \leq p_s$  the solution dispersed over time.

$\alpha$	.25	.5	1	1.5	2	3	4	5
$p_s^+$	n/a	n/a	5.78	8.93	12.68	21.5	31.9	43.6
$p_b^+$	n/a	n/a	5.79	8.94	12.69	21.6	32.0	43.7
$p_s^-$	.18	.69	2.50	5.11	8.337	16.2	25.8	36.8
$p_b^-$	.19	.70	2.51	5.12	8.338	16.3	25.9	36.9

TABLE 8.5. The numerical results for blow up and scattering thresholds for the off-centered Gaussian initial data with the phase  $\gamma = \pm \frac{1}{2}$ : blow up if  $p \geq p_b^\pm$  and global existence/scattering if  $p \leq p_s^\pm$ .

To compare all the above conditions (8.8) - (8.15) with the numerical data, we graph the dependence of  $p$  on  $\alpha$  in Figures 8.2 and 8.3. For clarity of presentation we plot  $\frac{p}{\alpha^{3/2}}$  on the vertical axis.

**8.3. Conclusions.** The above computations show

- (1) Consistency with Conjecture 3: if  $u_0$  is *real*, then  $\|u_0\|_{\dot{H}^{1/2}} < \|Q\|_{\dot{H}^{1/2}}$  implies  $u(t)$  scatters.
- (2) Consistency with Conjecture 4: Numerical simulations show that the blow up threshold line is higher than the line  $\|u_0\|_{\dot{H}^{1/2}} = \|Q\|_{\dot{H}^{1/2}}$ , although this profile is not monotonic.

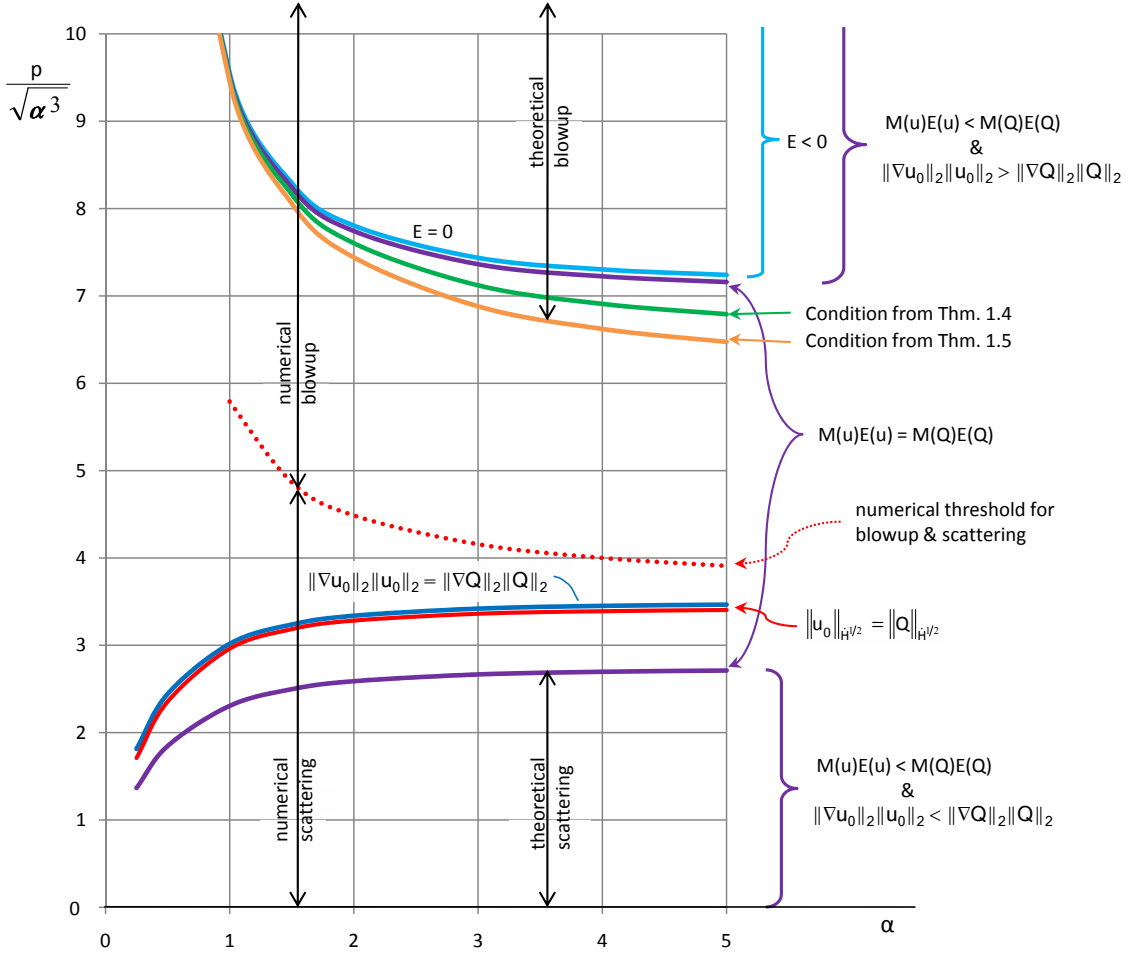


FIGURE 8.2. Global behavior of the solutions for the off-centered Gaussian initial data with positive quadratic phase. The curve denoted by “Condition from Thm. 1.4” comes from the largest positive root of the equation in (8.13), namely, values  $p_t/\sqrt[3]{\alpha^2}$  in Table 8.3. Similarly, the curve denoted by “Condition from Thm. 1.5” comes from the largest positive root of the equation in (8.15), namely, values  $p_t/\sqrt[3]{\alpha^2}$  in Table 8.4. The dotted line “numerical threshold” is plotted from the values  $p_s^+/\sqrt[3]{\alpha^2}$  and  $p_b^+/\sqrt[3]{\alpha^2}$  (indistinguishable) from Table 8.5. The curve “theoretical scattering” is provided by Thm. 1.1, see (8.10) and Table 8.2.



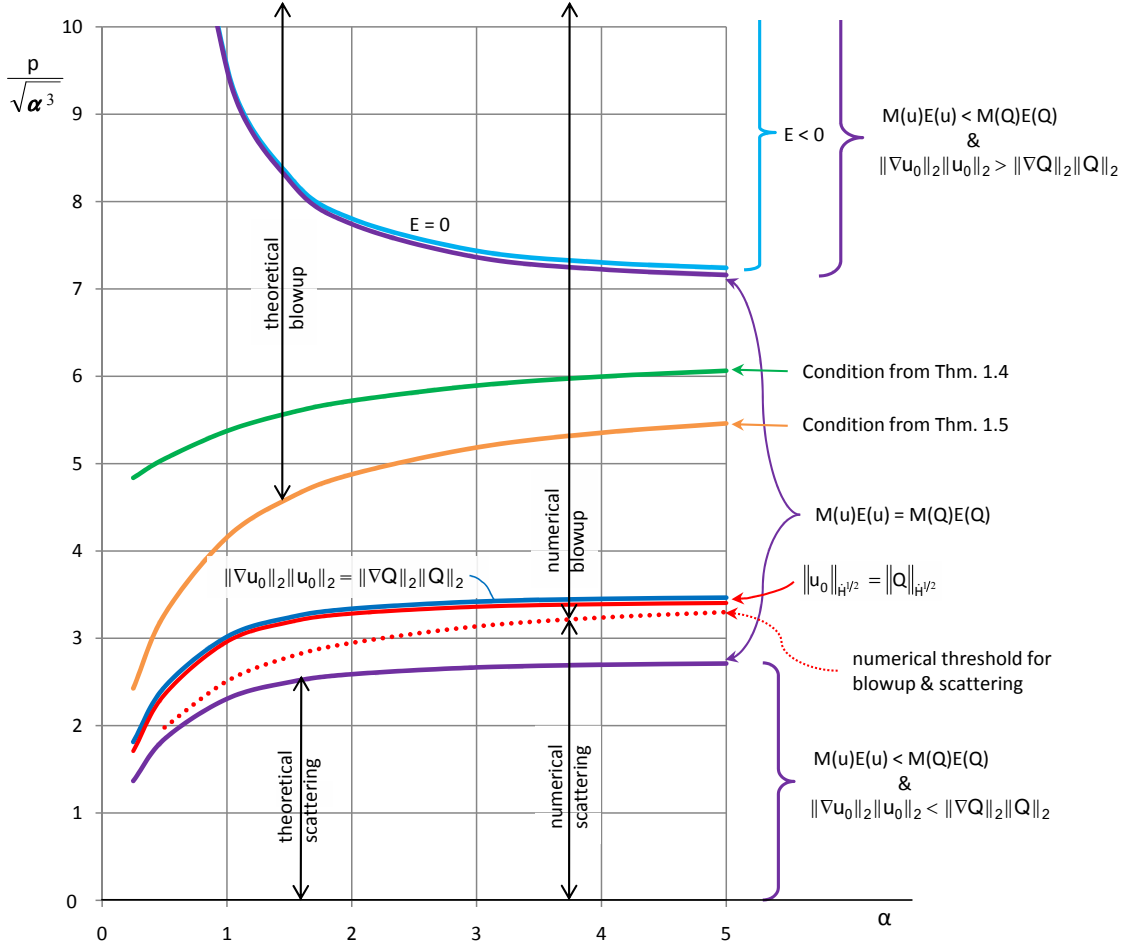


FIGURE 8.3. Global behavior of the solutions for the off-centered Gaussian initial data with negative quadratic phase. The curve denoted by “Condition from Thm. 1.4” comes from the smallest positive root of the equation in (8.13), namely, values  $p_b/\sqrt[3]{\alpha^2}$  in Table 8.3. Similarly, the curve denoted by “Condition from Thm. 1.5” comes from the smallest positive root of the equation in (8.15), namely, values  $p_b/\sqrt[3]{\alpha^2}$  in Table 8.4. The dotted line “numerical threshold” is plotted from the values  $p_s^-/\sqrt[3]{\alpha^2}$  and  $p_b^-/\sqrt[3]{\alpha^2}$  (indistinguishable) from Table 8.5. The curve “theoretical scattering” is provided by Thm. 1.1, see (8.10) and Table 8.2.

- (3) The condition “ $\|u_0\|_{L^2}\|\nabla u_0\|_{L^2} < \|Q\|_{L^2}\|\nabla Q\|_{L^2}$  implies scattering” is not valid (unless  $M[u]E[u] < M[Q]E[Q]$  as in Theorem 1.1), for example, when there is a negative initial phase present.
- (4) In all three cases (real data, data with positive phase and with negative phase) Theorems 1.4 and 1.5 provide new range on blow up than was previously known from our Theorem 1.1. Furthermore, Theorem 1.5 provides the best results.

## 9. OSCILLATORY GAUSSIAN PROFILE

Lastly we consider a Gaussian profile with oscillations (referred from now on as ‘oscillatory Gaussian’), it is a sign changing profile:

$$(9.1) \quad u_{\beta,0}(x) = p \cos(\beta r) e^{-r^2} e^{i\gamma r^2}.$$

Here, we fix the Gaussian  $e^{-r^2}$  itself and change the frequency of oscillation  $\beta$ . These data generate a solution to NLS denoted by  $u_\beta$ . We obtain:

$$\begin{aligned} M[u_\beta] &= \frac{\pi^{3/2}p^2}{4\sqrt{2}} m(\beta), \quad \|u_{\beta,0}\|_{L^2}^2 = \frac{\pi^{3/2}p^2}{4\sqrt{2}} a(\beta, \gamma), \\ E[u_\beta] &= \frac{\pi^{3/2}p^2}{8\sqrt{2}} (a(\beta, \gamma) - p^2 b(\beta)), \\ V(0) &= \frac{\pi^{3/2}p^2}{16\sqrt{2}} v(\beta), \quad V_t(0) = \gamma \frac{\pi^{3/2}p^2}{2\sqrt{2}} v(\beta), \\ \|u_{\beta,0}\|_{H^{1/2}}^2 &= 32\pi^2 p^2 \int_0^\infty R \left| \int_0^\infty r \cos(\beta r) \sin(2\pi Rr) e^{-r^2} dr \right|^2 dR \\ &= \frac{\pi}{8} p^2 \left( \sqrt{2\pi} \beta \operatorname{erf}\left(\frac{\beta}{\sqrt{2}}\right) - 2\sqrt{\pi}(\beta^2 - 4)e^{-\beta^2/2} \right), \end{aligned}$$

where

$$\begin{aligned} m(\beta) &= 1 + (1 - \beta^2)e^{-\beta^2/2}, \\ a(\beta, \gamma) &= 3(1 + \gamma^2) + \beta^2 + (3(1 + \gamma^2) - \beta^2(1 + 6\gamma^2) + \beta^4\gamma^2) e^{-\beta^2/2}, \\ b(\beta) &= \frac{1}{16\sqrt{2}} \left( 3 + (1 - 2\beta^2)e^{-\beta^2} + 2(2 - \beta^2)e^{-\beta^2/4} \right), \\ v(\beta) &= 3 + (3 - 6\beta^2 + \beta^4)e^{-\beta^2/2}, \\ \operatorname{erf}(x) &= \frac{2}{\sqrt{\pi}} \int_0^x e^{-t^2} dt. \end{aligned}$$

We list some values of the  $\dot{H}^{1/2}$  norm of  $u_{\beta,0}$  in Table 9.1.

$\beta$	0	0.25	0.5	1.0	2.0	3.0	4.0	5.0	6.0
$\frac{1}{2}\ u_{\beta,0}\ _{\dot{H}^{1/2}}^2$	$\pi$	3.046	2.788	2.101	1.879	2.901	3.933	4.922	5.906
$p_{1/2}$	2.97	3.02	3.15	3.63	3.84	3.09	2.65	2.37	2.17

$\beta$	7.0	8.0	9.0	10.0	15.0	20.0	25.0
$\frac{1}{2}\ u_{\beta,0}\ _{\dot{H}^{1/2}}^2$	6.890	7.875	8.859	9.844	14.765	19.687	24.609
$p_{1/2}$	2.01	1.88	1.78	1.68	1.37	1.19	1.06

TABLE 9.1. The  $\dot{H}^{1/2}$  norm of  $u_{\beta,0}$  and values of  $p$  for which  $\|u_{\beta,0}\|_{\dot{H}^{1/2}}^2 = \|Q\|_{\dot{H}^{1/2}}^2$ .

**9.1. Real oscillatory Gaussian.** First, we consider the real oscillatory Gaussian data ( $\gamma = 0$ ). We have

- $E[u] > 0$  if

$$(9.2) \quad p < \left( \frac{a(\beta, 0)}{b(\beta)} \right)^{1/2};$$

- the condition on the mass and gradient  $\|u_{\beta}\|_{L^2}^2 \|\nabla u_{\beta,0}\|_{L^2}^2 < \|Q\|_{L^2}^2 \|\nabla Q\|_{L^2}^2$  implies

$$(9.3) \quad p < 2 \|Q\|_2 \left( \frac{6}{\pi^3 m(\beta) a(\beta, 0)} \right)^{1/4};$$

- the mass-energy condition  $M[u]E[u] < M[Q]E[Q]$  gives

$$(9.4) \quad \pi^3 m(\beta) (a(\beta, 0) - p^2 b(\beta)) p^4 - 32 \|Q\|_2^4 < 0, \quad \text{or} \quad p < p_1 \quad \text{and} \quad p > p_2,$$

where  $p_1$  and  $p_2$ , the real positive zeros of the cubic polynomial (in  $p^2$ ) above, given in Table 9.2.

$\beta$	0	0.25	0.5	1.0	1.45	2.0	2.5	2.77	3.0	3.61	4.0
$p_1$	2.72	2.76	2.88	3.27	3.48	3.16	2.72	2.55	2.43	2.22	2.12
$p_2$	3.81	3.87	4.06	5.00	6.84	10.49	13.11	13.42	13.31	12.97	13.14

$\beta$	5.0	6.0	7.0	8.0	9.0	10.0	15.0	20.0	25.0
$p_1$	1.91	1.76	1.64	1.53	1.45	1.38	1.13	0.98	0.88
$p_2$	14.75	17.17	19.81	22.48	25.17	27.87	41.47	55.13	68.82

TABLE 9.2. The values of  $p$  in the mass-energy threshold for the real oscillatory Gaussian.

- the values of  $p$ , denoted by  $p_{1/2}$ , for which  $\|u_{\beta,0}\|_{\dot{H}^{1/2}}^2 = \|Q\|_{\dot{H}^{1/2}}^2$ , are given in Table 9.1.

- (Theorem 1.4) the condition (4.4) is

$$(9.5) \quad p \geq b(\beta)^{-1/2} \left( a(\beta, 0) - \frac{3m(\beta)^2}{v(\beta)} \right)^{-1/2};$$

- (Theorem 1.5) the condition (4.5) is

$$(9.6) \quad p > 2\sqrt{2} C^{7/2} \frac{a(\beta, 0)^{1/2} v(\beta)^{3/4}}{(\pi^{3/2} m(\beta)^{7/2} + 8C^7 v(\beta)^{3/2} b(\beta))^{1/2}};$$

- Numerical simulations: the results for the (real) oscillatory Gaussian initial data are in Table 9.3. For  $p \geq p_b$  the blow up was observed, for  $p \leq p_s$  the solution dispersed over time.

$\beta$	0	0.25	0.5	1.0	2.0	3.0	4.0	5.0	6.0
$p_s$	2.93	2.98	3.11	3.601	4.583	4.13	3.29	2.92	2.72
$p_b$	2.94	2.99	3.12	3.605	4.585	4.14	3.30	2.93	2.73

$\beta$	7.0	8.0	9.0	10.0	15.0	20.0	25.0
$p_s$	2.61	2.53	2.48	2.455	2.42	2.49	2.52
$p_b$	2.62	2.54	2.49	2.456	2.43	2.50	2.53

TABLE 9.3. Numerical simulations for the (real) oscillatory Gaussian. Here, the blow up was observed for  $p > p_b$  and global existence for  $p < p_s$ .

To compare all conditions (9.2) - (9.6) with numerical data, we graph the dependence of  $p$  on  $\beta$  in Figure 9.1. We plot  $p/\sqrt{1+\beta^2}$  on the vertical axis.

**9.2. Oscillatory Gaussian with quadratic phase.** When  $\gamma \neq 0$  we have

- $E[u] > 0$  if

$$(9.7) \quad p < \left( \frac{a(\beta, \gamma)}{b(\beta)} \right)^{1/2};$$

- the condition on the mass and gradient  $\|u_\beta\|_{L^2}^2 \|\nabla u_{\beta,0}\|_{L^2}^2 < \|Q\|_{L^2}^2 \|\nabla Q\|_{L^2}^2$  implies

$$(9.8) \quad p < 2 \|Q\|_2 \left( \frac{6}{\pi^3 m(\beta) a(\beta, \gamma)} \right)^{1/4};$$

- the mass-energy condition  $M[u]E[u] < M[Q]E[Q]$  gives

$$(9.9) \quad \pi^3 m(\beta) (a(\beta, \gamma) - p^2 b(\beta)) p^4 - 32 \|Q\|_2^4 < 0 \quad \text{or} \quad p < p_1^\gamma \quad \text{and} \quad p > p_2^\gamma,$$

where  $p_1^\gamma$  and  $p_2^\gamma$ , the real positive zeros of the polynomial above with  $\gamma = \pm \frac{1}{2}$ , given in Table 9.4.

$\beta$	0	0.25	0.5	1.0	1.6	2.0	2.4	2.66	3.0	4.0
$p_1^\gamma$	2.42	2.47	2.62	3.13	3.39	3.09	2.74	2.56	2.39	2.10
$p_2^\gamma$	4.46	4.50	4.61	5.29	7.97	10.94	13.37	13.92	13.77	13.40

$\beta$	5.0	6.0	7.0	8.0	9.0	10.0	15.0	20.0	25.0
$p_1^\gamma$	1.90	1.75	1.63	1.53	1.45	1.38	1.13	0.98	0.88
$p_2^\gamma$	14.95	17.34	19.95	22.61	25.28	27.97	41.54	55.18	68.86

TABLE 9.4. The values of  $p$  for the mass-energy threshold for the oscillatory Gaussian with the phase  $\gamma = \pm \frac{1}{2}$ .

- the values of  $p$ , denoted by  $p_{1/2}^\gamma$ , for which  $\|u_{\beta,0}\|_{\dot{H}^{1/2}}^2 = \|Q\|_{\dot{H}^{1/2}}^2$ , are given in Table 9.5.

$\beta$	0	0.25	0.5	1.0	2.0	3.0	4.0	5.0	6.0
$\frac{1}{2}\ u_{0,\beta}\ _{\dot{H}^{1/2}}^2$	$\frac{\sqrt{5}}{2}\pi$	3.384	3.042	2.165	1.933	2.959	3.942	4.922	5.906
$p_{1/2}^\gamma$	2.81	2.86	3.02	3.58	3.79	3.06	2.65	2.37	2.17

$\beta$	7.0	8.0	9.0	10.0	15.0	20.0	25.0
$\frac{1}{2}\ u_{0,\beta}\ _{\dot{H}^{1/2}}^2$	6.890	7.875	8.859	9.844	14.765	19.687	24.609
$p_{1/2}^\gamma$	2.01	1.88	1.78	1.68	1.37	1.19	1.06

TABLE 9.5. The values of  $\|u_{\beta,0}\|_{\dot{H}^{1/2}}^2/p^2$  for the oscillatory Gaussian initial data with phase  $\gamma = \pm \frac{1}{2}$  and values of  $p_{1/2}^\gamma$  for which the  $\dot{H}^{1/2}$  norm threshold holds.

- (Theorem 1.4) the condition (4.4) is

$$(9.10) \quad p \geq b(\beta)^{-1/2} \left( a(\beta, \gamma) - \frac{3m(\beta)^2}{v(\beta)} \right)^{-1/2},$$

and the condition (4.10) is

$$(9.11) \quad 2\sqrt{3}m(\beta) + \left( \frac{v(\beta)}{3m(\beta)^2} (a(\beta, 0) - p^2 b(\beta)) - 3 \right) (a(\beta, \gamma) - p^2 b(\beta))^{1/2} v(\beta)^{1/2} > 0,$$

the real positive zeros of which are in Table 9.6.

- (Theorem 1.5) the condition (4.5) is

$$(9.12) \quad p > \frac{2^{3/4} C^{7/2} v^{3/4} a(\beta, \gamma)^{1/2}}{(\pi^{3/2} m(\beta)^{1/2} + 2^{3/2} C^7 v(\beta)^{3/2} b(\beta))^{1/2}},$$

$\beta$	0	0.25	0.5	1	1.6	2	2.4	2.66	3	4
$p$	2.68	2.74	2.93	3.83	7.02	9.86	12.05	12.58	12.53	12.55
$p$	4.39	4.42	4.52	5.07	7.88	10.89	13.30	13.83	13.67	13.30

$\beta$	5	6	7	8	9	10	15	20	25
$p$	14.29	16.79	19.47	22.19	24.91	27.64	41.31	55.01	68.73
$p$	14.86	17.26	19.88	22.55	25.23	27.93	41.51	55.16	68.85

TABLE 9.6. Zeros of the function in the inequality (9.11) Theorem 1.4 .

and the condition (4.14) is

$$(9.13) \quad \left( \frac{\pi^{3/2} m(\beta)^{3/2}}{2^{1/2} C^7 v(\beta)^{1/2}} - \frac{v(\beta) b(\beta)}{m(\beta)^2} \right) p^2 + \frac{v(\beta) a(\beta, 0)}{m(\beta)^2} - \frac{27\pi^3 p^4}{8 C^{14}} m(\beta) (a(\beta, \gamma) - p^2 b(\beta)) > 0,$$

the positive real zeros of which are listed in Table 9.7.

$\beta$	0	0.25	0.5	1	1.6	2	2.4	2.66	3	4
$p_b$	2.81	2.87	3.06	3.90	6.71	9.10	10.45	10.57	10.35	10.56
$p_t$	4.46	4.49	4.60	5.14	7.91	10.86	12.05	13.37	12.01	12.52

$\beta$	5	6	7	8	9	10	15	20	25
$p_b$	12.22	14.41	16.74	19.11	21.49	23.88	35.92	48.03	60.15
$p_t$	13.96	16.11	18.44	20.80	23.18	25.58	37.61	49.72	61.85

TABLE 9.7. The positive real zeros of the polynomial in (9.13), by Theorem 1.5.

- Numerical simulations: the results for the oscillatory Gaussian initial data with the phase  $\gamma = \pm \frac{1}{2}$  are in Table 9.8. For  $p \geq p_b$  the blow up was observed, for  $p \leq p_s$  the solution dispersed over time.

To compare all the above conditions (9.7) - (9.13) with the numerical data, we graph the dependence of  $p$  on  $\alpha$  in Figures 9.3 and 9.2. For clarity of presentation we plot  $\frac{p}{\sqrt{1 + \beta^2}}$  on the vertical axis.

**9.3. Conclusions.** The above computations show

- (1) Consistency with Conjecture 3: if  $u_0$  is *real*, then  $\|u_0\|_{\dot{H}^{1/2}} < \|Q\|_{\dot{H}^{1/2}}$  implies  $u(t)$  scatters.

$\beta$	0	0.25	0.5	1.0	2.0	3.0	4.0	5.0
$p_s^+$	3.56	3.60	3.70	4.07	4.94	4.75	3.70	3.19
$p_b^+$	3.57	3.61	3.71	4.08	4.941	4.76	3.71	3.20
$p_s^-$	2.42	2.47	2.63	3.20	4.263	3.64	2.98	2.70
$p_b^-$	2.43	2.48	2.64	3.21	4.26	3.65	2.99	2.71

$\beta$	6.0	7.0	8.0	9.0	10.0	15.0	20.0	25.0
$p_s^+$	2.92	2.76	2.66	2.59	2.55	2.48	2.53	2.56
$p_b^+$	2.93	2.77	2.67	2.60	2.56	2.49	2.54	2.57
$p_s^-$	2.56	2.47	2.42	2.38	2.377	2.37	2.44	2.48
$p_b^-$	2.57	2.48	2.43	2.39	2.378	2.38	2.45	2.49

TABLE 9.8. Threshold for blow up and scattering in numerical simulations for the oscillatory Gaussian with the phase  $\gamma = \pm \frac{1}{2}$ .

- (2) Consistency with Conjecture 4: observe that the real oscillatory Gaussian initial data  $u_0$  is a radial profile that is not *monotonically decreasing*, thus, the condition  $\|u_0\|_{\dot{H}^{1/2}} > \|Q\|_{\dot{H}^{1/2}}$  does not necessarily imply that  $u(t)$  blows-up in finite time.
- (3) The condition “ $\|u_0\|_{L^2}\|\nabla u_0\|_{L^2} < \|Q\|_{L^2}\|\nabla Q\|_{L^2}$  *implies scattering*” is not valid (unless  $M[u]E[u] < M[Q]E[Q]$  as in Theorem 1.1) even for the real oscillatory Gaussian initial data.
- (4) In all three cases (real data, data with positive phase and with negative phase) Theorems 1.4 and 1.5 provide new range on blow up than was previously known from our Theorem 1.1. For small oscillations (small  $\beta$ ) Theorem 1.4 provides the best range for blow up and for large oscillations Theorem 1.5 provides a better result.

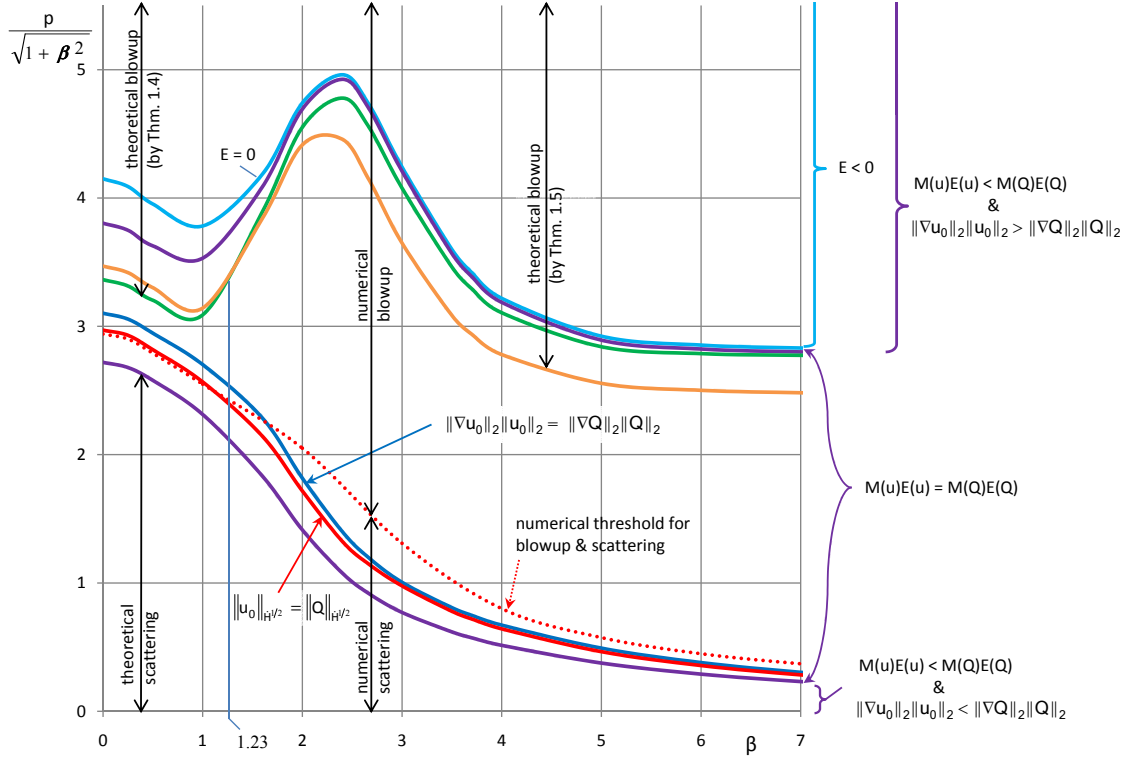


FIGURE 9.1. Global behavior of the solutions to (1.1) with the real oscillatory Gaussian initial data 9.1, with the rescaled vertical axis  $p/\sqrt{1+\beta^2}$ . The blow up threshold curve denoted “by Thm. 1.4” is given by (9.5) and the blow up threshold curve denoted “by Thm. 1.5” is given by (9.6). Observe that these curves intersect at  $\beta \approx 1.23$ . Therefore, for small oscillations ( $\beta < 1.23$ ) Theorem 1.4 provides the best range for blow up, correspondingly, for large oscillations ( $\beta > 1.23$ ) Theorem 1.5 gives a better range. The curve “theoretical scattering” is given by Thm. 1.1, see (9.4) and values  $p_1$  in Table 9.2. Observe that the numerical threshold (dotted curve, values are given in Table 9.3) for small oscillations coincide with the curve  $\|u_0\|_{\dot{H}^{1/2}} = \|Q\|_{\dot{H}^{1/2}}$ , see Table 9.1, and for large oscillations these curves separate.



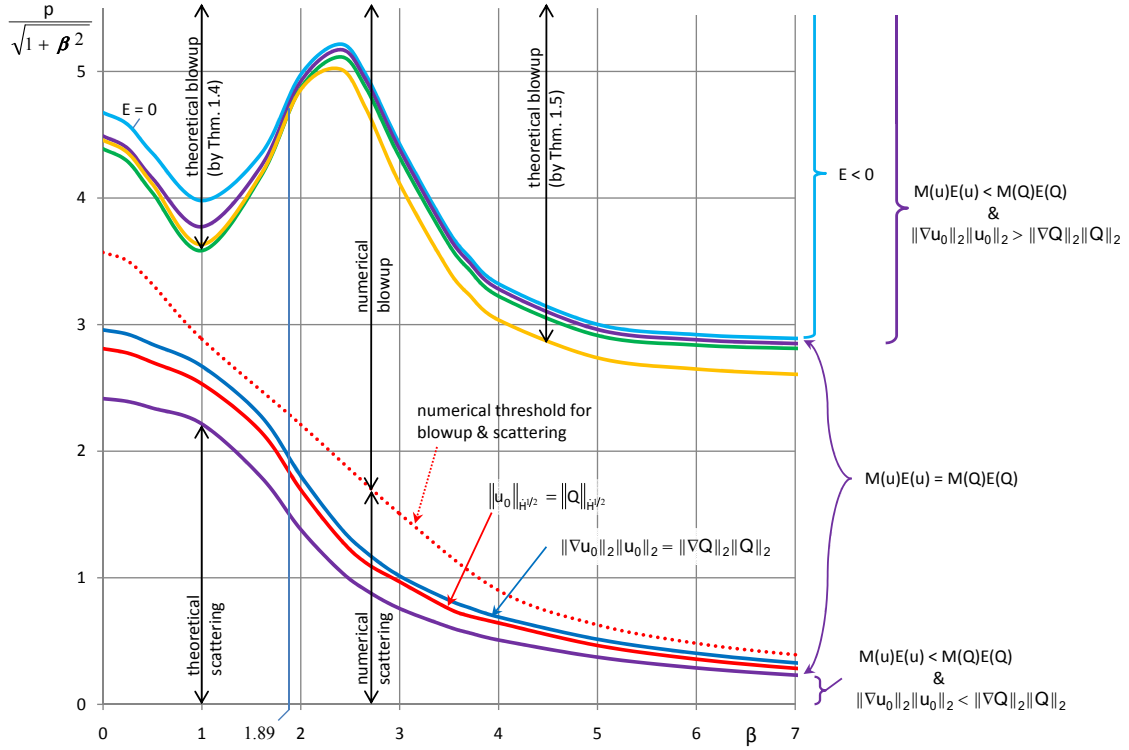


FIGURE 9.2. Global behavior of the solutions to (1.1) with the oscillatory Gaussian initial data with positive quadratic phase  $\gamma = +\frac{1}{2}$ , see (9.1). The vertical axis is rescaled  $p/\sqrt{1+\beta^2}$  to compare with the real case. The blow up threshold curve denoted “by Thm. 1.4” is given by (9.11), see values  $p_t$  in Table 9.6; the blow up threshold curve denoted “by Thm. 1.5” is given by (9.13), see values  $p_t$  in Table 9.7. Observe that these curves intersect at  $\beta \approx 1.89$ . Therefore, for small oscillations ( $\beta < 1.89$ ) Theorem 1.4 provides the best range for blow up, correspondingly, for large oscillations ( $\beta > 1.89$ ) Theorem 1.5 gives a better range. The curve “theoretical scattering” is given by Thm. 1.1, see (9.9) and values  $p_1^\gamma$ . The numerical threshold (dotted curve) is given in Table 9.8, values  $p_s^+$  and  $p_b^+$ . All  $p$  values in this graph are normalized by  $\sqrt{1+\beta^2}$ .

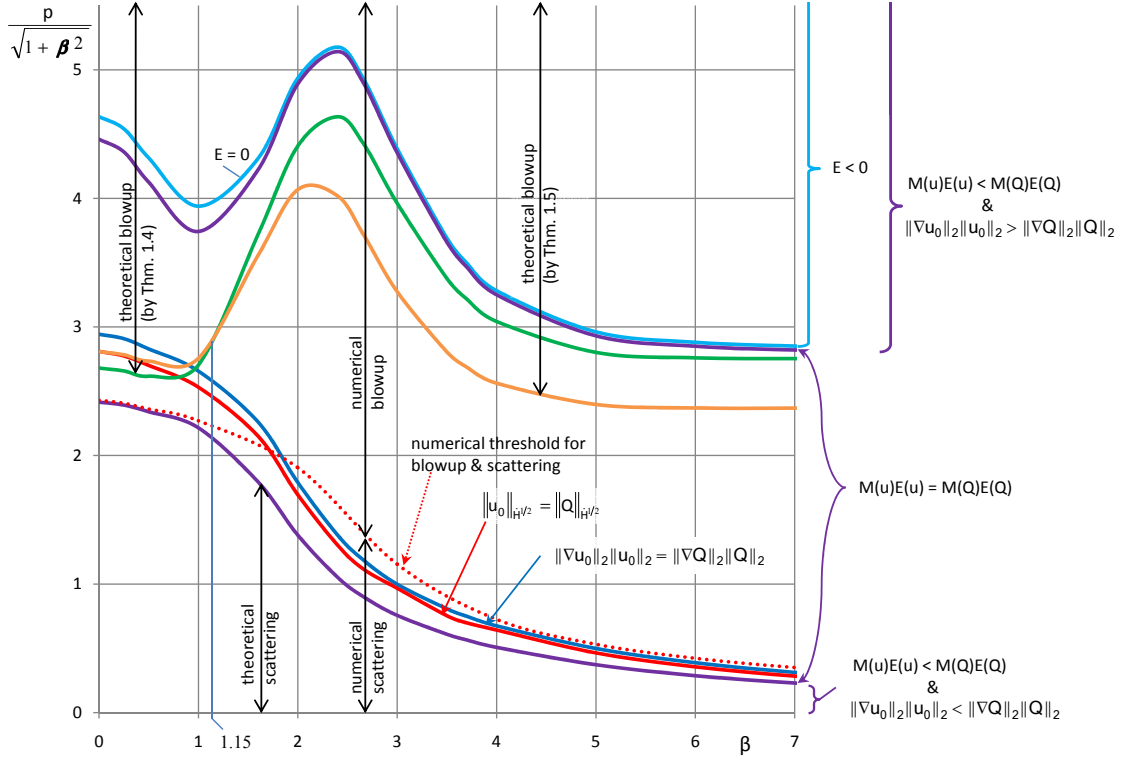


FIGURE 9.3. Global behavior of the solutions to (1.1) with the oscillatory Gaussian initial data with negative quadratic phase  $\gamma = -\frac{1}{2}$ , see (9.1). The vertical axis is rescaled  $p/\sqrt{1+\beta^2}$  to compare with the real case. The blow up threshold curve denoted “by Thm. 1.4” is given by the complement of (9.11), see values  $p_b$  in Table 9.6; the blow up threshold curve denoted “by Thm. 1.5” is given by the complement of (9.13), see values  $p_b$  in Table 9.7. Observe that these curves intersect at  $\beta \approx 1.15$ . Therefore, for small oscillations ( $\beta < 1.15$ ) Theorem 1.4 provides the best range for blow up, correspondingly, for large oscillations ( $\beta > 1.15$ ) Theorem 1.5 gives a better range. The curve “theoretical scattering” is the same as in Figure 9.2 and is given by Thm. 1.1, see (9.9) and values  $p_1^\gamma$ . The numerical threshold (dotted curve) is given in Table 9.8, values  $p_s^-$  and  $p_b^-$ . All  $p$  values in this graph are normalized by  $\sqrt{1+\beta^2}$ . Note that for small oscillations the numerical threshold dotted curve coincides with the “theoretical scattering” curve.

## REFERENCES

- [1] J. E. Barab, *Nonexistence of asymptotically free solutions for nonlinear Schrödinger equation*, J. Math Phys. 25 (1984), pp. 3270–3273.
- [2] M. Beceanu, *A critical centre-stable manifold for the Shrödinger equation in three dimensions*, arxiv.org preprint [arXiv:0909.1180 \[math.AP\]](#).
- [3] L. Bergé, T. Alexander, and Y. Kivshar, *Stability criterion for attractive Bose-Einstein condensates*, Phys. Rev. A, 62, 023607-6 (2000).
- [4] L. Bergé, and J. Juul Rasmussen, *Collapsing dynamics of attractive Bose-Einstein condensates*, Physics Letters A, 304 (2002), pp. 136–142.
- [5] T. Cazenave, *Semilinear Schrödinger equations*. Courant Lecture Notes in Mathematics, 10. New York University, Courant Institute of Mathematical Sciences, New York; American Mathematical Society, Providence, RI, 2003. xiv+323 pp. ISBN: 0-8218-3399-5.
- [6] F. Dalfovo, S. Giorgini, L. P. Pitaevskii, S. Stringari, *Theory of Bose-Einstein condensation in trapped gases*, Rev. Mod. Phys. 71 (1999) pp. 463–512.
- [7] E. Donley, N. Claussen, S. Cornish, J. Roberts, E. Cornell, and C. Wieman, *Dynamics of collapsing and exploding Bose-Einstein condensates*, Nature 412 (2001) pp. 295–299.
- [8] T. Duyckaerts, J. Holmer, and S. Roudenko, *Scattering for the non-radial 3d cubic nonlinear Schrödinger equation*, Math. Res. Lett. 15 (2008) pp. 1233–1250.
- [9] T. Duyckaerts and S. Roudenko, *Threshold solutions for the focusing 3d cubic Schrödinger equation*, to appear in Revista Math. Iber.
- [10] G. Fibich, *Some Modern Aspects of Self-Focusing Theory* in ‘Self-Focusing: Past and Present. Fundamentals and Prospects’, Springer Series: Topics in Appl. Physics, Vol. 114, Springer NY, 2009 Editors: Robert W. Boyd, Svetlana G. Lukishova, Y. Ron Shen 605 p. 299 illus., ISBN: 978-0-387-32147-9.
- [11] G. Fibich, N. Gavish, and X.P. Wang, *Singular ring solutions of critical and supercritical nonlinear Schrödinger equations* Physica D 231 (2007) pp. 55–86.
- [12] G. Fibich, N. Gavish, and X.P. Wang, *New singular solutions of the nonlinear Schrödinger equation*, Physica D 211 (2005) pp. 193–220.
- [13] R. Glassey, *On the blowing up of solutions to the Cauchy problem for nonlinear Schrödinger equation*, J. Math. Phys., 18 (1977) no. 9, pp. 1794–1797.
- [14] J.M. Gerton, D. Strekalov, I. Prodan, R.G. Hulet, *Direct observation of growth and collapse of a Bose-Einstein condensate with attractive interactions*, Nature 408 (2000) pp. 692–695.
- [15] N. Hayashi and P.I. Naumkin, *Asymptotics for large time of solutions to the nonlinear Schrödinger and Hartree equations*, American Journal of Mathematics 120 (1998), pp. 369–389.
- [16] J. Holmer, J. Marzuola, and M. Zworski, *Fast soliton scattering by delta impurities*, Comm. Math. Phys. 274 (2007), pp. 187–216.
- [17] J. Holmer and S. Roudenko, *On blow-up solutions to the 3D cubic nonlinear Schrödinger equation*, AMRX Appl. Math. Res. Express, v. 1 (2007), article ID abm004, 31 pp, doi:10.1093/amrx/abm004 .
- [18] J. Holmer and S. Roudenko, *A sharp condition for scattering of the radial 3d cubic nonlinear Schrödinger equation*, Comm. Math. Phys. 282 (2008), no. 2, pp. 435–467.
- [19] J. Holmer and S. Roudenko, *Divergence of infinite-variance nonradial solutions to the 3d NLS equation*, arxiv.org preprint [arXiv:0906.0203 \[math.AP\]](#).
- [20] P.M. Lushnikov, *Dynamic criterion for collapse*, Pis'ma Zh. Éksp. Teor. Fiz. 62 (1995) pp. 447–452.

- [21] M. Klaus and J.K. Shaw, *On the eigenvalues of Zakharov-Shabat systems*, SIAM J. Math. Anal. 34 (2003), pp. 759–773.
- [22] N.E. Kosmatov, V.F. Shvets and V.E. Zakharov, *Computer simulation of wave collapses in the nonlinear Schrödinger equation*, Physica D, 52 (1991), pp. 16–35.
- [23] E.A. Kuznetsov, J. Juul Rasmussen, K. Rypdal, S.K. Turitsyn, *Sharper criteria for the wave collapse*, Physica D, Vol. 87, Issues 1-4 (1995), pp. 273–284.
- [24] F. Merle and P. Raphaël, *Blow up of the critical norm for some radial  $L^2$  supercritical nonlinear Schrödinger equations*, Amer. J. Math. 130 (2008), no. 4, pp. 945–978.
- [25] W. Strauss, *Existence of solitary waves in higher dimensions*, Comm. Math. Phys. 55 (1977), no. 2, pp. 149–162.
- [26] C. Sulem and P.-L. Sulem, *The nonlinear Schrödinger equation. Self-focusing and wave collapse*. Applied Mathematical Sciences, 139. Springer-Verlag, New York, 1999. xvi+350 pp.
- [27] T. Tao, *Nonlinear dispersive equations. Local and global analysis*. CBMS Regional Conference Series in Mathematics, 106. Published for the Conference Board of the Mathematical Sciences, Washington, DC; by the American Mathematical Society, Providence, RI, 2006. xvi+373 pp. ISBN: 0-8218-4143-2.
- [28] S.N. Vlasov, V.A. Petrishchev, and V.I. Talanov, *Averaged description of wave beams in linear and nonlinear media (the method of moments)*, Radiophysics and Quantum Electronics 14 (1971) pp. 1062–1070. Translated from Izvestiya Vysshikh Uchebnykh Zavedenii, Radiofizika, 14 (1971) pp. 1353–1363.
- [29] S.N. Vlasov, L.V. Piskunova and V.I. Talanov. Zh. Eksp. Teor. Fiz. 95 (1989), 1945 [Sov. Phys JETP 68 (1989) 1125].
- [30] M. Weinstein, *Nonlinear Schrödinger equations and sharp interpolation estimates*, Comm. Math. Phys. 87 (1982/83), no. 4, pp. 567–576.
- [31] M. Weinstein, *On the structure and formation singularities in solutions to nonlinear dispersive evolution equations*, Comm. Partial Differential Equations 11 (1986) pp. 545–565.
- [32] V.E. Zakharov and A.B. Shabat, *Exact theory of two-dimensional self-focusing and one-dimensional self-modulation of waves in nonlinear media*, Soviet Physics JETP 34 (1972) pp. 62–69.
- [33] V.E. Zakharov, *Collapse of Langmuir waves*, Soviet Physics JETP (translation of the Journal of Experimental and Theoretical Physics of the Academy of Sciences of the USSR), 35 (1972) pp. 908–914.

BROWN UNIVERSITY

UNIVERSITY OF OXFORD

ARIZONA STATE UNIVERSITY